PB84-172618
BuMines OFR 50-84

A mining research contract report
SEPTEMBER 1983

STRESS ANALYSIS OF WIRE HOIST ROPE

Contract J0100011
University of Illinois at Urbana-Champaign
Department of Theoretical and Applied Mechanics

Bureau of Mines Open File Report 50-84

BUREAU OF MINES
UNITED STATES DEPARTMENT OF THE INTERIOR

The views and conclusions contained in this document are those of the authors and should not be interpreted as necessarily representing the official policies or recommendations of the Interior Department's Bureau of Mines or of the U.S. Government.

50272-101

REPORT DOCUMENTATION PAGE	1. REPORT NO. BuMines OFR 50-84	2.	3. Recipient's Accession No. PB84 172618
4. Title and Subtitle: Stress Analysis of Wire Hoist Rope			5. Report Date: September 30, 1983
			6.
7. Author(s): George A. Costello and James W. Phillips			8. Performing Organization Rept. No.
9. Performing Organization Name and Address: University of Illinois at Urbana-Champaign Department of Theoretical and Applied Mechanics 216 Talbot Laboratory, 104 South Wright St. Urbana, IL 61801-2983			10. Project/Task/Work Unit No. 11. Contract(C) or Grant(G) No. (C) J0100011 (G)
12. Sponsoring Organization Name and Address: Office of Assistant Director--Mining Research Bureau of Mines U.S. Department of the Interior Washington, DC 20241			13. Type of Report & Period Covered: Contract research, 1/7/80--9/30/83 14.

15. Supplementary Notes

Approved for release March 2, 1984.

16. Abstract (Limit: 200 words)

A theoretical analysis is presented for the static and dynamic response of wire rope in deep-shaft mining operations. Expressions for the stresses in the individual wires of complex wire ropes are derived, and specific results for simple strands are presented for the case of ropes subjected to a combination of axial loading and bending over a sheave. Consideration is also given to the dynamic overloading associated with certain mining operations, such as dumping ore into a suspended skip and accelerating a fully loaded skip upward. Experiments to determine the axial stiffness of wire rope are described. Factors affecting the service life of wire rope, such as residual stresses, contact stresses, and fatigue behavior, are discussed. Specific research areas in need of further investigation are identified.

17. Document Analysis a. Descriptors

Mining research
Wire rope
Stress analysis
Stresses
Modulus of elasticity
Elastic theory
Elastic analysis
Mine shafts
Mine hoisting
Cables
Strands

b. Identifiers/Open-Ended Terms

c. COSATI Field/Group: 02, 06G, 08I, 09D, 11F, 12B, 13I, 14A, 20A

18. Availability Statement	19. Security Class (This Report)	21. No. of Pages
Release unlimited by NTIS.	Unclassified	103
	20. Security Class (This Page) Unclassified	22. Price

(See ANSI-Z39.18) See Instructions on Reverse OPTIONAL FORM 272 (4-77) (Formerly NTIS-35) Department of Commerce

Preceding page blank

FOREWORD

This report was prepared by the University of Illinois at Urbana-Champaign, Department of Theoretical and Applied Mechanics, Urbana, IL 61801-2983, under USBM Contract number J0100011. The contract was initiated under the Minerals Health and Safety Technology Program. It was administered under the technical direction of the Spokane Research Center with Mr. Eugene H. Skinner acting as Technical Project Officer during the initial phase of the work, and with Mr. Grant L. Anderson, P.E., acting as Technical Project Officer during the final phase of the work. Mr. Francis M. Naughton was the contract administrator for the Bureau of Mines during the initial phase of the work; Mr. Doyne W. Teets served in this capacity during the final phase. This report is a summary of the work recently completed as part of this contract during the period January 7, 1980, to September 30, 1983. This report was submitted by the authors on September 30, 1983.

Table of Contents

List of Figures

List of Tables

Notation

A	metallic area of rope
a	acceleration
b	variable appearing in the contact-stress problem
$C_s^{\epsilon}, C_s^{\Delta\tau}$	constants relating Δr_s to ϵ_s and $\Delta\tau_s$, respectively
c	longitudinal wave speed in a rope
D	diameter of a sheave or drum
d	diameter of a rope
E	Young's modulus of the wire material
E_e	effective modulus of a strand or rope
e	base of natural logarithms
F, f	arbitrary functions
G, G'	normal and binormal bending-moment resultants, respectively, acting on a thin rod—see Eqns. (1-16)
G_s'	binormal bending-moment resultant acting on a strand in the sth strand layer
G_{si}'	binormal bending-moment resultant acting on a wire in the ith wire layer of the sth strand
g	acceleration due to gravity
H	twisting-moment resultant acting on a thin rod—see Eqns. (1-16)—or
H	total twisting-moment resultant acting on a rope
H_s	twisting-moment resultant acting on a strand in the sth layer of strands
H_{si}	twisting-moment resultant acting on a wire in the ith wire layer of the sth strand
I	mass moment of inertia of the rope about the x axis
i	number denoting a layer of wires within a strand
K, K'	normal and binormal external moment resultants per unit length, respectively, acting on a thin rod—see Eqns. (1-16)
K_1, K_2, K_3, K_4	nondimensional rope constants—see Eqns. (77-78)
k	axial spring constant of rope of length L
L	length of suspended rope
l	total number of layers of strands in a rope
l_s	total number of layers of wires in the sth strand
M	mass, or
M	bending moment in the residual-stress problem
m	ratio of suspended mass to the mass of rope
m_s	number of strands in the sth strand layer
m_{si}	number of wires in the ith wire layer of the sth strand
N, N'	normal and binormal shear-force resultants, respectively, acting on a thin rod—see Eqns. (1-16)
N_s'	binormal shear-force resultant acting on a strand in the sth strand layer

N'_{si}	binormal shear-force resultant acting on a wire in the ith wire layer of the sth strand
R	wire radius—see Eqns. (1-16)—or
R	rope radius, equal to $d/2$
R_s	strand radius of a strand in the sth strand layer
R_{si}	wire radius of a wire in the ith wire layer of the sth strand
r	helix radius of a thin rod—see Fig. 2
r_s	helix radius of a strand in the sth strand layer
r_{si}	helix radius of a wire in the ith wire layer of the sth strand
s	position along the centerline of a thin rod—see Eqns. (1-16)—or
s	number designating a layer of strands within a rope
T	tensile force resultant acting on a thin rod—see Eqns. (1-16)—or total tensile force on a rope
T_D	dynamic tensile force applied to a rope
T_s	tensile force resultant acting on a strand in the sth strand layer
T_{si}	tensile force resultant acting on a wire in the ith wire layer of the sth strand
t	time
t_D	dumping time of muck into a skip
u	axial displacement of a rope element
V	initial velocity of descending rope and skip
X	normal external force resultant per unit length acting on a thin rod—see Eqns. (1-16)
X_s	normal external force resultant per unit length acting on a strand in the sth strand layer
X_{si}	normal external force resultant per unit length acting on a wire in the ith wire layer of the sth strand
x	coordinate measured along the centerline of the rope
Y, Z	binormal and tangential external force resultants per unit length, respectively, acting on a thin rod—see Eqns. (1-16)
z_{si}^T, z_{si}^B	nondimensional factors relating maximum wire stresses to the D/d ratio—see Eqn. (76)
α	helix angle of a thin rod, measured counter-clockwise from a plane normal to the helix centerline—see Fig. 2
α_s	helix angle of the sth strand layer, measured counter-clockwise from a plane normal to the rope centerline
α_{si}	helix angle of the ith wire layer in the sth strand, measured counter-clockwise from a plane normal to the strand centerline
β	rotational strain of a rope—see Eqn. (79)
γ	included half-angle in certain types of strand
$\Delta( )$	small change in ( )
Δr_{si}^p	the portion of Δr_{si} that is due to strains in the $i-1$ wires beneath the ith wire in the sth strand
Δ	constant used in the contact-stress problem
ϵ	axial wire strain—see Eqns. (1-16)—or

ϵ	axial strain of a rope
ϵ_s	axial strain of a strand in the sth strand layer
ϵ_{si}	axial strain of a wire in the ith wire layer of the sth strand layer
ϵ_Y	yield strain for a bilinear material
ζ	$ct-x$ or $ct+x$, as required
η_{sij}	nondimensional constants relating r_{si} to the various R_{sj} in a given strand
η_{s0j}	nondimensional constants relating R_s to the various R_{sj} in a given strand
η_{0st}	nondimensional constants relating r_s to the various R_t in a rope
Θ	tangential external twisting-moment resultant per unit length acting on a thin rod—see Eqns. (1-16)
θ	angle of rotation of a rope element about the x axis
κ, κ'	normal and binormal curvature, respectively, of a thin rod—see Eqns. (1-16)
κ_s'	binormal curvature of a strand in the sth strand layer
κ_{si}'	binormal curvature of a wire in the ith wire layer of the sth strand
ν	Poisson's ratio of the wire material
ρ	mass per unit length of the rope, or
ρ	radius of curvature of wire centerline
ρ_f	final (residual) radius of curvature of a wire centerline
σ_{si}	maximum tensile stress in a wire in the ith wire layer of the sth strand
σ_{max}	$= \sigma_{si}$ (used in figure labels)
σ_{nom}	nominal stress in the rope, equal to T/A
$\sigma_=$	maximum (compressive) contact stress between wires
τ	twist of a thin rod—see Eqns. (1-16)
τ_s	twist of a strand in the sth strand layer
τ_{si}	twist of a wire in the ith wire layer of the sth strand
ω	circular frequency

Executive Summary

An important part in assessing the performance of wire rope as a structural machine is a determination of the stresses in the individual wires in the rope. This report is concerned with such a determination, in both the static and dynamic case, for those loading conditions associated with deep-shaft hoisting.

The rope is assumed to consist of one or more layers of strands wound around an axis called the centerline of the rope. Each strand in the rope consists of one or more layers of wires wound around the centerline of that strand.

Expressions and plots are presented for the axial wire stresses in the individual wires where the rope is subjected to both tension and bending around a sheave. In this analysis friction is neglected. This is felt to be a reasonable assumption for the static case of well lubricated ropes.

The results indicate that, for a rope with an independent-wire-rope core, the maximum axial wire stress occurs in the center wire of the core when the rope is subjected to tension only and not allowed to rotate. When a rope is subjected to both tension and bending the maximum axial wire stress may shift to the center wire of the strand, since this wire has a larger diameter than the center wire of the core. This shift to the center wire of the strand depends upon the radius of curvature of the sheave. For ropes with a fiber core, the maximum axial stresses occur in the center wire of the strand.

A static analysis of a rope shows that the axial force and twisting moment can be represented as linear functions of the axial strain and the axial rotational strain. The dynamic equations of motion based on these results are presented. Solutions are presented for the following problems: (1) upward acceleration of a loaded skip, (2) dumping muck into a skip, and (3) arresting a descending skip.

Experiments are conducted on a representative wire rope, wire strand and an individual wire to determine experimentally the relationship between the loads and the elastic response of a rope. It is found that the effective modulus for the rope is about 60 percent of the modulus of the wire material.

Recommendations for further study, based on the results of this report, are made. These are concerned mainly with the application of the aforementioned stresses to a fatigue criterion to determine the useful life of a wire rope in a mine shaft.

I. Introduction

The mining industry today depends very heavily upon the use of wire rope to accomplish its mission. With the increase in depths of shafts, wire rope is being called upon more and more to perform under severe working conditions. Increased speeds and tonnage also place additional burdens on the ability of wire to perform satisfactorily. An important element in assessing the performance of wire rope as a structural element is a determination of the stresses in the individual wires in the rope. This report is concerned with such a determination, in both the static and dynamic case, for those loading conditions associated with deep-shaft hoisting.

A. Previous work

A property common to all ropes is an ability to resist tensile loads that are large in comparison to bending and torsional loads. In spite of the importance of ropes and the length of time that ropes have been used, a rational method of analysis has long escaped theoreticians pursuing the problems that arise in wire-rope use. In the work of Suslov [1],† the statement is made that a mathematical calculation of the stress (in wire rope) by the theory of elasticity is impossible "owing to a great number of unknown changeable units which enter as a part in the solution of such a problem."

The basic element of a wire rope is, as the name implies, a single thin metallic wire. The various components of a wire rope are shown in Fig. 1 and as the figure indicates, a wire rope is constructed by laying several strands around a core [2]. The core may be either wire rope, natural fibers, or polypropylene. The strands themselves have a center that is the axial member around which the individual metallic wires are wrapped helically. It is apparent that a precise static response of a wire rope with this type of cross section would be extremely difficult to ascertain unless certain assumptions are made.

In view of the complexity of the problem, relatively few theoretical papers of any significance have appeared, and—as is the case in many engineering areas—the experimental work preceded the theory. Extensive testing of wire rope running over sheaves has been reported by the British Wire Rope Research Commission under the supervision of Schoble [3] and by the Institut fur Fordertechnick in Stuttgart under the direction of Woernle [4]. Test results are also reported in the works of de Forest and Hopkins [5] and Skillman [6]. In the work of Drucker and Tachau [7] a design criterion for wire rope, based on a dimensionless bearing-pressure ratio, is presented. There has been, of course, considerable testing by various wire rope manufacturers but detailed reports are difficult to obtain.

Hall, in a theoretical paper [8], makes various assumptions concerning the loads acting on the individual strands in small wire ropes. All rope loads are equally distributed among the several strands, and all strand loads are equally distributed over the individual wires. Three articles by Hruska [9,10,11] were stimulated by Hall's paper. The first of Hruska's articles is concerned with the calculation of stresses in rope, the second with radial forces, and the third with tangential forces. Contact stresses in wire rope are investigated in an article by Leissa [12]. The results are based on assumptions made previously by Hruska. The radial forces between strands and between individual wires in each strand are expressed as functions of the tensile loading and geometry of the rope.

The critical stresses and modes of failure of wire rope are discussed in an article by Starkey and Cress [13]. The work is again based on Hruska's assumptions. It is found that the greatest stresses occur as a result of the high contact stresses between wires. The assertion is made that the usual mode of failure is fretting fatigue initiated at such points of contact. Contact stresses are also discussed in an article by Bert and Stein [14].

†Numbers in brackets denote References at end of report.

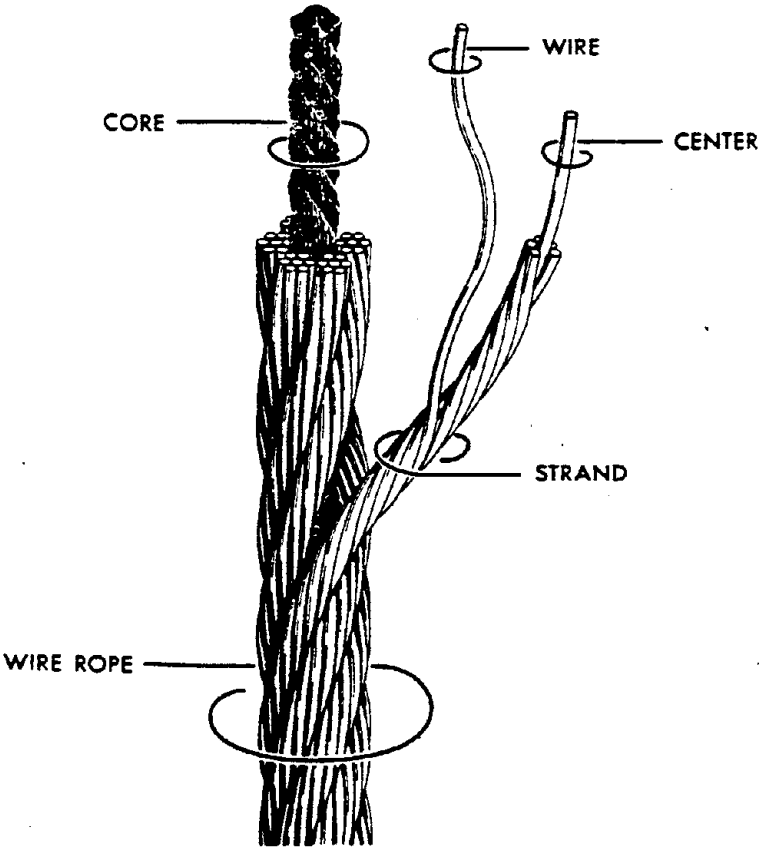

Fig. 1. Components of a wire rope.

Machida and Durelli [15] treat the response of a strand subjected to axial and torsional displacements. Explicit expressions are given for the determination of the axial force and the bending and twisting moments in helical wires, and for the axial force and twisting moment in the core of a seven-wire strand subjected to axial and torsional displacements. Using mechanical and electrical strain gages, dial gages, and brittle coatings, Durelli and Machida [16] also determined the strains, stresses, and displacements in epoxy oversized models. An analysis of multi-wire strands in tension and combined tension and torsion is reported in the work of Chi [17].

Costello and Phillips [18,19,20] pursued the method of separating the strand into thin wires and of solving the six nonlinear differential equations of equilibrium [21] for each wire. In their procedure, the wires are then placed together to form a strand. It is assumed that the strand is loaded by an axial force and an axial twisting moment, that there are no frictional forces between the wires, and that in the initial unloaded state the wires are just touching each other. An exact solution of the nonlinear equations is presented; from the solution all the stresses (bending, axial, torsional, and contact) can be calculated.

The problem of coupled extensional-torsional oscillations in wire rope has been examined by Samras, Skop and Milburn [22]. The equations of motion for a straight rope section loaded simultaneously in tension and torsion are derived, and constitutive equations relating these loadings to the extensional and rotational deformations of the rope are postulated. It is shown that, in general, two types of waves can propagate through a straight rope section.

The elongation and rotation of a strand is considered in a paper by Costello and Phillips [23], where again the nonlinear equations are solved. There it is shown that a strand is much stiffer if the ends are prevented from rotating, which is not the case for a helical spring [21]. In [23], a plot of the effective modulus is shown as a function of the original strand helix angle; the effective modulus is determined by investigating the slope of the load-deflection curve at the origin. Phillips and Costello [24] also investigated the axial impact of strands. In their paper, the longitudinal impact of a finite-length strand fixed at one end is considered in detail, and numerical results are presented.

There are many types of cross sections of wire rope. Costello and Sinha [25] extended the methods developed by Costello, et. al. [18-20,23,24] so that cross sections similar to that shown in Fig. 1 could be analyzed. This was accomplished by determining first the axial, bending, and torsional stiffness for a strand and by subsequently treating the strand as a wire with these properties when the complex cross section was "pieced together." The bending stiffness of the strand was determined by a theory that is presented in the works of Costello [26] and Costello and Miller [27]; the torsional stiffness is discussed in an article by Costello and Sinha [28]. Recently, Costello and Miller [29] investigated the construction requirements for a reduced-rotation strand (a strand that tends not to twist when subjected only to an axial force).

Theoretical expressions are presented for the localized stresses due to the contact forces between wires in adjacent layers of a strand in the work of Phillips, Miller and Costello [30]. The results were applied to a specific strand, but it is felt that the approach can be generalized so as to treat more complex rope geometries.

The differential equations of motion governing the axial and rotational displacements of a straight single-lay wire rope are presented in a thesis by Butson [31] and in a related article by Butson, Phillips and Costello [32]. The boundary conditions and initial conditions are those associated with various deep-shaft hoisting systems. Butson's work should be regarded as initial groundwork in the complex analysis of the dynamics of deep-shaft hoisting systems.

A simplified bending theory for wire rope bent over a sheave has recently been developed by Costello and Butson [33]. The rope is subjected to axial, bending, and torsional loads; it is pointed out that, in addition to the radial pressure applied by the sheave to the rope, other generalized forces must be applied by the sheave to the rope if the rope itself is subjected to a twisting moment (which is generally the case).

In works by Velinsky [34] and Velinsky, Anderson and Costello [35], an important step toward the analysis of complex-cross-section wire rope was taken. The equations governing the static behavior of wire rope were linearized rigorously in a manner that allows previously discussed theories to be applied to rope of complex cross section with relative ease. It is on the work of Velinsky, et. al., that much of the first part of this Report is based.

B. Need for research

It is difficult to find another area of structural mechanics where so much testing is involved and where, at the same time, so little theoretical work has been done. The mechanical tests on rope can generally be divided into two categories: (1) direct axial tests where the ends are prevented from rotating, and the breaking strength of the rope is recorded; and (2) fatigue tests where the rope progressively fractures due to localized wire damage from fluctuating stresses, subsequently culminating in multiple fractures and rope failure.

The breaking strength of a rope is an important parameter in design. For a given loading system acting on a rope, the "working" rope size is usually determined by applying an appropriate factor of safety to the given loading. Design procedures based on the breaking strength of rope require that the loads acting on the rope be known; but generally such procedures do not take into account the fatigue life.

Fatigue tests, on the other hand, are performed on a given rope for a given loading. Since there are so many parameters that can vary—for example, the rope construction, the loading, the rope diameter, the sheave diameter—the number of tests quickly becomes enormous.

In view of the preceding remarks it is clear that a rational method of analysis is needed. A useful theoretical analysis would first manifest itself in the form of a determination of the stresses in the individual wires of a wire rope. The stress determination would depend upon the rope construction and the known loads acting on the rope. Initially, the response of the rope would be determined in the static case, and then the results of the static analysis would be extended to the dynamic case by means of Newton's laws of motion. Such a determination would result in a better rope design since, with the aid of a computer solution based on the analytical formulation, the many parameters affecting the stress distribution could be varied systematically in an effort to achieve optimum rope performance under given loading conditions.

Since many ropes fail by a mechanism called fretting fatigue [36], a knowledge of the time dependence of stresses in the wire material should lead to a better criterion for determining the useful life of a wire rope.

It is felt that the results presented in this report meet many of the goals just set. At the same time, it is obvious that more work is needed, principally in the area of theoretical analysis of complex wire-rope cross sections other than the ones treated to date, and in the determination of contact stresses, residual stresses, and other factors affecting the fatigue performance of rope.

II. Theoretical analysis of wire rope

In this section, an analysis is presented for the static and dynamic response of wire rope subjected to mechanical loading. Axial, torsional, and bending loads are considered for static loading; for dynamic loading, only axial and torsional effects are treated. Throughout the discussion, the effects of friction are neglected.

A. Static analysis

A *rope* consists of one or more layers of *strands* wound about an axis called the centerline of the rope. Each strand in the rope consists of one or more layers of *wires* wound about the centerline of that strand.

When a straight length of rope is pulled and twisted, every wire in the rope is subjected to tensile, torsional, bending, and transverse-shear stresses, as well as stresses due to either line or point contact with neighboring wires. Furthermore, when a rope is bent around a sheave, additional stresses due principally to bending are induced in each wire.

The analysis of stresses in wire rope can be rather elementary, or it can be exceedingly complex, depending upon the nature of the assumptions made in the analysis. In the present work, the static analysis of *wire* stresses due to the axial and torsional deformation of the *strand* containing that wire is rigorous in the sense that the linearized coupled equations of equilibrium for each wire in a straight strand are satisfied exactly. Likewise, the analysis of the generalized forces acting on the *strand* due to the axial and torsional deformation of the *rope* is rigorous in the sense that the linearized coupled equations of equilibrium for each strand in a straight rope are satisfied exactly. Important assumptions that are made in the analysis include the following:

- The rope is free of defects such as kinks or broken wires.
- The effects of friction can be neglected.
- The strains in the wires are small.
- The wire stresses can be related to wire strains by means of Hooke's law for an isotropic linear elastic material.
- The effects of residual stresses induced during rope manufacture can be neglected.
- The wires have circular cross section.
- The bending stiffness of a strand is the sum of the individual bending stiffnesses of the helically bent wires comprising the strand.
- The (coupled) torsional and axial response of a strand in the rope is the same as that of a straight strand.

It is appropriate to discuss some of these assumptions at this point. First of all, the ropes used in deep-shaft mining, particularly those ropes used to hoist personnel, are carefully installed so as to avoid kinking, bird-caging, crushing, and other physical abuse. Broken wires will occur with normal use, and wherever a break in a wire occurs, the load formerly carried by that wire must be carried by neighboring wires; but the effect of a broken wire is localized to within a rope's lay length or so of such a defect. In any event, a major objective of the current research is the prediction of the stresses in flawless rope, so that a criterion based on stress cycling can be employed to estimate the life of the individual wires under ideal conditions.

Neglecting friction is probably reasonable since the ropes used in deep-shaft mining are

lubricated to reduce wear of the ropes and sheaves. The inclusion of friction in the basic equilibrium and kinematics relations greatly complicates the analysis, even for a simple strand, as Butson [31] has noted. Reference to Butson's work will be made later.

The strains in the wires are in fact very small, since the stresses in the wires are generally much smaller than the tensile yield strength of the wire material. For example, the high-strength steels commonly employed in wire-rope manufacture have yield strengths of the order of 300,000 lb./in.^{2} and a Young's modulus of approximately 29.0×10^6 lb./in.^{2}; thus, even at yield, the magnitude of the strain is only of the order of 0.01. The fact that the strains are small is important when one considers the geometry of deformation of a wire.

The wire used in wire rope has some ductility despite the high degree of cold working induced in the wire-drawing process. Some ductility is required so that the wire can be plastically deformed when constructing the strand, and additional ductility is required when the strand is preformed during the rope-laying process. Once the rope is constructed, however, the *additional* strains induced mechanically during normal use are much smaller in magnitude than the strains that would be required to cause additional plastic deformation. The use of linear elastic constitutive relations is therefore appropriate for these additional strains.

1. Analysis of a wire

Ropes are made from strands, which in turn are composed of many helically shaped wires. Each helical wire represents a special case of a thin rod bent into an arbitrary shape, for which the equations of equilibrium [21] are:

$$\frac{dN}{ds} - N'\tau + T\kappa' + X = 0, \tag{1}$$

$$\frac{dN'}{ds} - T\kappa + N\tau + Y = 0, \tag{2}$$

$$\frac{dT}{ds} - N\kappa' + N'\kappa + Z = 0, \tag{3}$$

$$\frac{dG}{ds} - G'\tau + H\kappa' - N' + K = 0, \tag{4}$$

$$\frac{dG'}{ds} - H\kappa + G\tau + N + K' = 0, \tag{5}$$

and

$$\frac{dH}{ds} - G\kappa' + G'\kappa + \Theta = 0, \tag{6}$$

where s denotes the position along the centerline of the wire, N and N' are the normal and binormal shear force resultants, T is the tensile force resultant, G and G' are the normal and binormal bending moment resultants, and H is the twisting moment resultant acting on the wire. Other variables appearing in Eqns. (1-6) are the external force resultants per unit length X, Y, and Z, acting in the normal, binormal, and tangential directions, respectively; and the external moment resultants per unit length K, K', and Θ, acting about the normal, binormal, and tangential directions, respectively. See Fig. 2.

The equations of equilibrium simplify tremendously when one considers the special case of a helical wire that is bent into the shape of another helix. Even so, the governing equations are nonlinear if one (correctly) regards the generalized curvatures κ, κ', and τ as those associated with the

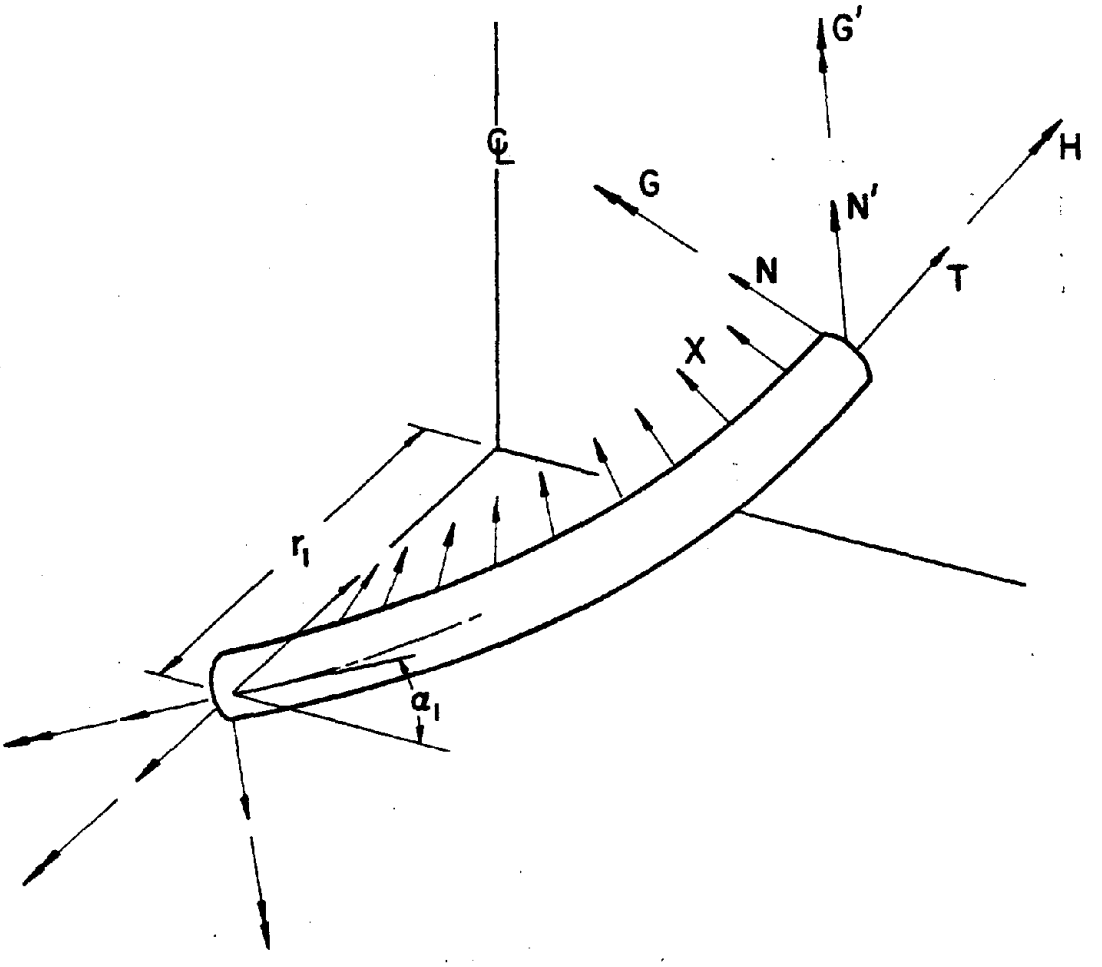

Fig. 2. Generalized forces on a wire or strand.

deformed configuration of the appropriate helix. This was the approach taken by the authors in earlier work [18-20,23]. As a practical matter, however, the *changes* in the values of the generalized curvatures for wires in a rope strand are very small and have negligible effect on the equations of equilibrium for a wire. With negligible loss of accuracy, the generalized curvatures appearing in Eqns. (1-6) are taken to be [18-20,23]

$$\kappa = 0, \quad \kappa' = \frac{\cos^2\alpha}{r}, \quad \text{and} \quad \tau = \frac{\sin\alpha\,\cos\alpha}{r}, \tag{7}$$

where α and r are the *original* values of the helix angle (measured from a plane normal to the helix centerline) and helix radius, respectively, of the wire within the strand.

It is in writing down the formulas for the generalized moments G, G', and H that the *changes* in generalized curvatures are important, just as they were in [18-20,23]. Specifically, for a circular wire of radius R,

$$G = \frac{\pi ER^4}{4}\Delta\kappa, \quad G' = \frac{\pi ER^4}{4}\Delta\kappa', \quad \text{and} \quad H = \frac{\pi ER^4}{4(1+\nu)}\Delta\tau, \tag{8}$$

where $\Delta\kappa$ denotes the *change* in κ from its original value, etc., and E and ν denote Young's modulus

and Poisson's ratio, respectively, for the wire material.

When a helical wire is deformed into the shape of another helix, there is no change in the normal curvature, i.e.

$$\Delta\kappa = 0. \tag{9}$$

It follows from the first of Eqns. (8) that $G = 0$. The other generalized curvature changes generally do not vanish, but it is assumed that they are independent of the coordinate s. Also, it is assumed that the wire tension T does not depend on s. If the wire is not subjected to external bending moments per unit length (i.e. $K = K' = 0$), then it follows from Eqns. (1-6) that

$$-N'\tau + T\kappa' + X = 0, \tag{10}$$

$$Y = 0, \tag{11}$$

$$Z = 0, \tag{12}$$

$$-G'\tau + H\kappa' - N' = 0, \tag{13}$$

$$N = 0, \tag{14}$$

and

$$\Theta = 0. \tag{15}$$

Note that Eqn. (13) can be used to determine N' if G' and H are known. Then, if T is known, the normal force per unit length X can be determined from Eq. (10). For a single wire with axial wire strain ϵ, the tension T is given by

$$T = \pi ER^2\epsilon. \tag{16}$$

The wire strain was denoted by ξ in previous work [18-20,23].

Notation for wires and wire variables

In order to identify the various wires in a wire rope, one needs to introduce some kind of numbering scheme. The one used in this report is due originally to Velinsky [35], and involves the use of two subscrips—one to identify the strand, and another to identify a given wire in that strand. Specifically, the subscripts si will denote the ith wire within the sth strand, or more precisely, any of the wires in the ith layer of wires in a given strand in the sth layer of strands within the rope. The numbering scheme for a 6x19 Seale IWRC is illustrated in Fig. 3, where a comma (,) is used to separate the values of s and i for a given wire.

If Eqns. (10), (13) and (16) are rewritten in this notation, they become, respectively,

$$-N'_{si}\tau_{si} + T_{si}\kappa'_{si} + X_{si} = 0, \tag{17}$$

$$-G'_{si}\tau_{si} + H_{si}\kappa'_{si} - N'_{si} = 0, \tag{18}$$

and

$$T_{si} = \pi ER^2\epsilon_{si}. \tag{19}$$

The curvature κ'_{si} and the twist τ_{si} of a given wire are given by

$$\kappa'_{si} = \frac{\cos^2\alpha_{si}}{r_{si}} \tag{20}$$

and

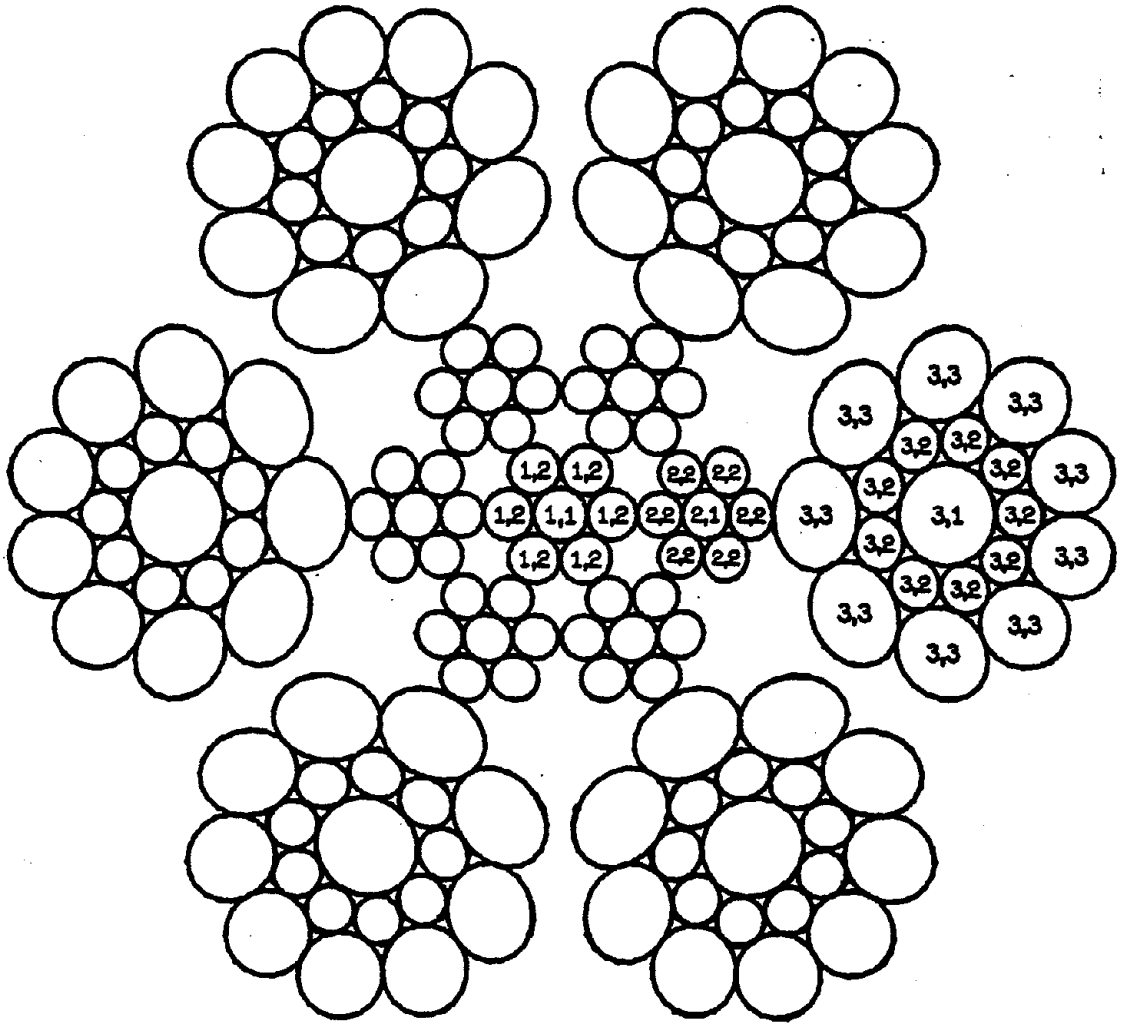

Fig. 3. Wire identification for a Seale 6x19 IWRC.

$$\tau_{si} = \frac{\sin\alpha_{si}\cos\alpha_{si}}{r_{si}}, \tag{21}$$

where r_{si} denotes the helix radius of the wire.

Changes in curvature and twist

Note that small changes in r_{si} and α_{si} will give rise to small changes in the curvature and twist. Starting with Eqns. (20) and (21), one can show by the chain rule of partial differentiation that

$$r_{si}\,\Delta\tau_{si} = -\frac{\cos\alpha_{si}\sin\alpha_{si}}{r_{si}}\,\Delta r_{si} + (\cos^2\alpha_{si} - \sin^2\alpha_{si})\,\Delta\alpha_{si} \tag{22}$$

and

$$r_{si}\,\Delta\kappa'_{si} = -\frac{\cos^2\alpha_{si}}{r_{si}}\,\Delta r_{si} - 2\cos\alpha_{si}\sin\alpha_{si}\,\Delta\alpha_{si}. \tag{23}$$

For reasons that will become apparent only later, one notes that Eqns. (22) and (23) can be inverted to give Δr_{si} and $\Delta\alpha_{si}$ in terms of $\Delta\kappa'_{si}$ and $\Delta\tau_{si}$:

$$\frac{\Delta r_{si}}{r_{si}} = -2\tan\alpha_{si}\,(r_{si}\,\Delta\tau_{si}) + (\tan^2\alpha_{si} - 1)\,(r_{si}\,\Delta\kappa'_{si}) \tag{24}$$

and

$$\Delta\alpha_{si} = (r_{si}\,\Delta\tau_{si}) - \tan\alpha_{si}\,(r_{si}\,\Delta\kappa'_{si}). \tag{25}$$

2. Analysis of a strand

A strand is composed of layers of helical wires all wrapped concentrically about a common axis called the centerline of the strand. Generally a strand has a central straight wire called a center wire—see Fig. 1—but this is not essential. The layers of wires can each contain an arbitrary number of wires; let m_{si} denote the number of wires in the ith layer of wires in a *single* strand from the sth layer of strands in a rope. Values of m_{si} for a 6x19 Seale rope with a 7x7 IWRC, for example, would be: $m_{11} = 1$ and $m_{12} = 6$ for the central strand of the IWRC, $m_{21} = 1$ and $m_{22} = 6$ for each of the outer strands of the IWRC, and $m_{31} = 1$, $m_{32} = 9$, and $m_{33} = 9$ for each of the Seale strands.

Initial helix radii of wires within strands

One of the first tasks in describing a wire rope cross section is the determination of initial helix radii of wires within the strands. This is not a difficult task if (as is generally the practice in the manufacture of many rope strands) the wire diameters have been chosen so that the wires in a given layer rest on wires in the layer beneath it, rather than on each other. The 6x19 Seale IWRC is an example of such a rope: the six outer wires of the central strand rest on the center wire, and consequently

$$r_{12} = R_{11} + R_{12}$$

where r_{12} is the helix radius of the "12" wires and R_{11} and R_{12} are the wire radii for the central ("11") wire and any one of the "12" wires. The strands in the outer layer of strands in the IWRC are similarly constructed, i.e.

$$r_{22} = R_{21} + R_{22},$$

and, in fact, so are the Seale strands—at least as far as the central wire and the first layer of nine wires covering the central wire are concerned:

$$r_{32} = R_{31} + R_{32}.$$

An expression for the helix radius r_{33} of the nine *outer* Seale wires is not written down as quickly as those for the other wires. If it is assumed for simplicity that the cross sections of the wires *in the strand* are circular, then it is readily shown that

$$r_{33} = (R_{31}+R_{32})\cos\frac{\pi}{m_{32}} + (R_{32}+R_{33})\cos\gamma,$$

where γ satisfies the equation

$$(R_{32}+R_{33})\sin\gamma = (R_{31}+R_{33})\sin\frac{\pi}{m_{32}},$$

that is,

$$\gamma = \arcsin\left[\frac{R_{31}+R_{32}}{R_{32}+R_{33}}\sin\frac{\pi}{m_{32}}\right]. \tag{26}$$

It is noted in passing that this expression for r_{33} is only approximate because in its derivation, no account was taken of the fact that the cross sections of the wires *in the strand* are essentially elliptical. Although the point is worthy of consideration, it will not be discussed in this report because of the additional complexity involved. The fact that, in general, *all* wires have essentially elliptical cross sections does *not* affect the results for r_{12}, r_{22}, and r_{32} because the minor half-axis of the elliptical cross section is always equal to the wire radius (regardless of the helix angle).

An important observation to be made is that the helix radius r_{si} is always representable by the summation

$$r_{si} = \sum_{j=1}^{i} \eta_{sij} R_{sj}, \tag{27}$$

where, at least in the present context, the η_{sij} are *constants*. The complete set of η_{sij} for the wire helix radii in a Seale IWRC, including the central wires in each strand, are:

$$\begin{aligned}
&\eta_{111} = 0;\ \eta_{121} = 1 \text{ and } \eta_{122} = 1;\\
&\textit{and}\\
&\eta_{211} = 0;\ \eta_{221} = 1 \text{ and } \eta_{222} = 1;\\
&\textit{and}\\
&\eta_{311} = 0;\ \eta_{321} = 1 \text{ and } \eta_{322} = 1; \text{ and}\\
&\eta_{331} = \cos\frac{\pi}{m_{32}},\ \eta_{332} = \cos\frac{\pi}{m_{32}} + \cos\gamma,\ \eta_{333} = \cos\gamma.
\end{aligned} \tag{28}$$

The value of γ is determined from Eqn. (26).

Initial radius of a strand

The radius of a strand is the radius of the envelope that encloses the outermost wires in the strand. Generally there is no confusion as to which are the "outermost" wires in a strand, but in some strands, such as the Warrington, there are two different "outer" wire diameters and some care is required in identifying which of the corresponding wire sets is actually the "outermost."

In the following discussion, it will be assumed that the layers of wires in the strand have been numbered in such a way that, if l_s is the total number of layers of wires in the sth strand, then the l_sth layer is the outermost layer. For example, in reference to Fig. 3, it will be seen that the values of l_s for the 6x19 Seale IWRC would be $l_1 = 2$, $l_2 = 2$, and $l_3 = 3$. If this convention is always followed, then a simple expression for the strand radius R_s can be written down, since the strand radius is equal to the sum of the helix radius of the outermost wires and the wire radius of wires in that layer:

$$R_s = r_{si} + R_{si}, \quad (i = l_s \text{ only}). \tag{29}$$

In particular, for the 6x19 Seale with the 7x7 core, one would have

$$R_1 = r_{12} + R_{12}, \quad R_2 = r_{22} + R_{22}, \quad \text{and} \quad R_3 = r_{33} + R_{33}.$$

Strand strain and strand twist, in terms of wire variables

In the present context a strand is regarded as a collection of l_s layers of wires all preformed helically about a *straight* centerline. The generalized strains that such a strand can experience—and yet remain straight—consist of an axial strand strain ϵ_s and a change in twist $\Delta\tau_s$. (The change in twist $\Delta\tau_s$ has units of angular rotation per unit length, and in much of the work of Costello et. al., this quantity has been rendered dimensionless by multiplying it by some suitable radial dimension and calling the product a "rotational strain." In the analysis of multi-stranded ropes, however, such a nondimensionalization is neither necessary nor beneficial at this stage.)

The rest of this section deals with the determination of the generalized *wire* strains that are developed in a strand when the strand is deformed. There are three conditions that each wire must satisfy: two "compatibility" conditions that relate the generalized wire strains to the two strand strains presently allowed, and one "relative motion" condition ensuring continued contact between wires in the cross section (allowing for Poisson contraction). Since there are three conditions to be met, three generalized wire strains must be introduced for each wire, and in the following analysis, the three generalized wire strains are chosen to be the axial wire strain ϵ_{si}, the change in wire twist $\Delta\tau_{si}$, and the change in wire curvature $\Delta\kappa_{si}'$.

The first conditions to be treated are the two displacement-strain relations that ensure that *each* of the wires within a given strand will deform in a manner that is compatible with the overall deformation of that strand. Of these relations, the first concerns the axial strand strain ϵ_s, and the second concerns the change in strand twist $\Delta\tau_s$. From earlier work (for example, [23]), it will be seen that for *any* of the layers of wires in the sth strand ($i = 1, \ldots, l_s$), the axial strand strain depends upon the wire strain and the change in wire helix angle according to the relation

$$\epsilon_s = (1+\epsilon_{si}) \frac{\sin(\alpha_{si}+\Delta\alpha_{si})}{\sin\alpha_{si}} - 1 \tag{30}$$

where ϵ_{si} is the axial wire strain and $\Delta\alpha_{si}$ is the change in wire helix angle. Since ϵ_{si} and $\Delta\alpha_{si}$ are very small quantities, Eqn. (30) can be linearized; the result of the linearization is:

$$\epsilon_s = \epsilon_{si} + \cot\alpha_{si}\,\Delta\alpha_{si}. \tag{31}$$

Alternatively, Eqn. (31) may be written in terms of the wire strain and the changes in twist and curvature of the wire, by recalling Eqn. (25); the result is:

$$\epsilon_s = \epsilon_{si} + \cot\alpha_{si}\,(r_{si}\,\Delta\tau_{si}) - (r_{si}\,\Delta\kappa_{si}'). \tag{32}$$

The second of the two displacement-strain relations concerns the change in twist $\Delta\tau_s$. The fundamental nonlinear relation for $\Delta\tau_s$ is [23]

$$\Delta\tau_s = \frac{1}{r_{si}+\Delta r_{si}}(1+\epsilon_{si}) \frac{\cos(\alpha_{si}+\Delta\alpha_{si})}{\sin\alpha_{si}} - \frac{1}{r_{si}}\cot\alpha_{si}. \tag{33}$$

Linearization of this equation for small Δr_{si}, ϵ_{si} and $\Delta\alpha_{si}$ leads to the expression:

$$\Delta\tau_s = \frac{1}{r_{si}}\left[\cot\alpha_{si}\left(-\frac{\Delta r_{si}}{r_{si}}+\epsilon_{si}\right) - \Delta\alpha_{si}\right], \tag{34}$$

which, like Eqn. (31), can be rewritten in terms of the wire strain and the changes in wire twist and curvature, by employing Eqns. (24) and (25):

$$r_{si}\,\Delta\tau_s = \cot\alpha_{si}\,\epsilon_{si} + (r_{si}\,\Delta\tau_{si}) + \cot\alpha_{si}\,(r_{si}\Delta\kappa_{si}'). \tag{35}$$

Change in wire helix radius

The third condition on the generalized wire strains is provided by a consideration of the *deformed* helix radii of the wires within the strand. Recall that the *undeformed* helix radius of the ith wire in the sth strand is given by Eqn. (27):

$$r_{si} = \sum_{j=1}^{i} \eta_{sij} R_{sj}.$$

Now suppose that the η_{sij} are constants, so that the change in the helix radius is due solely to Poisson contraction of the individual wires; then the change in helix radius Δr_{sij} will be given by

$$r_{si} + \Delta r_{si} = \sum_{j=1}^{i} \eta_{sij} (1 - \nu \epsilon_{sj}) R_{sj}, \tag{36}$$

where the ϵ_{sj} are the strains in any of the wires up to and including the ith wire in the given strand, or

$$\Delta r_{si} = -\nu \sum_{j=1}^{i-1} \eta_{sij} \epsilon_{sj} R_{sj} - \nu \eta_{sii} \epsilon_{si} R_{si}. \tag{37}$$

The expression for Δr_{si} in Eqn. (37) is written as the sum of two terms, namely, a summation over all wires *beneath* the ith wire, and a term involving *only* the ith wire. One now observes that if the strains in all the wires *beneath* the ith wire have already been determined, then Eqn. (37) provides the third condition needed to solve for all the generalized strains in the ith wire. Equation (24) is now used to rewrite Eqn. (37) in the form:

$$\frac{1}{r_{si}} \Delta r_{si}^{p} = \frac{1}{r_{si}} \nu \eta_{sii} R_{si} \epsilon_{si} - 2 \tan\alpha_{si} (r_{si} \Delta\tau_{si}) + (\tan^2\alpha_{si} - 1)(r_{si} \Delta\kappa_{si}'), \tag{38}$$

where

$$\Delta r_{si}^{p} \equiv -\nu \sum_{j=1}^{i-1} \eta_{sij} \epsilon_{sj} R_{sj} \tag{39}$$

is the *known* portion of the total change in helix radius due to previously calculated strains in the wires beneath the ith wire.

Solution for the generalized wire strains

Three independent linear equations—Eqns. (32), (35) and (38)—have now been derived for the generalized wire strains $\Delta\tau_{si}$, $\Delta\kappa_{si}'$ and ϵ_{si} associated with the ith wire in the sth strand. Multiplying Eqn. (38) by $\cot^2\alpha_{si}$, and collecting the equations together, one finds that governing relations are:

$$\begin{aligned}
\cot\alpha_{si} (r_{si} \Delta\tau_{si}) \quad &- 1 (r_{si} \Delta\kappa_{si}') \quad &+ 1 \epsilon_{si} &= \epsilon_{s} \\
1 (r_{si} \Delta\tau_{si}) \quad &+ \cot\alpha_{si} (r_{si} \Delta\kappa_{si}') \quad &+ \cot\alpha_{si} \epsilon_{si} &= r_{si} \Delta\tau_{s} \\
-2\cot\alpha_{si} (r_{si} \Delta\tau_{si}) + (1 - \cot^2\alpha_{si}) (r_{si} \Delta\kappa_{si}') &+ \nu \eta_{sii} (R_{si}/r_{si}) \cot^2\alpha_{si} \epsilon_{si} &= (\cot^2\alpha_{si}/r_{si}) \Delta r_{si}^{p}
\end{aligned} \tag{40}$$

For any imposed strand strain ϵ_s, strand twist change $\Delta\tau_s$ and partial helix-radius change Δr_{si}^{p}, one can solve Eqns. (40) uniquely for the generalized strains in a given wire. The equations remain valid even in the often encountered case where a wire or layer of wires is parallel to the strand, i.e. $\cot\alpha_{si} = 0$. When this occurs, the solution to Eqns. (40) is simply

$$\begin{aligned}
\Delta\tau_{si} &= \Delta\tau_{s}, \\
\Delta\kappa_{si}' &= 0, \quad \text{and} \\
\epsilon_{si} &= \epsilon_{s}.
\end{aligned} \tag{41}$$

In the general case where $\cot\alpha_{si} \neq 0$, Eqns. (40) are quickly solved since the equations are linear and there are only three unknowns to be determined. It should be appreciated that the *number* of layers of

wires in the given strand is not a matter of concern: one starts with the innermost layer of wires in the strand and solves for each layer one set of three equations in three unknowns; the procedure is ideally suited for numerical computation.

Generalized forces on the strand: tension, torsion and bending

Once the generalized strains in all the wires of a given strand are known, the total tensile force T_s and total twisting moment H_s acting on the strand can be determined, as follows. First the bending moment G'_{si}, the twisting moment H_{si}, and the tensile force T_{si} acting on the individual wires are found by substituting the known values of $\Delta\kappa'_{si}$, $\Delta\tau_{si}$, and ϵ_{si} into Eqns. (8) and Eqn. (16). The equilibrium equations for a wire, Eqns. (17) and (18), are then used to determine the shear force N'_{si} and the distributed normal force X_{si} acting on the individual wires. The total tensile force T_s acting on the strand is the sum of the components of the wire forces in the direction of the strand axis:

$$T_s = \sum_i^{l_s} m_{si} (T_{si} \sin\alpha_{si} + N'_{si} \cos\alpha_{si}), \tag{42}$$

while the twisting moment H_s acting on the sth strand is the sum of the axial components of the wire moments and of the moments of wire forces:

$$H_s = \sum_i^{l_s} m_{si} [(H_{si} \sin\alpha_{si} + G'_{si} \cos\alpha_{si}) + r_{si} (T_{si} \cos\alpha_{si} - N'_{si} \sin\alpha_{si})]. \tag{43}$$

To complete the analysis for a strand, one needs to specify how the bending moment G'_s will be computed for the strand once it is preformed into the rope and subjected to a change in *strand* curvature $\Delta\kappa'_s$. For purposes of computing this bending moment, it is assumed that the strand is a collection of helical wires free to slide relative to each other. It then follows from a recent paper by Costello [26] that

$$G'_s = \left(\sum_i^{l_s} m_{si} \frac{\sin\alpha_{si}}{1 + \frac{1}{2}\nu \cos^2\alpha_{si}} \frac{\pi E R_{si}^4}{4} \right) \Delta\kappa'_s, \tag{44}$$

i.e. the bending moment required to change the curvature of the entire strand by an amount $\Delta\kappa'_s$ is equal to the sum of the bending moments required to bend all the component helical wires in the strand by the same amount. Experimental results reported by McConnell and Zemke [37] on the flexural stiffness of stranded conductors indicate that Eqn. (44) is certainly accurate enough for the current purposes of analysis, since the role that G'_s plays in the overall response of a *straight* rope is generally relatively minor.

3. Analysis of a rope

A rope is formed from strands in a manner that greatly resembles the manner in which strands are formed from wires. Correspondingly, much of the theory developed for the analysis of strands applies directly to the analysis of ropes. One feature that complicates the analysis of ropes, however, is that the deformed radius of a strand is a function not only of the axial strain of the strand, but also of the change in twist of the strand. This matter will be addressed after some preliminaries regarding the geometry of strands within a rope have been presented.

Initial helix radii of strands within the rope

Let l denote the number of layers of strands in a rope; the analysis to be presented here will be valid for any value of l, including $l = 1$. Much of the rope used for hoisting has a two-layer internal-

wire-rope core about which is wrapped a third layer of strands of a particular type, such as a Seale, Warrington, filler-wire, or flattened strand. For all these types of rope, $l = 3$.

The initial helix radii of the strands in a rope are usually easy to specify in terms of the radii of the strands, since strands are rarely "nested" among themselves. Consider the 6x19 Seale IWRC shown in Fig. 3. If one starts at the center of the rope, one finds that the helix radii r_s of the three strand layers are:

$$r_1 = 0,$$
$$r_2 = R_1 + R_2, \quad \text{and}$$
$$r_3 = R_1 + 2R_2 + R_3,$$

where R_1, R_2 and R_3 are the known strand radii previously computed from Eqn. (29). Note that each r_s is given by a summation of the form

$$r_s = \sum_{t=1}^{s} \eta_{0st} R_t, \tag{45}$$

where for this rope—and for most ropes having a two-layer internal-wire-rope core—the η_{0st} are:

$$\eta_{011} = 0;$$
$$\eta_{021} = 1, \quad \eta_{022} = 1; \quad \text{and}$$
$$\eta_{031} = 1, \quad \eta_{032} = 2, \quad \eta_{033} = 1.$$

Initial radius of the rope

The radius R of the entire rope is the radius of the envelope that encloses the outermost strands. It will be assumed that the l layers of strands have been numbered in such a way that the lth layer of strands is the outermost one. Then the radius of the rope will be simply

$$R = r_s + R_s \quad (s = l \text{ only}). \tag{46}$$

Rope strain and rope twist, in terms of strand variables

Each preformed strand in the rope has its own twist τ_s and curvature κ_s' given by

$$\tau_s = \frac{\sin\alpha_s \cos\alpha_s}{r_s} \quad \text{and} \quad \kappa_s' = \frac{\cos^2\alpha_s}{r_s}, \tag{47}$$

where α_s is the helix angle of that strand within the rope. When the rope is loaded axially by a tensile force T and twisting moment H, each of the individual strands within the rope is subjected to an axial strain ϵ_s and *changes* in strand twist and curvature, which are denoted by $\Delta\tau_s$ and $\Delta\kappa_s'$, respectively.

As was the case for wires within a strand, there arise three conditions governing the behavior of strands within a rope, and these conditions lead to a set of three simultaneous equations for the generalized strand strains ϵ_s, $\Delta\tau_s$ and $\Delta\kappa_s'$. The first two of these conditions are "compatibility" relations that ensure that each strand will deform in a manner that is compatible with a specified axial rope strain ϵ and rope change-in-twist $\Delta\tau$. (In earlier work [18-20,23], the change in twist was normalized with respect to a suitable radial dimension and called a "rotational strain." That procedure will not be followed in the present section.) The analysis of the "compatibility" relations is identical to that encountered previously for the wires within the strand, and leads to the expressions

$$\epsilon = \epsilon_s + \cot\alpha_s (r_s \Delta\tau_s) - (r_s \Delta\kappa_s') \tag{48}$$

and

$$r_s \Delta\tau_s = \cot\alpha_s \epsilon_s + (r_s \Delta\tau_s) + \cot\alpha_s (r_s \Delta\kappa_s'). \tag{49}$$

Change in strand radius

The third relation governing the behavior of the sth strand within the rope concerns the change in strand helix radius Δr_s that occurs because of the Poisson contraction of all the wires in the sth strand and in the $s-1$ strand layers beneath it. Viewed more simply, the change in helix radius Δr_s is related directly to changes in the strand radii of the $(s-1)$ strands beneath the sth strand, as well as to the change in the strand radius of the sth strand itself, by virtue of Eqn. (45). The strand radii, in turn, depend on the amount of axial strain and twist applied to the individual strands; it is this matter which must now be addressed.

Recall that the initial strand radius R_s of a given strand is equal to the sum of the helix radius of the outermost (l_sth) wire in that strand and the radius of that wire, i.e. from Eqns. (28) and (29),

$$R_s = \sum_{j=1}^{i} \eta_{sij} R_{sj} + R_{si} \quad (i = l_s \text{ only}). \tag{50}$$

It proves helpful to shorten this expression by incorporating the "$+R_{si}$" term automatically into a single summation over the R_{sj}, as follows: let

$$\eta_{s0j} \equiv \begin{cases} \eta_{sij}, & i = l_s \text{ and } j \neq l_s \\ \eta_{sij} + 1, & i = l_s \text{ and } j = l_s \end{cases} \tag{51}$$

Then Eqn. (50) can be written in the more compact form

$$R_s = \sum_{j=1}^{l_s} \eta_{s0j} R_{sj}. \tag{52}$$

Now consider the change ΔR_s in the radius of the sth strand due to Poisson contraction of the wires within the strand. This change will satisfy the relation

$$R_s + \Delta R_s = \sum_{j=1}^{l_s} \eta_{s0j} (1 - \nu \epsilon_{sj}) R_{sj}, \tag{53}$$

where the ϵ_{sj} are the strains in the individual wires, i.e.

$$\Delta R_s = -\nu \sum_{j=1}^{l_s} \eta_{s0j} \epsilon_{sj} R_{sj}. \tag{54}$$

It should be noted that both tension and twisting of a strand give rise to strains ϵ_{sj} in the individual wires of a strand and consequently both modes of loading must be considered when determining the change in strand radius. The fact that the twisting of a strand affects the radius of the strand is one of the features that distinguishes strand behavior from that of a solid wire.

Since the ϵ_{sj} are linear functions of both ϵ_s and $\Delta\tau_s$, and since the ϵ_{sj} equal zero when both ϵ_s and $\Delta\tau_s$ are equal to zero, it follows that

$$\epsilon_{sj} = \frac{\partial\epsilon_{sj}}{\partial\epsilon_s}\epsilon_s + \frac{\partial\epsilon_{sj}}{\partial\Delta\tau_s}\Delta\tau_s, \tag{55}$$

where the partial derivatives $\frac{\partial\epsilon_{sj}}{\partial\epsilon_s}$ and $\frac{\partial\epsilon_{sj}}{\partial\Delta\tau_s}$ can be computed (numerically if necessary) from the previously developed solution for wire strains in a loaded strand:

$$\frac{\partial \epsilon_{sj}}{\partial \epsilon_s} \equiv \left.\frac{\Delta \epsilon_{sj}}{\Delta \epsilon_s}\right|_{\Delta \tau_s = 0} \quad \text{and}$$
$$\frac{\partial \epsilon_{sj}}{\partial \Delta \tau_s} \equiv \left.\frac{\Delta \epsilon_{sj}}{\Delta (\Delta \tau_s)}\right|_{\epsilon_s = 0}. \tag{56}$$

Using Eqn. (55), one can rewrite Eqn. (54) in the form

$$\Delta R_s = \frac{\partial R_s}{\partial \epsilon_s} \epsilon_s + \frac{\partial R_s}{\partial \Delta \tau_s} \Delta \tau_s \tag{57}$$

where

$$\frac{\partial R_s}{\partial \epsilon_s} = -\nu \sum_{j=1}^{l_s} \eta_{s0j} \frac{\partial \epsilon_{sj}}{\partial \epsilon_s} R_{sj} \quad \text{and}$$
$$\frac{\partial R_s}{\partial \Delta \tau_s} = -\nu \sum_{j=1}^{l_s} \eta_{s0j} \frac{\partial \epsilon_{sj}}{\partial \Delta \tau_s} R_{sj} \tag{58}$$

are the *known* derivatives for all strands up to and including the sth one.

Change in strand helix radius

One can now return to Eqn. (45) and note that the change in strand helix radius Δr_s must satisfy the equation

$$r_s + \Delta r_s = \sum_{t=1}^{s} \eta_{0st} (R_s + \Delta R_t), \tag{59}$$

that is, with the aid of Eqn. (57),

$$\Delta r_s = \Delta r_s^p + \eta_{0ss} \frac{\partial R_s}{\partial \epsilon_s} \epsilon_s + \eta_{0ss} \frac{\partial R_s}{\partial \Delta \tau_s} \Delta \tau_s, \tag{60}$$

where Δr_s^p denotes that portion of Δr_s that is due solely to the known changes in strand radii of strands *underlying* the sth one:

$$\Delta r_s^p \equiv \sum_{t=1}^{s-1} \eta_{0st} \left(\frac{\partial R_t}{\partial \epsilon_t} \epsilon_t + \frac{\partial R_t}{\partial \Delta \tau_t} \Delta \tau_t \right). \tag{61}$$

Equation (60) will now be transformed so that the variables describing the strand's deformation will be the same as those used in Eqns. (48) and (49). This is done by recalling a fundamental relation—similar to Eqn. (24)—that gives the change in helix radius Δr_s as a function of the change in twist $\Delta \tau_s$ and the change in curvature $\Delta \kappa_s'$. Performing this substitution, multiplying both sides of the resulting equation by $\cot^2 \alpha_s$, and introducing the definitions

$$C_s^{\epsilon} \equiv \eta_{0ss} \frac{\partial R_s}{\partial \epsilon_s}, \quad C_s^{\Delta \tau} \equiv \eta_{0ss} \frac{\partial R_s}{\partial \Delta \tau_s}, \tag{62}$$

one finds that

$$\left[-2 \cot \alpha_s - \frac{\cot^2 \alpha_s}{r_s} C_s^{\Delta \tau}\right] (R_s \Delta \tau_s) + (1 - \cot^2 \alpha_s) (r_s \Delta \kappa_s') - \frac{\cot^2 \alpha_s}{r_s} C_s^{\epsilon} \epsilon_s = \frac{\cot^2 \alpha_s}{r_s} \Delta r_s^p. \tag{63}$$

Solution for the generalized strand strains

Three independent linear equations have now been derived for the generalized strains ϵ_s, $\Delta \tau_s$

and $\Delta\kappa_s'$ associated with the sth strand: Eqns. (48) and (49), which ensure that the strand will deform in a manner compatible with that of the rope, and Eqn. (63), which ensures that the various layers of strands will remain in contact with each other in the deformed configuration of the rope. The three equations, when collected together, are:

$$\begin{aligned} \cot\alpha_s\, r_s\, \Delta\tau_s \quad &- 1\, r_s\, \Delta\kappa_s' \quad + 1\, \epsilon_s = \epsilon \\ 1\, r_s\, \Delta\tau_s \quad &+ \cot\alpha_s\, r_s\, \Delta\kappa_s' \quad + \cot\alpha_s\, \epsilon_s = r_s\, \Delta\tau \\ [-2\cot\alpha_s - (\cot^2\alpha_s/r_s)\, C_s^{\Delta\tau}]\, r_s\, \Delta\tau_s &+ (1-\cot^2\alpha_s)\, r_s\, \Delta\kappa_s' - (\cot^2\alpha_s/r_s)\, C_s^{\epsilon}\, \epsilon_s = (\cot\alpha_s/r_s)\, \Delta r_s^p \end{aligned} \tag{64}$$

These equations governing strands in a rope are nearly identical in form to Eqns. (40), which govern the individual wires in a strand. In fact, if one merely rewrites the third of Eqns. (40) as

$$[-2\cot\alpha_{si} - \frac{\cot^2\alpha_{si}}{r_{si}}\, C_{si}^{\Delta\tau}]\, (r_{si}\, \Delta\tau_{si}) + (1-\cot^2\alpha_{si})\, (r_{si}\, \Delta\kappa_{si}') + \frac{\cot^2\alpha_{si}}{r_{si}}\, C_{si}^{\epsilon}\, \epsilon_{si} = \frac{\cot^2\alpha_{si}}{r_{si}}\, \Delta r_{si}^p$$

and sets

$$C_{si}^{\Delta\tau} = 0 \quad \text{and} \quad C_{si}^{\epsilon} = -\nu\, \eta_{sii},$$

then the forms of Eqns. (40) and of Eqns. (64) *will* be identical. As a practical matter, this means that a computer subroutine written to solve one of these sets of equations can be used without modification to solve the other.

Generalized forces on the rope

Having solved Eqns. (64) for each strand in the rope, one can use Eqns. (42-44) to determine the tensile force T_s, the twisting moment H_s, and the bending moment G_s' acting on each strand. Equilibrium equations identical in form to Eqns. (10) and (13) can then be used to determine the shearing force N_s' and the distributed normal load X_s acting on each strand:

$$\begin{aligned} N_s' &= H_s\, \kappa_s' - G_s'\, \tau_s \quad \text{and} \\ X_s &= N_s'\, \tau_s - T_s\, \kappa_s', \end{aligned} \tag{65}$$

where τ_s and κ_s' are the twist and curvature of the sth strand, given by Eqns. (47).

The total force T and twisting moment H sustained by the rope can now be computed by resolving in the axial direction of the rope the forces and moments acting on individual strands. The process is analogous to the procedure used for each strand, in terms of the wires within strands—see Eqns. (42) and (43)—and the results are:

$$T = \sum_{s=1}^{l} m_s\, (T_s \sin\alpha_s + N_s' \cos\alpha_s) \tag{66}$$

and

$$H = \sum_{s=1}^{l} m_s\, [(H_s \sin\alpha_s + G_s' \cos\alpha_s) + r_s\, (T_s \cos\alpha_s - N_s' \sin\alpha_s)], \tag{67}$$

where m_s is the number of strands in the sth layer of strands, and l is the number of strand layers.

Concluding remarks

A general procedure has been outlined for determining the axial, bending, shear, torsional, and distributed normal loads on each wire, and on each strand of wires, in a rope containing an arbitrary number of layers of strands, each strand containing an arbitrary number of layers of wires. Poisson contraction of individual wires is accounted for. The rope may be given an arbitrary axial strain ϵ and an arbitrary twist $\Delta\tau$.

The procedure has been developed with the following solution technique in mind: first, one specifies the construction of a given rope according to a relatively simple numbering scheme for strands and for wires within strands; then, starting with the innermost strand, one determines the generalized strand strains required to match the specified rope strains ϵ and $\Delta\tau$, at the same time allowing for individual Poisson contraction of wires within the strand and the resulting "Poisson contraction" of the strand itself. All equations are linear, and the maximum number of simultaneous equations to be solved at *any* stage of the procedure is three.

An ANSI 77 Fortran computer program has been written to analyze the stresses in wire rope loaded axially and bent over a sheave. The program is listed in the Appendix to this Report and contains a subroutine ROPE that is based entirely on the theoretical analysis developed up to this point. An analysis of the bending of ropes over sheaves, and further details concerning the entire computer program listed in the Appendix, will be presented subsequently.

4. Analysis of loaded rope bent over a sheave

The preceding analysis has dealt with a rope that remains straight in its loaded configuration. A practical example of such a rope is a boom pendant rope that is subjected principally to an axial load. Most rope, however, is cyclically subjected not only to axial loads but also to additional loads that are induced when the rope is wound around a drum or passed over a sheave, as illustrated in Fig. 4. An example of this loading arrangement would be the drum-and-sheave hoisting system commonly used in deep-shaft mining.

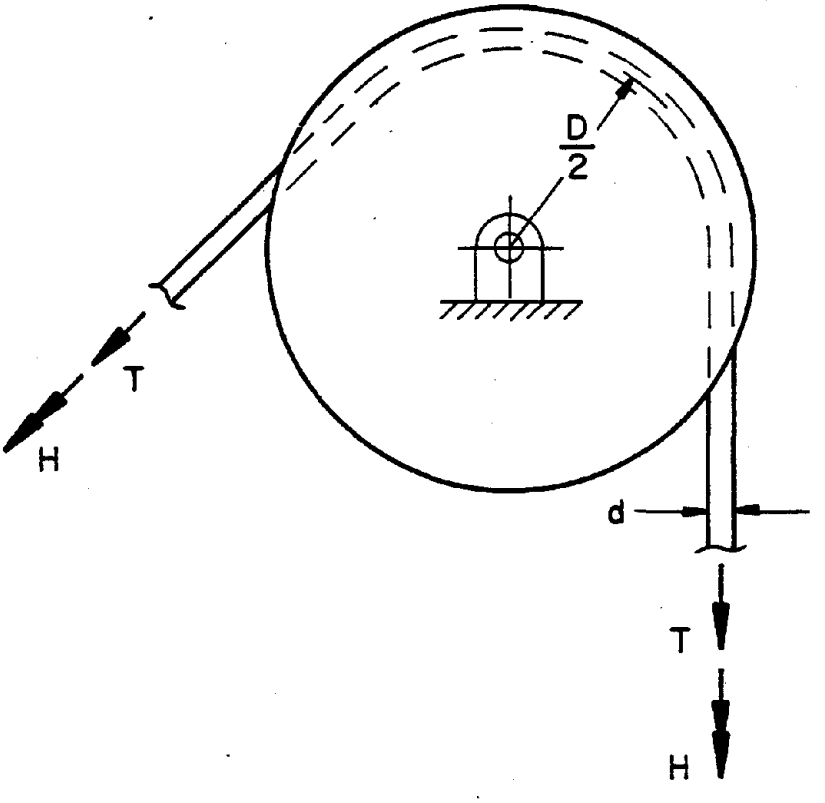

Fig. 4. Wire rope passed over a sheave and loaded axially.

It must be recognized that an "exact" analysis of the deformation of a loaded wire rope passed over a sheave would be exceedingly complex, especially if an attempt were made to analyze in detail the transition regions where the rope enters and leaves the sheave. An approximate method of analysis will be employed here.

It will be assumed that the stresses in the individual wires of an axially loaded rope bent around a sheave consist of the stresses that would exist in the same axially loaded rope if it were straight, *plus* the bending stresses that would be induced in the individual preformed wires, each in the shape of a double helix, bent elastically into the rope-centerline curvature that is imposed by the sheave. Except perhaps for questions concerning the redistribution of wire loads within the transition regions, one can argue that this assumption is a reasonable one for well-lubricated wire rope.

Wire stresses in a straight rope

Consider first the stresses in the wires of a *straight* wire rope subjected to an axial tension T and an axial twisting moment H. To simplify the discussion, it will be assumed that the rope is prevented from twisting *everywhere* along its length, i.e.

$$\Delta\tau = 0,$$

in which case the twisting moment H becomes proportional everywhere to the tension T. This condition is imposed, at least approximately, by most methods of rope termination after a rope has been placed in service.

The only *wire* stresses that will be considered here are those stresses that are induced by the axial force T_s, the twisting moment H_s, and the bending moment G_s' applied to the *strand* in which a given wire resides.

Of these three strand loads, the first two—T_s and H_s—are mutually coupled and together they give rise to five types of wire load: a tension T_{si}, a bending moment G_{si}', a twisting moment H_{si}, a transverse shear N_{si}', and a resultant distributed load X_{si}. The tension T_{si} gives rise to a uniform stress

$$\frac{T_{si}}{\pi R_{si}^2}$$

over the wire cross section, while the bending moment G_{si}' gives rise to a linearly varying stress distribution having extreme (tensile and compressive) stress values of

$$\pm \frac{G_{si}' R_{si}}{\pi R_{si}^4/4}.$$

The stresses due to the torsion H_{si} and shear N_{si}' are shearing stresses acting tangent to the plane of the cross section; they are relatively small in magnitude and they are not directly additive to the normal stresses produced by the tension and bending. For simplicity, these shearing stresses will be neglected. The distributed load X_{si} is related to line and point contact with neighboring wires. The subject of localized stresses due to contact is an important but complicated one [30] requiring further analysis, but no attempt will be made to analyze contact stresses here.

The third strand load, G_s', gives rise to additional wire bending stresses that must be superimposed on the previously considered wire stresses induced by T_s and H_s. Recall that G_s' is proportional to the change in strand curvature $\Delta\kappa_s'$ from Eqn. (44). The corresponding maximum bending stresses are given approximately† by

†In Costello's paper [26] on the flexure of a helical wire, it is shown that the wire sustains not only a bending moment about both the normal and binormal axes in the cross section, but also a twisting moment about the wire centerline. In the case of the helical wires in a rope strand, however, the helix angle is very close to $\pi/2$ and it follows from Eqn. (19) of [26] that the dominant stresses are those due to bending.

$$\pm E \frac{\sin\alpha_{si}}{1+\frac{1}{2}\nu\cos^2\alpha_{si}} R_{si}\,\Delta\kappa_s',$$

where R_{si} and α_{si} are the *wire* radius and helix angle (within the strand), respectively. It should be recognized that the axis about which these additional wire bending stresses are developed is the binormal axis of the *strand,* whereas the axis about which the G_{si}'-produced bending stresses are developed is the binormal axis of the individual *wire.* Generally these two axes do not coincide, but within every lay length of wires within a strand there will be one wire for which the two types of bending will combine detrimentally; consequently, for purposes of computing the *maximum* stresses in the wire cross section, the two bending stress contributions will simply be added algebraically.

The principal effect, then, of applying an axial load T to a straight rope is to produce maximum tensile stresses σ_{si}^{T} of magnitude

$$\sigma_{si}^{T} = \frac{1}{\pi R_{si}^2} T_{si} + \frac{R_{si}}{\pi R_{si}^4/4} |\,G_{si}'\,| + \frac{E R_{si}\sin\alpha_{si}}{1+\frac{1}{2}\nu\cos^2\alpha_{si}} |\,\Delta\kappa_s'\,| \tag{68}$$

in the individual wires of the rope, where absolute values of G_{si}' and $\Delta\kappa_s'$ have been taken to ensure that, regardless of the signs of the various G_{si}''s and $\Delta\kappa_s'$'s, it will be the maximum *tensile* values of the associated bending distributions that will be added to the uniform tensile stresses induced by the wire tensions T_{si}, when individual wire-stress maxima are determined.

As it turns out, the stresses σ_{si}^{T} are generally larger in magnitude than the *nominal* stress

$$\sigma_{\text{nom}} \equiv \frac{T}{A}, \tag{69}$$

which is theoretically the value that all wires in a straight rope would have if all the wires were straightened out and loaded in parallel; in Eqn. (69), T is the tensile load applied to the rope and A is the "metallic area" given by

$$A \equiv \sum_{s=1}^{l} m_s \sum_{i=1}^{l_s} m_{si}\,\pi R_{si}^2, \tag{70}$$

i.e. A is just the sum of all the *circular* cross sectional areas of the wires. The nominal stress is a quantity that can be calculated easily for any rope; it is used in the presentation of subsequent results.

Wire stresses due to bending over a sheave

In keeping with the approximation mentioned at the beginning of this section, one considers the stresses that would be induced in a wire of radius R_{si}, preformed into the shape of a "helix on a helix", and bent around a sheave or drum of diameter D. The radius of curvature of the rope centerline is equal to $D/2$, and consequently [26] the maximum change of normal curvature of the sth strand, $\Delta\kappa_s$, is given by

$$\Delta\kappa_s = \frac{\sin\alpha_s}{1+\frac{1}{2}\nu_s\cos^2\alpha_s}\,\frac{1}{D/2} \tag{71}$$

where ν_s is a "strand Poisson's ratio." The term $\frac{1}{2}\nu_s\cos^2\alpha_s$ has a magnitude much smaller than unity and with negligible error, ν_s may be set equal to the Poisson's ratio of the wire material, ν. A wire within the sth strand, in turn, will suffer a maximum change in normal curvature, $\Delta\kappa_{si}$, that is related to the strand's maximum change in normal curvature by the relation

$$\Delta\kappa_{si} = \frac{\sin\alpha_{si}}{1+\frac{1}{2}\nu\cos^2\alpha_{si}}\,\Delta\kappa_s. \tag{72}$$

It follows that the maximum wire stress due to pure bending, σ_{si}^{B}, induced in the preformed wire is given by

$$\sigma_{si}^{B} = E R_{si} \frac{\sin\alpha_s}{1+\frac{1}{2}\nu\cos^2\alpha_s} \frac{\sin\alpha_{si}}{1+\frac{1}{2}\nu\cos^2\alpha_{si}} \frac{1}{D/2}, \tag{73}$$

where the superscript B denotes "bending due to sheave curvature." The magnitudes of the factors $\frac{\sin\alpha_s}{1+\frac{1}{2}\nu\cos^2\alpha_s}$ and $\frac{\sin\alpha_{si}}{1+\frac{1}{2}\nu\cos^2\alpha_{si}}$ are generally between 0.9 and unity for typical strands and typical wires within strands.

Equation (73) can be rewritten in a more usable form by introducing the rope diameter d, which is simply

$$d = 2R,$$

R being the rope radius defined by Eqn. (46). The result is that

$$\sigma_{si}^{B} = E \frac{R_{si}}{R} \frac{\sin\alpha_s}{1+\frac{1}{2}\nu\cos^2\alpha_s} \frac{\sin\alpha_{si}}{1+\frac{1}{2}\nu\cos^2\alpha_{si}} \left(\frac{d}{D}\right), \tag{74}$$

where the appearance of the factor $\frac{R_{si}}{R}$ suggests that for a given D/d ratio, the bending stresses due to sheave curvature can be reduced by using wire rope containing many fine wires, as is generally well known.

Combined stresses due to axial loading and bending over a sheave

Substitution of the stresses due to the axial loading T (Eqn. (68)) and those due to bending of the rope over a sheave of diameter D (Eqn. (74)) give an expression of the form

$$\frac{\sigma_{si}}{\sigma_{\text{nom}}} = \frac{\sigma_{si}^{T}}{\sigma_{\text{nom}}} + \frac{\sigma_{si}^{B}}{\sigma_{\text{nom}}} = z_{si}^{T} + z_{si}^{B}\left(\frac{D}{d}\cdot\frac{\sigma_{\text{nom}}}{E}\right)^{-1}, \tag{75}$$

where the nominal stress σ_{nom} (Eqn. (69)) has been introduced as a normalizing factor, and where

$$z_{si}^{T} \equiv \frac{\sigma_{si}^{T}}{\sigma_{\text{nom}}} \quad \text{and} \quad z_{si}^{B} \equiv \frac{R_{si}}{R} \frac{\sin\alpha_s}{1+\frac{1}{2}\nu\cos^2\alpha_s} \frac{\sin\alpha_{si}}{1+\frac{1}{2}\nu\cos^2\alpha_{si}}. \tag{76}$$

The important observation to be made is that both z_{si}^{T} and z_{si}^{B} are completely determined by an analysis of a *straight* rope. The parameter $\frac{D}{d}\cdot\frac{\sigma_{\text{nom}}}{E}$, on the other hand, involves the D/d ratio and is easily evaluated for a given sheave diameter, rope diameter, nominal rope stress, and rope material.

Results for selected rope constructions

Equation (75) has been used to determine the maximum wire stresses in a solid rod, a 1x7 strand, a 7x7 rope, a 6x19 Seale fiber-core rope, and a 6x19 Seale IWRC bent over a sheave and loaded axially, and the results are shown in Figs. 5 through 9, respectively. Results for ropes of 6x25 filler-wire construction, both with a fiber core and with an IWRC, are presented in Figs. 10 and 11, respectively. In each of these figures, there are as many curves as there are wire types in the given cross section. The abscissa scale has been chosen so that values of $\frac{D}{d}\cdot\frac{\sigma_{\text{nom}}}{E}$ in the range

$$0 < \frac{D}{d}\cdot\frac{\sigma_{\text{nom}}}{E} \leqslant 0.3$$

are considered. This range is typical of conditions commonly encountered in hoisting operations: recommended values of D/d for headframe sheaves lie between about 60 and about 100 (depending on the rope diameter, the rope construction, and the type of application [38]), and σ_{nom} is typically about

0.003 times the modulus of elasticity E of the wire material (at least for steel rope, with the usual factors of safety applied).

The results in any of these figures can be interpreted as follows. First, a value of σ_{nom} is computed from Eqn. (69), with T set equal to the load in the rope at the sheave. Then, with a given D/d ratio, and a known value of E for the wire material, one computes a value for $\frac{D}{d}\cdot\frac{\sigma_{nom}}{E}$ and examines the curves above the corresponding point along the abscissa, to determine which wire in the cross section has the greatest stress. For example, if a given Seale 6x19 IWRC rope has a metallic area of 1.00 in.^{2} carries a load of 50 tons at the sheave, then from Eqn. (69),

$$\sigma_{nom} = \frac{T}{A} = \frac{50 \times 2{,}000\,\text{lb.}}{1.00\,\text{in.}^2} = 100{,}000\ \text{lb./in.}^2.$$

Then, if the D/d ratio is 20 and the rope is made of steel, the corresponding value of $\frac{D}{d}\cdot\frac{\sigma_{nom}}{E}$ is

$$\frac{D}{d}\cdot\frac{\sigma_{nom}}{E} = 20 \times \frac{100{,}000\,\text{lb./in.}^2}{30\times10^6\,\text{lb./in.}^2} = 0.067,$$

and from Fig. 9 it is determined that the maximum stress occurs in the center wire of the outer Seale strand and has a value of about 2.47 times the nominal stress or about 247,000 lb./in.^{2}. If the D/d ratio in this example were increased from 20 to, say, 90, then $\frac{D}{d}\cdot\frac{\sigma_{nom}}{E}$ would be equal to 0.30 and the critical wire would no longer be the Seale-strand center wire but rather the center wire in the strand core of the IWRC, which would then be subjected to a maximum stress of about 1.59 times the nominal stress, or about 159,000 lb./in.^{2}.

Note that in the example of the Seale IWRC, regardless of the value of the D/d ratio, the maximum stresses occur in wires that are *not* visible from the outside. Visual inspection for wire failure would be particularly prone to error for ropes "helped" by large D/d ratios, since in this case it is the innermost wires of the core, and of the Seale strand, that are subjected to the largest stresses and which would presumably break first during cyclic loading.

It is interesting to observe that the maximum stresses are generally reduced as the number of wires in a rope is increased from 1 (Fig. 5) to 7 (Fig. 6), etc., up to 163 for the Seale IWRC (Fig. 9). A curious but somewhat less obvious result is that, regardless of the type of rope, it appears difficult to reduce the maximum stresses much below about $1.6\sigma_{nom}$ even if the D/d ratio is raised to an extremely large value. There appear to be two different mechanisms that account for this second observation, namely that in a *straight* rope, (1) strand center wires are subjected to larger-than-average *axial* strains, whereas (2) strand outer wires are subjected to larger-than-average *bending* strains. It must be remembered that throughout this discussion, it has been assumed that the rope is prevented from twisting; if this condition is not met, then still other mechanisms—such as the *twist* of individual wires—may become important.

Results for the filler-wire constructions (Figs. 10 and 11) indicate that the stresses among the various wires are remarkably uniform, with the exception of the filler wire itself, which is notably understressed. Since the filler wire is very small, it accounts for a small fraction of the total rope weight; it would therefore seem that the understressing of the filler wire is tolerable from the point of view of optimum rope performance.

(Next section begins after the following figures)

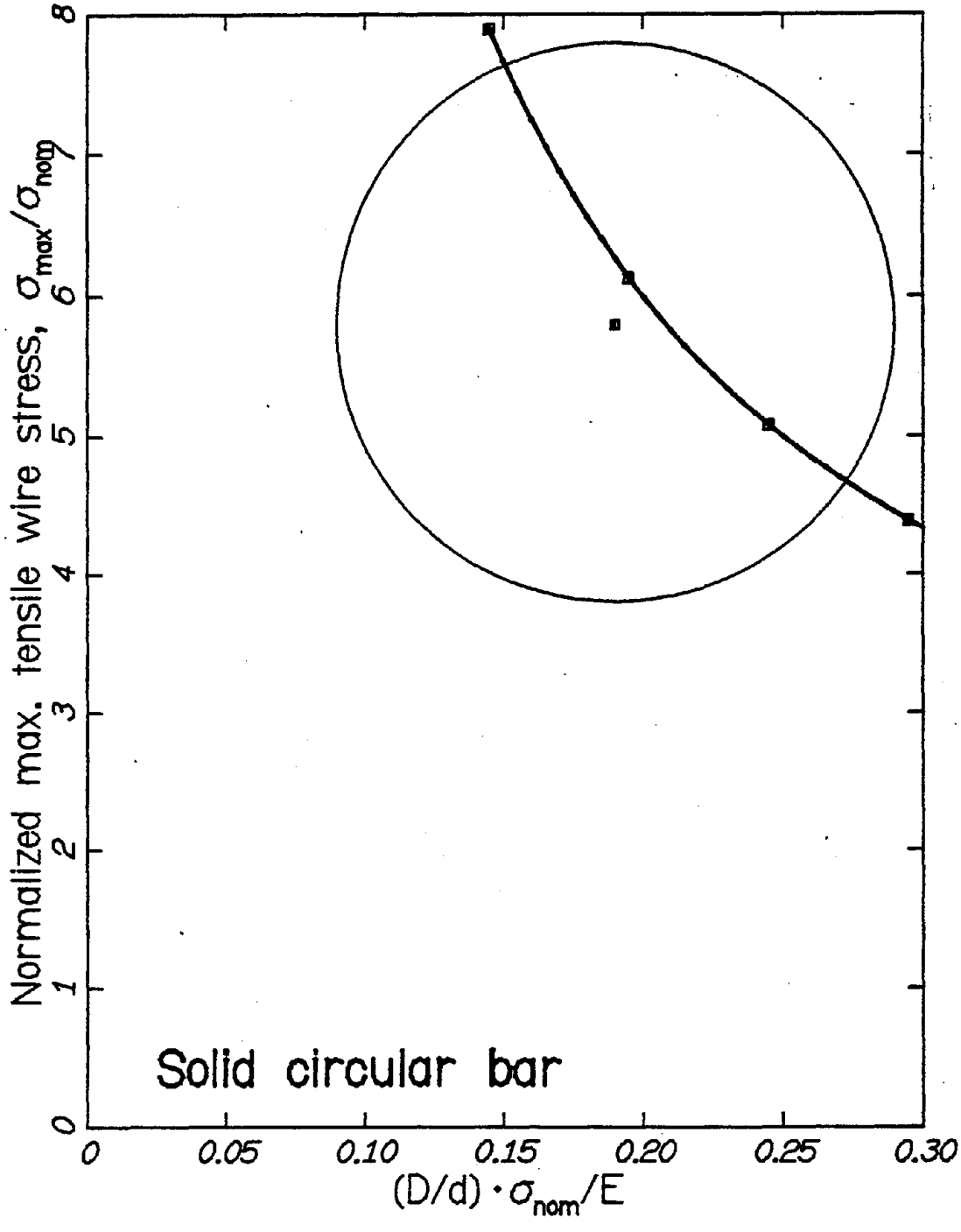

Fig. 5. Maximum tensile stress in a solid rod bent over a sheave.

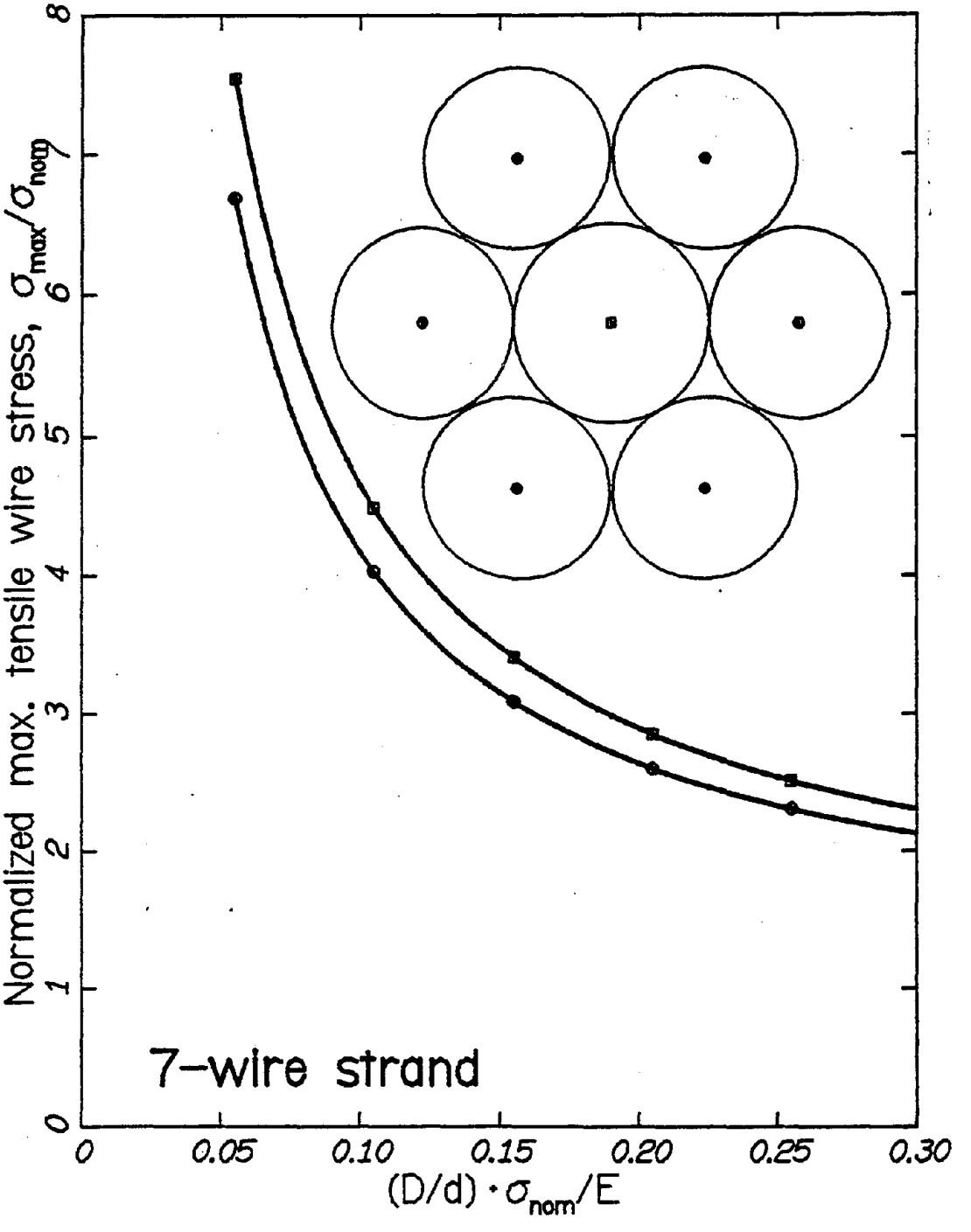

Fig. 6. Maximum tensile stresses in a 1x7 strand bent over a sheave.

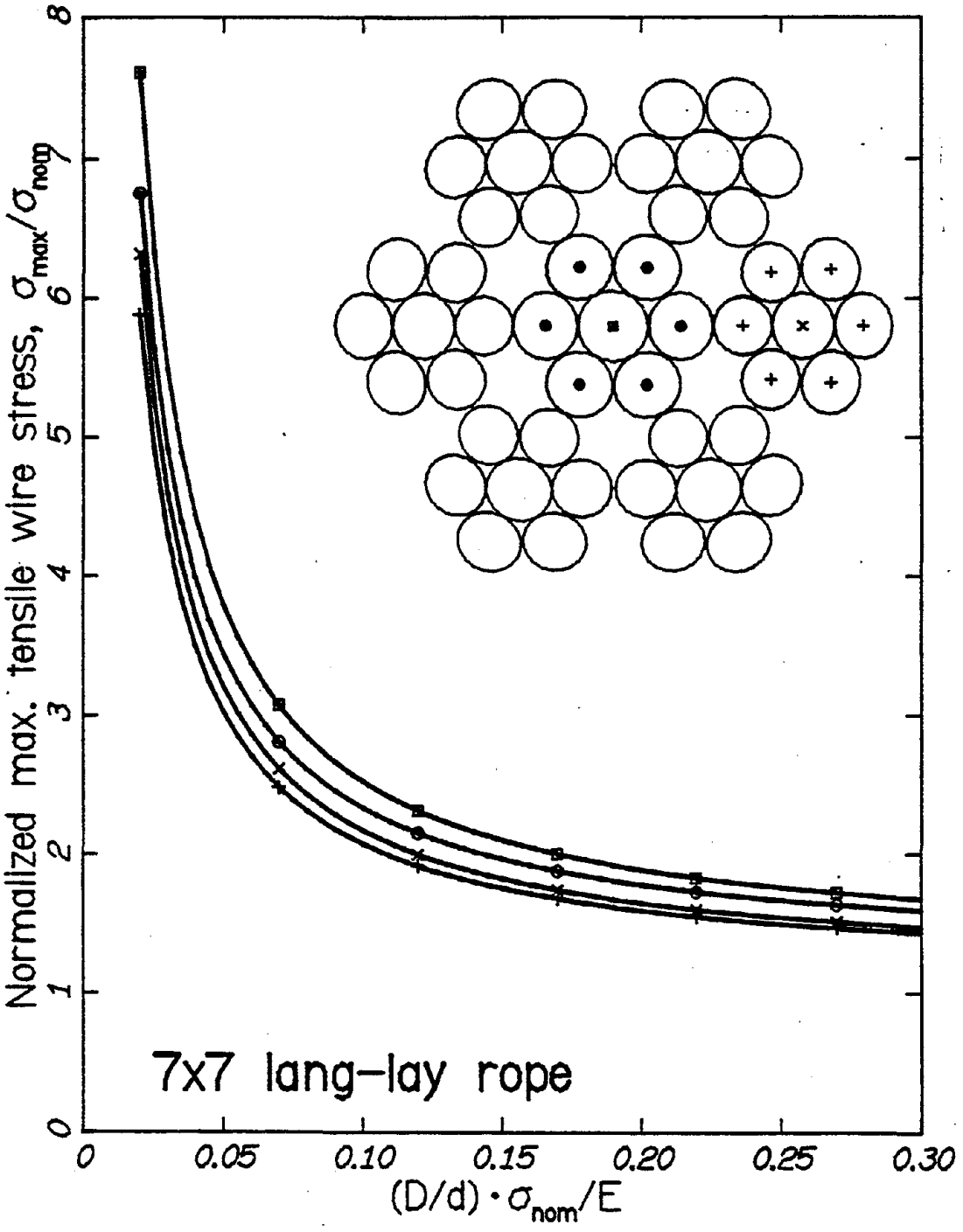

Fig. 7. Maximum tensile stresses in a 7x7 wire rope bent over a sheave.

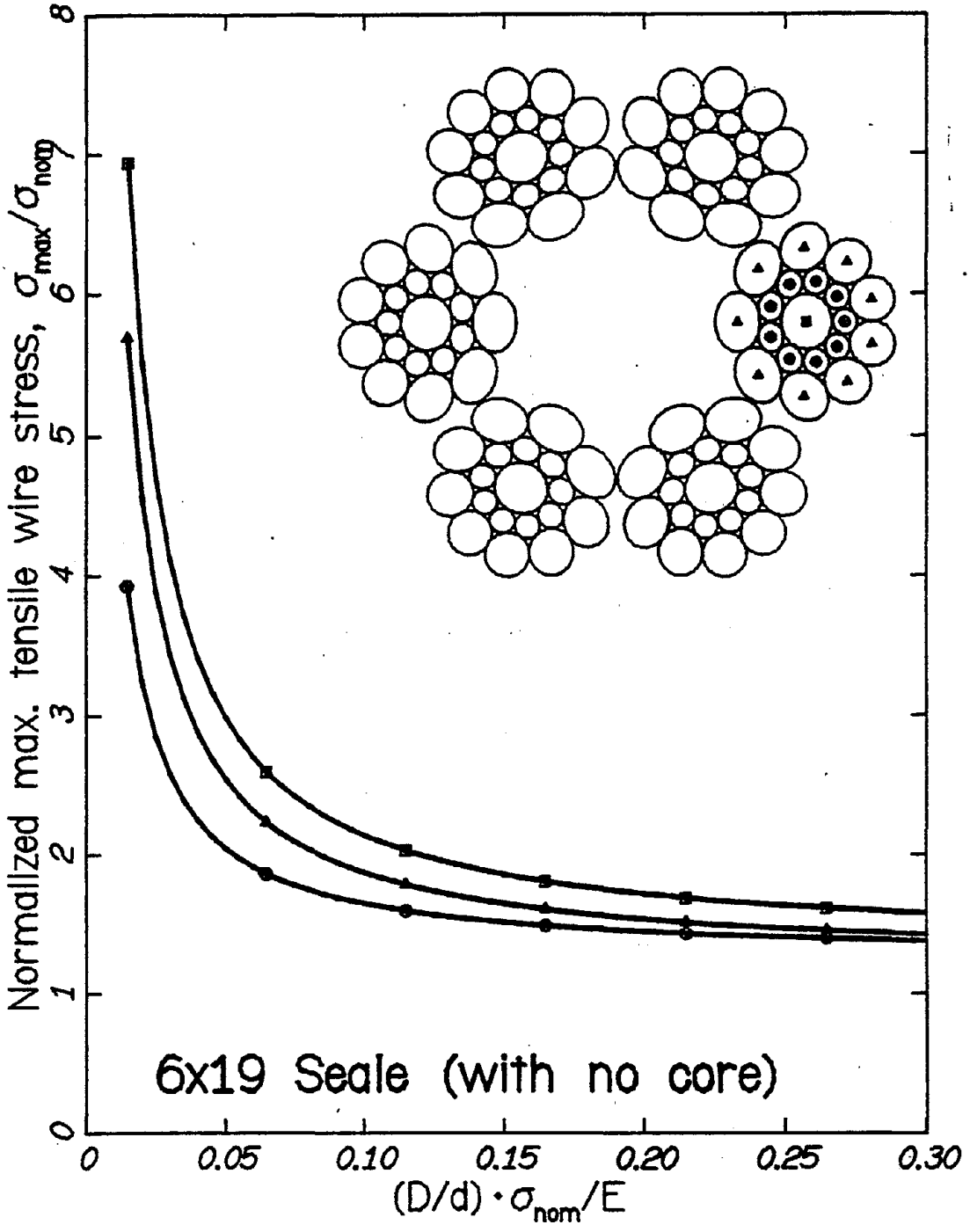

Fig. 8. Maximum tensile stresses in a 6x19 Seale bent over a sheave.

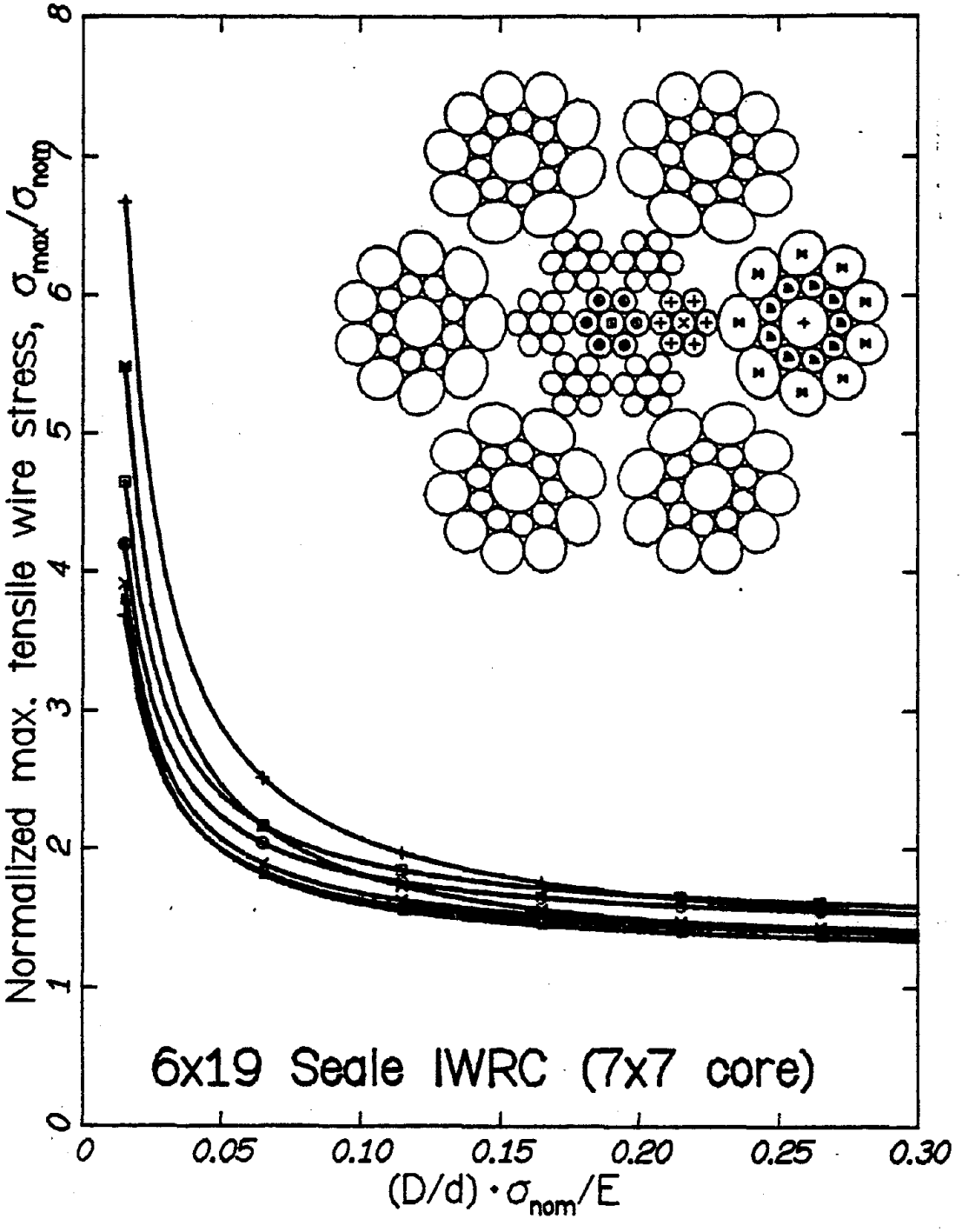

Fig. 9. Maximum tensile stresses in a 6x19 Seale IWRC bent over a sheave.

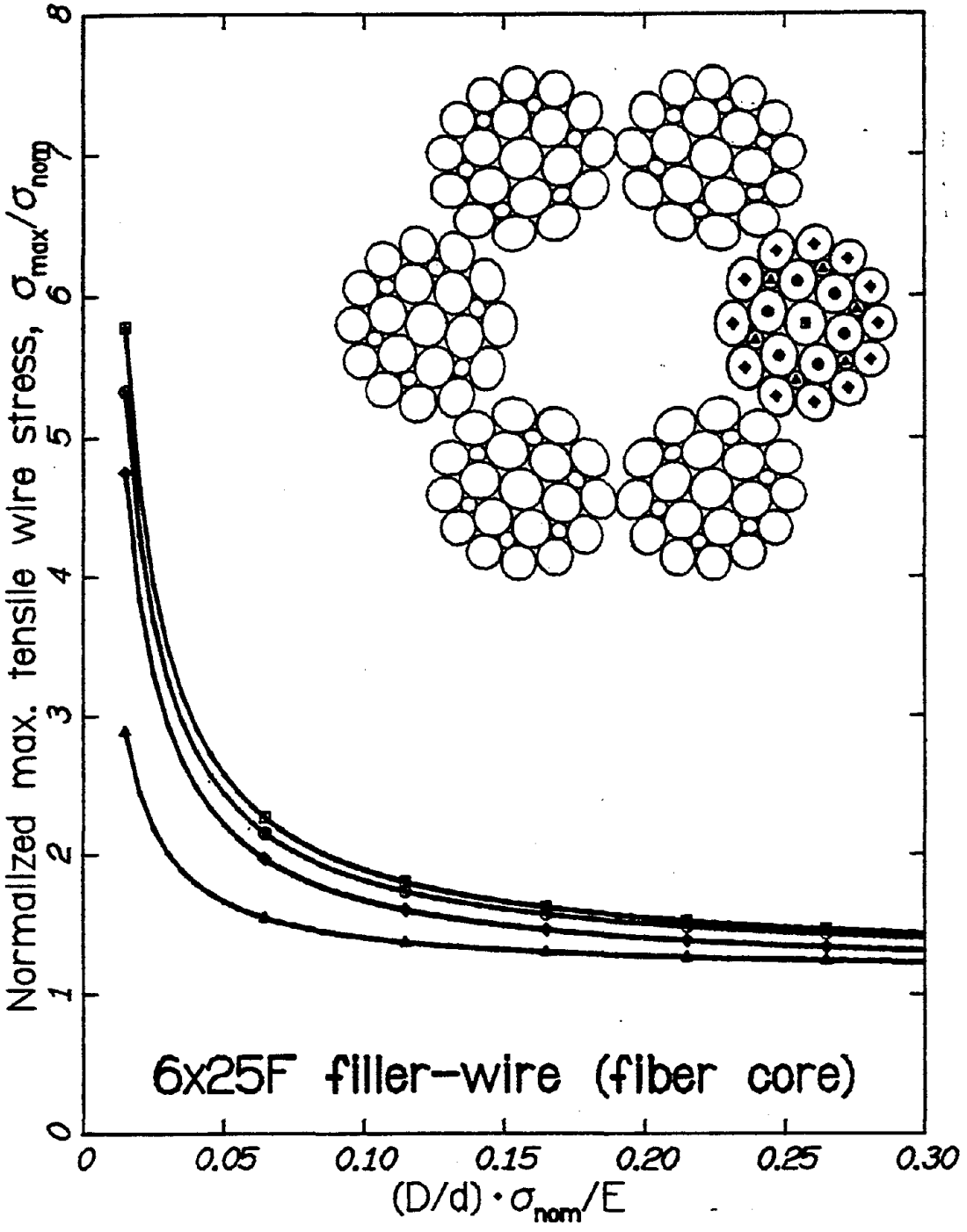

Fig. 10. Maximum tensile stresses in a 6x25 filler-wire rope bent over a sheave.

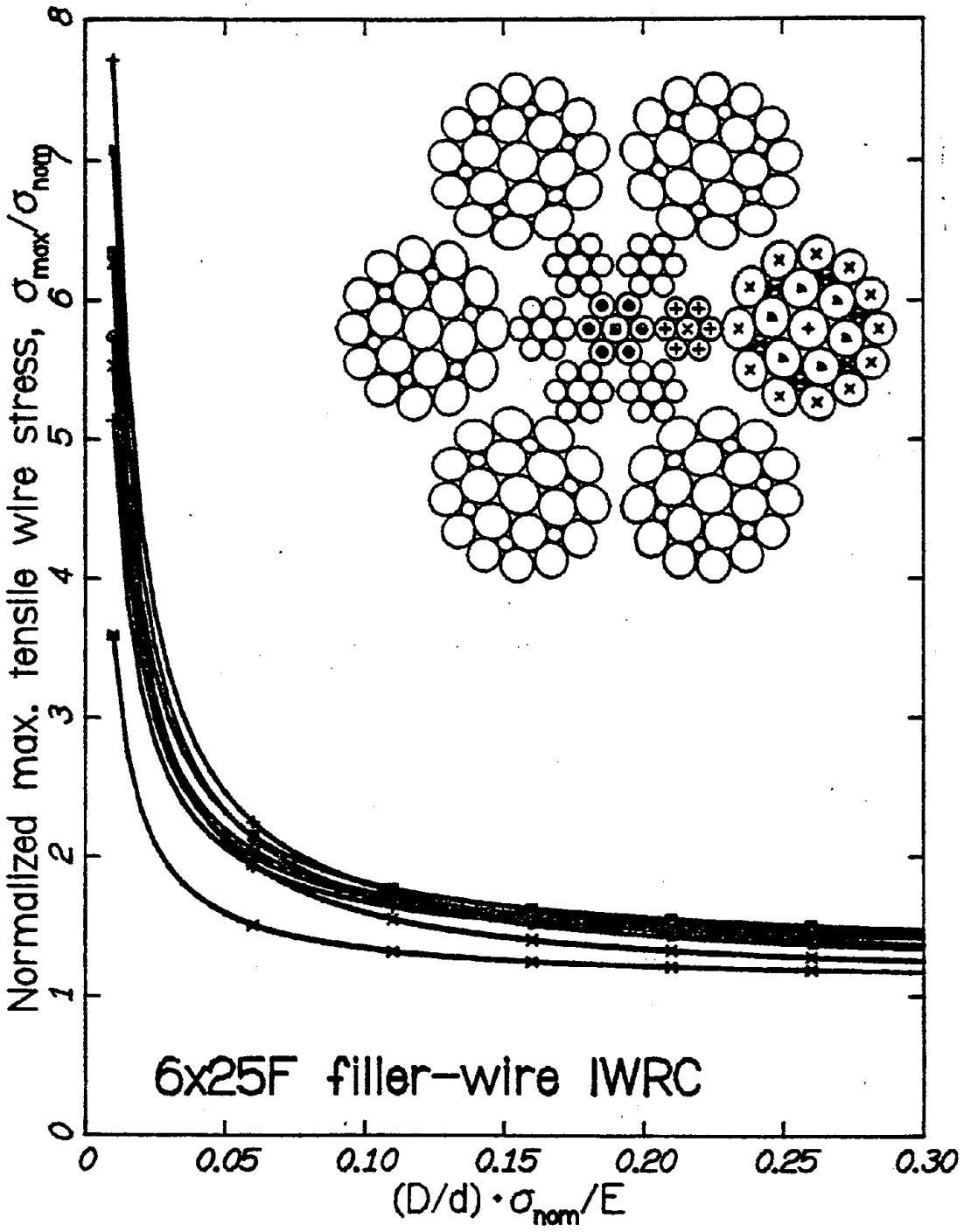

Fig. 11. Maximum tensile stresses in a 6x25 IWRC filler-wire rope bent over a sheave.

5. Programming considerations

An ANSI 77 Fortran computer program has been written to generate graphs like the ones shown in Figs. 5 through 11, and to print out other intermediate data, such as the generalized wire strains and forces, the generalized strand strains and forces, and the generalized rope strains and forces, for a rope of arbitrary cross section. The program is listed in the Appendix to this report, along with a sample output for the Seale 6x19 IWRC that has been used throughout this document as a particular example. As mentioned in the Notes preceding the source listing, every attempt has been made to follow the notation used in the theoretical development contained in this report. For this reason, it is felt that an extensive "user's manual" for the program is unnecessary; the principal effort required in using the program for rope constructions other than those considered in this report is the writing of an appropriate subroutine GEOM for each rope of interest to the user.

Program organization

The main entry point is a program called SHEAVE, which is written in accordance with the theory presented in §II.4 of this report. Program SHEAVE makes calls to subroutines, which in turn may make further subroutine calls, as follows:

```
SHEAVE
    > GEOM
    & ROPE
        > STRAND
            > DEFORM
                > SOL3B3
        & DEFORM
            > SOL3B3
    & Plotting routines
    & XSECTN
        > CIRCLE
            > Plotting routines
        & Plotting routines
```

where the symbol > means "which calls", and the symbol & means "and calls". Subroutine GEOM is the user-supplied subroutine defining the number of strand layers, the number of wires in each layer, the wire radii, etc., according to the rules given in §§II.2-3 of this report. Further comments on subroutine GEOM are given subsequently. Subroutine ROPE is based on the theory of §II.3; subroutine STRAND is based on the theory of §II.2. Both STRAND and ROPE make use of subroutine DEFORM, whose only function is to set up three simultaneous equations of the type (40) or (64), respectively, and pass them to SOL3B3, which solves the equations by Cramer's rule.

Program SHEAVE produces printed output—a sample of which is given in the Appendix—and also plotter output, by means of the "Plotter routines", namely, PLOTS, PLOT, NEWPEN, LINE, SYMBOL, and AXIS. Documentation for the plotter routines is furnished by the manufacturer of the user's plotter; if the user does not have a plotter, the user should "comment out" the calls to the plotter routines or create a dummy subroutine with the names of these routines as entry points.

Subroutine GEOM

When the program was being written, several types of data-input schemes were considered, including BLOCK DATA subprograms, SUBROUTINE subprograms, and READ statements in the main procedure. Of these, the SUBROUTINE subprogram method was chosen because it allows the

user to code *executable* statements in his "input file."

The subroutine begins with the SUBROUTINE statement, followed by a PARAMETER statement that can be changed, if the maximum number, K, of wire layers within a strand (usually 2 or 3), or the maximum number of strand layers in the rope (usually 3), *exceeds* the number 3:

```
      SUBROUTINE     GEOM
      PARAMETER      (PI=3.14159265, K=3)
```

Note: if it is necessary to raise K to a higher value (as would be the case for a 6x25 filler-wire construction, for example), then the value of K must be raised in *all* program units that contain this parameter. On the other hand, it is not necessary to decrease K if a smaller value of K would also suffice. The following declarations are common to most of the program units and should appear exactly as shown:

```
      REAL           ALPHA(K,0:K),  BIGR(0:K,0:K),  ETA(0:K,0:K,K),
     &               EPS(0:K,0:K),  DTAU(0:K,0:K),  DKAP(0:K,0:K),
     &               DRDEPS(K),     DRDTAU(K),
     &               NU, SOL(3)
      INTEGER        S, T, M(K,0:K), LAYERS(0:K)
      COMMON /VAR/   ALPHA, BIGR, ETA, EPS, DTAU, DKAP,
     &               DRDEPS, DRDTAU, NU, M, LAYERS
      REAL           BIGT(0:K,0:K), GPRIME(0:K,0:K),
     &               BIGH(0:K,0:K), NPRIME(0:K,0:K),
     &               KAP(0:K,0:K),  TAU(0:K,0:K),
     &               R(0:K,0:K),    E,
     &               OFFANG(K,0:K)
      COMMON /VAR/   BIGT, GPRIME, BIGH, NPRIME,
     &               KAP, TAU, R, E, OFFANG
      CHARACTER*60   DESC
      COMMON /CVAR/  DESC
```

Now that all variables have been typed, dimensioned, and placed in labelled common blocks, values can be assigned using either DATA statements or assignment statements, as required.

As an example, consider a right-lay, regular-lay, 6x19 Seale rope *without* an independent-wire-rope core.† This rope is shown in Fig. 8 and again in Fig. 12, this time with the s,i designations of the various wires. This rope differs from the Seale IWRC in that the number of strand layers has been reduced from 3 to 1; also, the formula for determining the helix radius of the Seale strands within the rope is not as straightforward as it was for the Seale IWRC. Pertinent preliminary data are contained in the statement

```
      DATA           DESC /'6X19 SEALE -- NO CORE'/,
     &               E    /30.E+6/,
     &               NU   /0.29/
```

where it has been assumed that the rope is made of steel. The rope has one layer of strands, i.e.

```
      DATA           LAYERS(0) /1/
```

and within this layer there are 6 strands, each making an angle of 70.24° measured counter-clockwise

†The rope can be assumed to have either no core at all, or a fiber core that keeps the strands from touching each other. In either case the resultant distributed line load acting on a given strand will be directed radially.

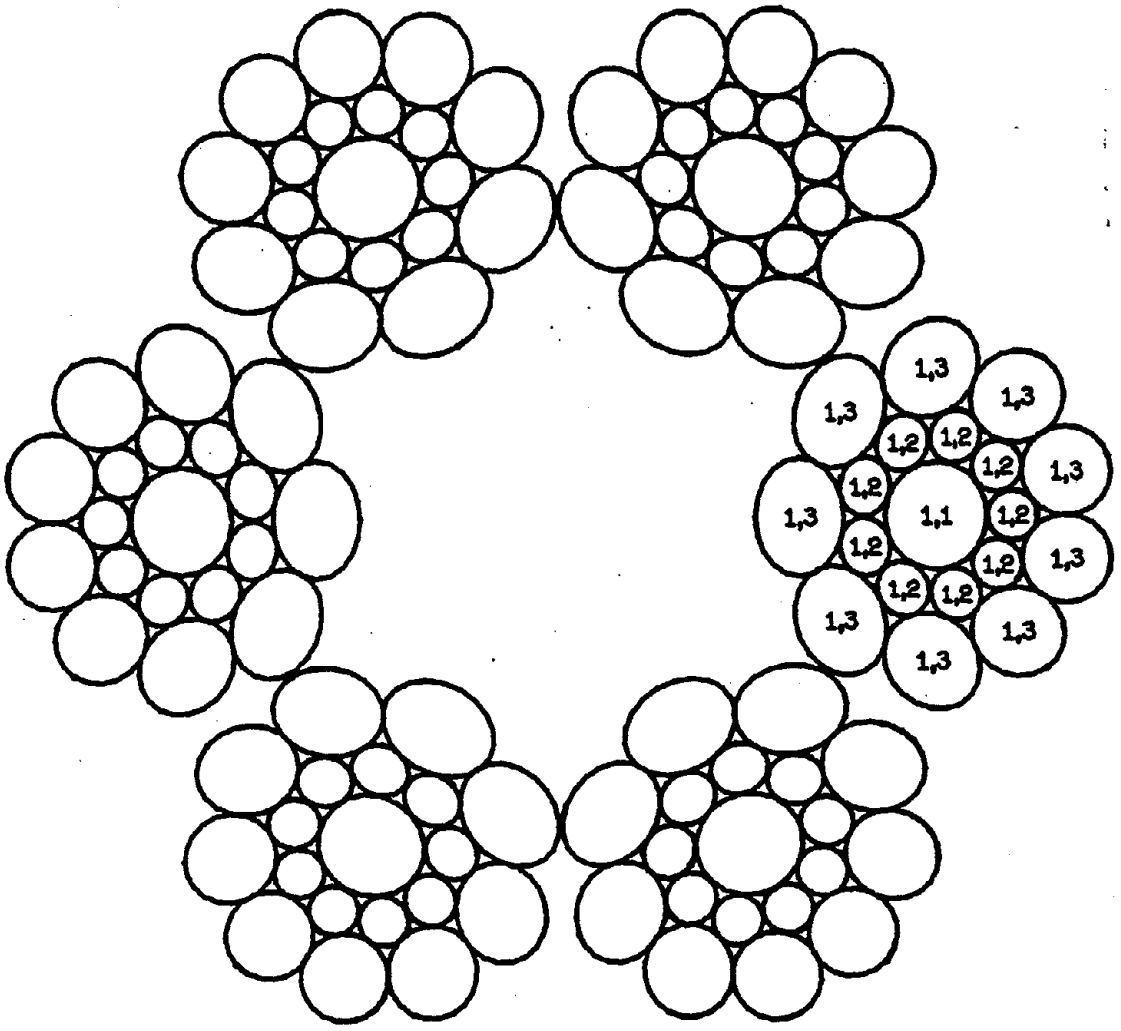

Fig. 12. Cross section of a 6x19 Seale with no core.

from a plane perpendicular to the rope's axis, i.e.

```
 DATA          M     (1,0) /6/,
&              ALPHA(1,0) /70.24/
```

As for the wire variables, it is noted that each of the strands in strand layer 1 has 3 layers of wires, and that there are 1, 9, and 9 wires in these layers, respectively:

```
 DATA          LAYERS(1)      /3/,
&             (M(1,I),I=1,3) /1, 9, 9/
```

The helix angles of the wires within strands, and the corresponding wire radii are:

```
      DATA          (ALPHA(1,I),I=1,3) /90.,      102.27,  111.23 /,
     &              (BIGR (1,I),I=1,3) /0.05731,  0.02805, 0.04993/
```

where angles greater than 90° have been entered for the non-central Seale wires because the strand is of *left-lay* construction. Some words of caution are in order here: (1) even though the outer wires are "nested" among those in the next inner layer, and consequently the two outer layers have the same lay length within the strand, the corresponding helix angles are *not* equal; and (2) one must enter the *radius* of an individual wire and not the diameter.

It is assumed that the strands are just touching each other in the unloaded configuration of the rope, that is [23],

$$\frac{r_1}{R_1} = \left[1 + \frac{1}{[\tan(\pi/m_1)\,\sin\alpha_1]^2}\right]^{\frac{1}{2}}.$$

Using Fortran, one can handle such a formula in different ways; the statement function is particularly suitable, and since no *executable* statements have been written down so far, a statement function can appear here:

```
      HRBYR(M,RAD) = SQRT(1.+1./(TAN(PI/M)*SIN(RAD))**2)
```

Since a formula for the helix radius of the first (and only) strand is now available, and since—recall Eqn. (45)—

$$r_s = \sum_{i=1}^{s} \eta_{0si} R_i,$$

where s in this case assumes only the value 1, there is only one value of η_{0si} to be concerned with:

```
      ETA(0,1,1) = HRBYR(M(1,0),PI*ALPHA(1,0)/180.)
```

The rest of the η's concern the wires within the Seale strand itself. For these layers of wires, the η_{sij} satisfying Eqn. (27) must be found, i.e.

$$r_{si} = \sum_{j=1}^{i} \eta_{sij} R_{sj}.$$

The first two layers of wires in the Seale strand form a simple strand, and consequently $r_{11} = 0\,R_{11}$ and $r_{12} = 1\,R_{11} + 1\,R_{12}$, i.e.

```
      DATA           ETA(1,1,1)          /0./,
     &              (ETA(1,2,J),J=1,2) /1., 1./
```

The helix radius of an outer wire in the Seale strand is determined by drawing a triangle consisting of the following three line segments: one from the center of the 11 wire to the center of the 13 wire, another from the center of the 11 wire to the center of the 12 wire, and one from the center of the 12 wire to the center of the 13 wire. See Fig. 12. The first of these three line segments will pass through a gap between adjacent 12 wires, but the other two will pass through the contact points between wires in adjacent layers. It is readily determined by drawing a fourth line segment from the center of the 12 wire perpendicular to the "11-13" line segment that

$$r_{13} = (R_{11}+R_{12})\cos\frac{\pi}{m_{12}} + (R_{12}+R_{13})\cos\gamma,$$

where γ is the angle between the "12-13" line and the "11-13" line:

$$\gamma = \arcsin\left[\frac{R_{11}+R_{12}}{R_{12}+R_{13}}\sin\frac{\pi}{m_{12}}\right].$$

In Fortran, these geometrical relations can be coded as follows:

```
      ETA(1,3,1) = COS(PI/M(1,2))
      GAMMA      = ASIN((BIGR(1,1) + BIGR(1,2))
     &                 /(BIGR(1,2) + BIGR(1,3))
     &                 *SIN(PI/M(1,2))
      ETA(1,3,2) = COS(PI/M(1,2)) + COS(GAMMA)
      ETA(1,3,3) = COS(GAMMA)
```

This completes the data needed for the stress analysis of the rope.

The following data are added to aid in drawing the cross section properly. (See subroutine XSECTN in the Appendix.) It is helpful to know, when drawing the cross section, where the first strand (in a given layer of strands), and the first wire (in a given layer of wires in a strand) is positioned in the respective layer of strands or wires. In most cases, specifying 0° is fine. However, in the case of the Seale strand, if a given wire in the *second* layer of wires is positioned at 0°, then a reference wire in the *third* layer will be positioned at π/m_{12}, or 20°, if $m_{12} = 9$:

```
      DATA           OFFANG(1,0)          /0./,
     &              (OFFANG(1,I),I=1,3) /0., 0., 20./
      RETURN
      END
```

The specification of the right-lay, regular-lay 6x19 Seale with no core is now complete.

As with other subroutines called by the main program, this subroutine must be compiled and added to the run stream when the program is executed.

Input/Output

There are no READ statements in the main program or in any of the subroutines. There are, however, WRITE statements in the main program SHEAVE and in subroutine ROPE. All WRITE statements are to unit 6. Sample output for the Seale IWRC appears at the end of the Appendix.

Plotter output is written to unit 9. If two different pen sizes are available, the smaller pen should be put in pen holder #1 and the larger in #2. The total length of paper used in the x-direction is 17 inches, and in the y-direction, 10 inches. Fanfold 8½x11-in. paper can be used. Additional notes are given in the Appendix.

B. Dynamic analysis

In this section, the equations governing the dynamic (axial and rotational) motion of a wire rope are derived and then solved by various techniques for three specific dynamics problems common to most deep-shaft mining operations.

Derivation of the governing equations

The previous section has dealt with the static behavior of wire rope. The linearized analysis presented there gives rise to expressions for the axial force T and the axial twisting moment H that are *linear* in the axial strain ϵ and the rotational strain β, that is:

$$\frac{T}{AE} = K_1\epsilon + K_2\beta \tag{77}$$

and

$$\frac{H}{ER^3} = K_3\epsilon + K_4\beta \tag{78}$$

where A denotes the metallic cross sectional area of the rope $(= \sum_s m_s \sum_i m_{si}\pi R_{si}^2)$, R denotes the outside radius of the rope, E is the modulus of elasticity of the wire material, ϵ is the axial strain of the rope, β is the rotational strain of the rope, and K_1, K_2, K_3 and K_4 are dimensionless constants which can be calculated by the previous static theory. The rotational strain is defined by the equation

$$\beta = R\,\Delta\tau, \tag{79}$$

where $\Delta\tau$ is the angle of twist per unit length of the rope. For example, in the case of a straight wire, $K_1 = 1$, $K_2 = 0$, $K_3 = 0$ and $K_4 = \frac{\pi}{4(1+\nu)}$. Velinsky [34] has obtained the following result for a Seale IWRC wire rope:

$$\frac{T}{AE} = 0.7019\epsilon + 0.1232\beta \tag{80}$$

and

$$\frac{H}{ER^3} = 0.2060\epsilon + 0.0403\beta. \tag{81}$$

Consider now a small length of an axially loaded rope shown in Fig. 1. A summation of forces along the axis of the rope yields the following equation of motion:

$$\frac{\partial T}{\partial x} = \rho\,\frac{\partial^2 u}{\partial t^2}, \tag{82}$$

where x denotes the inital coordinate locating the particle of the rope under discussion, t denotes time, ρ is the mass per unit length of rope, and u is the displacement of the particle along the x axis. The force T is a function of ϵ and β, where ϵ and β are now regarded as functions of x and t. Consequently Eqn. (82) can be written as

$$\frac{\partial T}{\partial \epsilon}\frac{\partial \epsilon}{\partial x} + \frac{\partial T}{\partial \beta}\frac{\partial \beta}{\partial x} = \rho\,\frac{\partial^2 u}{\partial t^2}, \tag{83}$$

and since

$$\epsilon = \frac{\partial u}{\partial x} \tag{84}$$

and

$$\beta = R\frac{\partial\theta}{\partial x}, \tag{85}$$

where $\theta(x,t)$ is the angle of rotation about the x axis, Eqn. (83) becomes

$$AEK_1\frac{\partial^2 u}{\partial x^2} + AEK_2R\frac{\partial^2\theta}{\partial x^2} = \rho\frac{\partial^2 u}{\partial t^2}. \tag{86}$$

A summation of the moments about the x axis for a small length of the axially loaded rope yields:

$$\frac{\partial H}{\partial x} = I\frac{\partial^2\theta}{\partial t^2}, \tag{87}$$

where I is the mass moment of inertia per unit length about the x axis. Equation (87) can now be written as

$$\frac{\partial H}{\partial\epsilon}\frac{\partial\epsilon}{\partial x} + \frac{\partial H}{\partial\beta}\frac{\partial\beta}{\partial x} = I\frac{\partial^2\theta}{\partial t^2}, \tag{88}$$

which becomes, as a result of Eqns. (84) and (85),

$$ER^3K_3\frac{\partial^2 u}{\partial x^2} + ER^4K_4\frac{\partial^2\theta}{\partial x^2} = I\frac{\partial^2\theta}{\partial t^2}. \tag{89}$$

Equations (86) and (89) constitute the two equations of motion which must be solved together with the appropriate initial conditions and boundary conditions. Since the equations are linear, the stresses due to the static loads (e.g. the weight of the rope) can be added to those produced by the dynamic loads.

In the remainder of this section three different problems associated with hoisting operations in deep mineshafts will be analyzed: (1) the upward acceleration of a loaded skip, (2) the dumping of muck into a suspended skip, and (3) the sudden arresting of a descending skip. Various solution techniques, including normal-mode solutions, effective-mass vibration solutions, and travelling-wave solutions, will be illustrated; the particular technique(s) chosen to solve a given problem are usually suggested by the nature of the problem.

1. Upward acceleration of a loaded skip

Consider for example the problem of a loaded skip at rest at the bottom of a shaft, where the top end of the rope (of length L) is given an upward constant acceleration a. Since the system is at rest initially, the initial conditions are:

$$u(x,0) = 0, \quad \theta(x,0) = 0, \tag{90}$$

$$\frac{\partial u}{\partial t}(x,0) = 0, \text{ and } \frac{\partial\theta}{\partial t}(x,0) = 0. \tag{91}$$

The boundary conditions are:

$$u(0,t) = -\frac{at^2}{2}, \tag{92}$$

$$\theta(0,t) = 0, \tag{93}$$

$$\theta(L,t) = 0, \tag{94}$$

and

$$K_1 \frac{\partial u}{\partial x}\bigg|_{x=L} + K_2 R \frac{\partial \theta}{\partial x}\bigg|_{x=L} = -\frac{M_{S+M}}{AE} \frac{\partial^2 u}{\partial t^2}\bigg|_{x=L}, \tag{95}$$

where M_{S+M} is the total mass of the skip and the muck.

Laplace-transform solution to the coupled equations

The solution to the above problem has, in principle, been treated in the work of Butson [31], by the method of Laplace transforms. The solution is rather complex and hence it will not be presented here. The interested reader is referred instead to Butson's thesis [31].

An important result in the thesis [31], however, is that, in the case of ropes where the ends are not allowed to rotate, the rotation θ of the rope can be neglected. This of course reduces the complexity of the problem to a large extent since the response of the rope can be described effectively by an *uncoupled* one-dimensional wave equation.

Normal-mode solution to the uncoupled equation

In this approximation, Eqn. (86) yields

$$AEK_1 \frac{\partial^2 u}{\partial x^2} = \rho \frac{\partial^2 u}{\partial t^2}, \tag{96}$$

and the appropriate initial and boundary conditions become

$$u(x,0) = 0 \quad \text{and} \quad \frac{\partial u}{\partial t}(x,0) = 0 \tag{97}$$

and

$$u(0,t) = -\frac{at^2}{2} \quad \text{and} \quad AEK_1 \frac{\partial u}{\partial x}\bigg|_{x=L} = -M_{S+M} \frac{\partial^2 u}{\partial t^2}\bigg|_{x=L}. \tag{98,99}$$

Using the normal-mode method [39], one determines that the dynamic force T_D at the top of the rope is given by

$$T_D = M_{S+M} a(1-\cos\omega t) + AEK_1 \frac{p_1}{c} D_1 \phi_1(t), \tag{100}$$

where $\omega = \sqrt{k/M_{S+M}}$, $k = AEK_1/L$, $c^2 = AEK_1/\rho$, and p_1 and D_1 are determined from the following equations:

$$\frac{p_1 L}{c} \tan\frac{p_1 L}{c} = \frac{\rho L}{M_{S+M}} \tag{101}$$

and

$$D_1^2 \left[\frac{L}{2} - \frac{c}{2p_1}\sin\frac{p_1 L}{c}\cos\frac{p_1 L}{c} + \frac{M_{S+M}}{\rho}\sin^2\frac{p_1 L}{c}\right] = 1, \tag{102}$$

and the function $\phi_1(t)$ is given by the expression

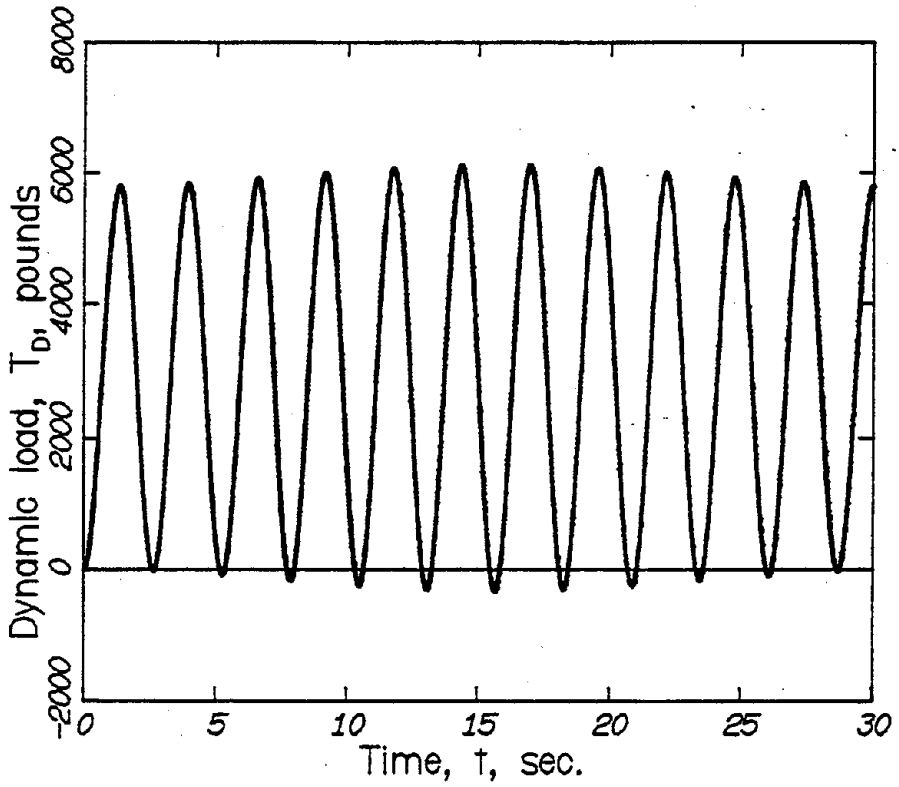

Fig. 13. Dynamic load, T_D, as a function of time, t, for the upward-acceleration problem.

$$\phi_1(t) = \frac{aD_1}{p_1}\left[\frac{c}{p_1^2}\left(1-\cos\frac{p_1 L}{c}\right)(1-\cos p_1 t) - \frac{c^2}{p_1 L}\left(\sin\frac{p_1 L}{c} - \frac{p_1 L}{c}\cos\frac{p_1 L}{c}\right)\frac{\cos\omega t - \cos p_1 t}{p_1^2-\omega^2}\right] \tag{103}$$

Let the rope, for example, be a 1½-in.-dia. 6x19 fiber-core rope where

L	= 2,800 ft.,
weight of skip	= 9,000 lb.,
weight of muck	= 12,000 lb.,
weight of rope (3.78×2800)	= 10,600 lb.,
maximum speed	= 2,500 ft./min.,
period of acceleration	= 12 sec., and
a	= 3.47 ft./sec.^{2}

The total static load at the top is 31,600 lb. Evaluation of Eqn. (100) for these parameters yields a maximum dynamic load of about 6,100 lb. which must be added to the static load to compute the maximum load in the rope. The dynamic load is plotted in Fig. 13. It is noted that the maximum load

does not occur in the first cycle, but rather after several cycles of the oscillation.

2. Dumping muck into a skip

Consider now the problem of dumping the muck into a skip when the skip is at the bottom of the shaft.

Vibration solution using "effective mass" of the rope

The system will be approximated by a one-degree-of-freedom system in which the "effective mass" of the rope is considered. This approximation, based on the assumption that the displacement of the rope varies linearly, can be used in this case with sufficient accuracy. In order to estimate the effect of the mass of the rope on the period of natural vibration, this approximation results in an addition of one-third the weight of the rope to the weight of the skip and the muck. If, for example, the weight of the rope is one-half the weight of the skip and the muck, the error in the approximate solution is about 0.5%. Hence, with almost negligible error, the equation of motion governing the loading of the muck into the skip can be written as

$$\left(M_{S+M}+\frac{M_R}{3}\right)\frac{d^2u}{dt^2}+k\,u\;=\;f(t), \tag{104}$$

where M_{S+M} denotes the mass of the skip and the muck, M_R is the mass of the rope, $k = AEK_1/L$, and u is the stretch of the rope at the bottom end measured from the static equilibrium position when the rope is loaded by its weight and the weight of the skip and the muck. During the dumping process, the force $f(t)$ acting on the skip is given by

$$f(t)\;=\;-M_M g[1-t/t_D], \qquad t\leqslant t_D \tag{105}$$

where t_D is the total dumping time, and

$$f(t)\;=\;0, \qquad t\geqslant t_D \tag{106}$$

which means that, at $t = 0$, the force applied to the end of the rope is equal to the weight of the skip alone. For this problem the following solution is obtained:

$$u(t)\;=\;\frac{M_M g}{k}\left[\frac{t}{t_D}-1-\frac{\sin\omega_n t}{\omega_n t_D}\right], \qquad t\leqslant t_D \tag{107}$$

where

$$\omega_n^2\;=\;\frac{k}{M_{S+M}+M_R/3}. \tag{108}$$

Also,

$$u(t)\;=\;\bar{A}\cos\omega_n t+\bar{B}\sin\omega_n t, \qquad t\geqslant t_D \tag{109}$$

where the constants $\bar{A}$ and $\bar{B}$ are determined by matching the displacement and the velocity at time $t = t_D$.

Let the rope, for example, be a 1¼-in.-dia. Seale IWRC, weighing 2.89 lb./ft., with $K_1 = 0.7$ (as given in Eqn. (80)—see also Velinsky, et al. [35, p. 13]), and let

L	= 3,000 ft.,
weight of skip	= 5,000 lb.,
weight of muck	= 10,000 lb.,
E	= 29.0×10^6 lb./in.^{2},

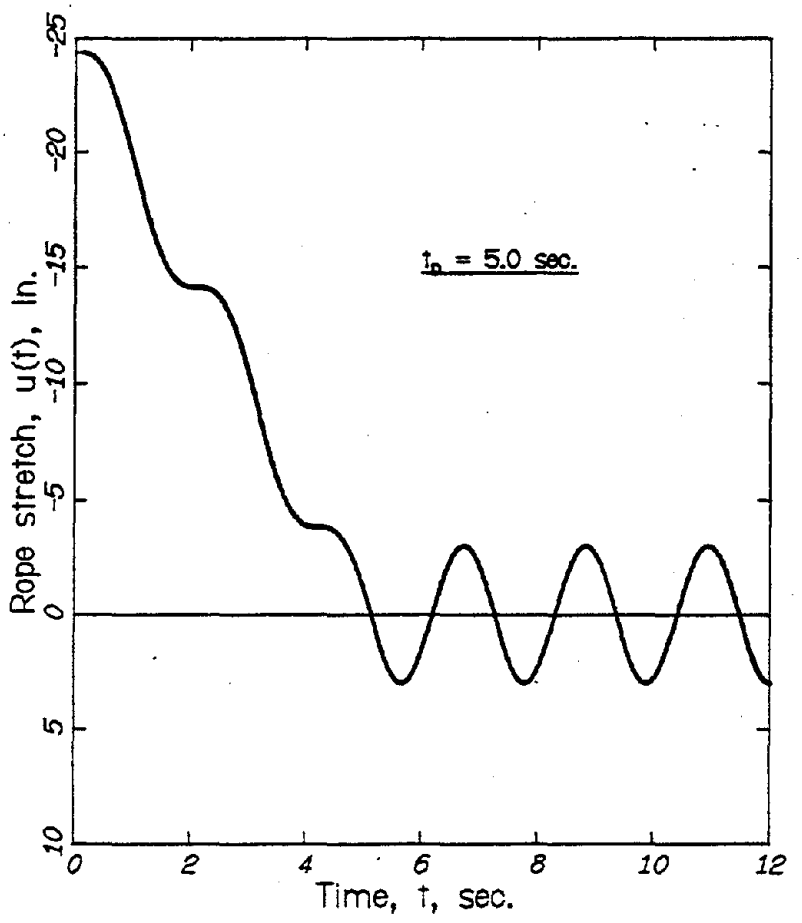

Fig. 14. Dynamic stretch, $u(t)$, in a rope supporting a skip, with a dumping time t_D equal to 5 sec.

A = 0.727 in.^{2},
t_D = 5 sec.

Hence

$$k = \frac{AEK_1}{L} = 410 \text{ lb./in.},$$

$$M_{S+M} + \frac{M_R}{3} = 46.3 \text{ lb.-sec.}^2/\text{in.},$$

and

$$\omega_n = \left[\frac{k}{M_{S+M} + M_R/3}\right]^{1/2} = 2.98 \text{ rad./sec.}$$

The total static force at the top of the rope is

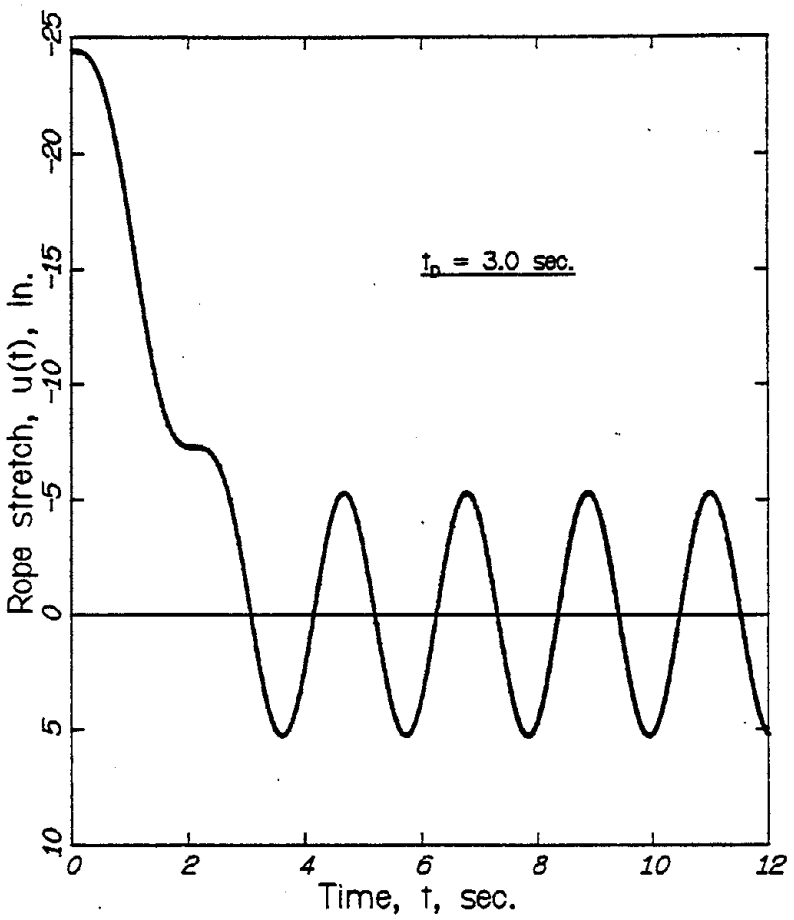

Fig. 15. Dynamic stretch, $u(t)$, in a rope supporting a skip, with a dumping time t_D equal to 3 sec.

$$T_S = (8{,}670 + 5{,}000 + 10{,}000) \text{ lb.} = 23{,}670 \text{ lb.}$$

The total *static* stretch of the rope Δ_T due only to the weight of the rope and to the weight of the skip and the muck is

$$\Delta_T = \frac{8670 \times 3000 \times 12}{2 \times 0.727 \times 0.7 \times 29.0 \times 10^6} + \frac{15000 \times 3000 \times 12}{0.727 \times 0.7 \times 29.0 \times 10^6} = 47.2 \text{ in.}$$

Evaluation of Eqn. (109) for the given loading conditions reveals that the *additional* stretch due to the dynamic effects is about 3 in. (past the equilibrium position), as shown in Fig. 14. Hence the maximum force at the top of the rope—with dynamic effects included—is

$$23{,}670 + 3 \times 410 = 24{,}900 \text{ lb.}$$

It is interesting to consider the effect of the dumping time on the additional stretch of the rope. Results for t_D = 3 sec., 2 sec., and 1.5 sec. are shown in Figs. 15, 16 and 17, respectively. Note that a decrease in the dumping time may or may not increase the maximum dynamic stretch.

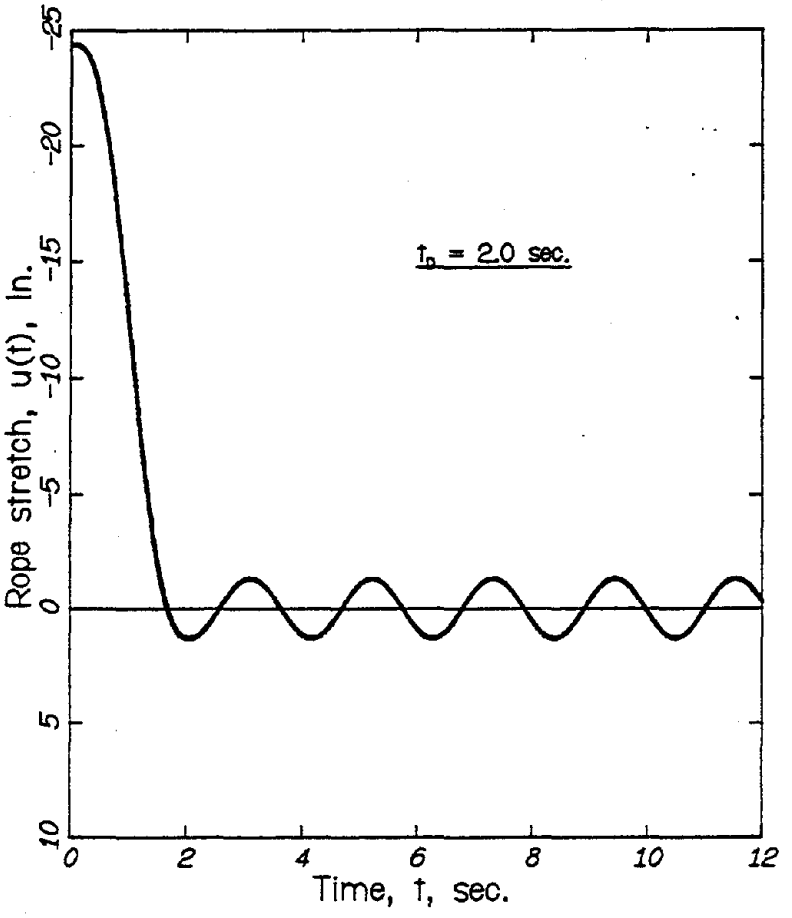

Fig. 16. Dynamic stretch, $u(t)$, in a rope supporting a skip, with a dumping time t_D equal to 2 sec.

3. Arresting a descending skip

Consider now a rope with a suspended mass M at the lower end, travelling downward with a constant velocity V, suddenly arrested at its upper end by a clamp.

Travelling-wave solution

The differential equation of motion, Eqn. (96), can be written as:

$$\frac{\partial^2 u}{\partial t^2} = c^2 \frac{\partial^2 u}{\partial x^2}, \tag{110}$$

where

$$c^2 = \frac{AEK_1}{\rho}, \tag{111}$$

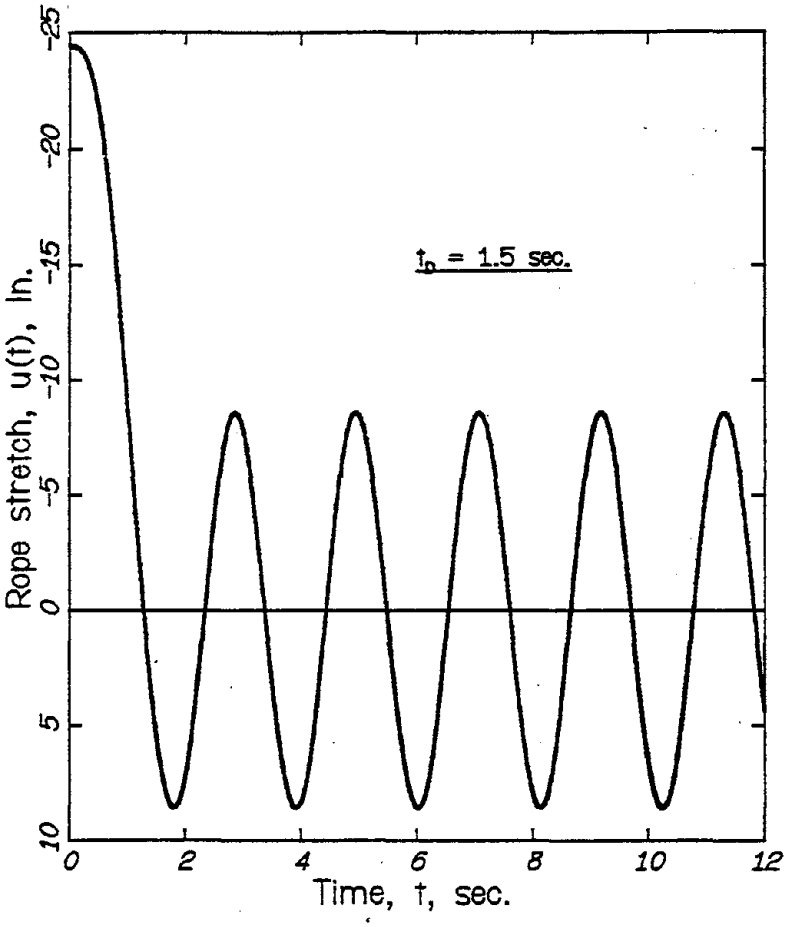

Fig. 17. Dynamic stretch, $u(t)$, in a rope supporting a skip, with a dumping time t_D equal to 1.5 sec.

in which ρ is the mass per unit length of the rope. At the lower end,

$$-T\Big|_{x=L} = M\frac{\partial^2 u}{\partial t^2}\Big|_{x=L} \tag{112}$$

and hence

$$-c^2\frac{\partial u}{\partial x}\Big|_{x=L} = mL\frac{\partial^2 u}{\partial t^2}\Big|_{x=L}, \tag{113}$$

where L denotes the length of the rope and m is defined as $M/\rho L$, that is, m is the ratio of the suspended mass M to the mass of the rope.

The solution to Eq. (110) can be written as

$$u(x,t) = f(ct-x) + F(ct+x), \tag{114}$$

and since the upper end of the rope is clamped (for $t \geqslant 0$),

$$u(0,t) = 0 \tag{115}$$

and Eq. (114) becomes

$$u(x,t) = f(ct-x) - f(ct+x). \tag{116}$$

Once the function $f(\zeta)$ is known, the displacement $u(x,t)$ can be determined by placing the appropriate value of ζ in $f(\zeta)$ and by using Eqn. (116) to evaluate the displacement u.

The velocity v can be evaluated by the expression

$$v = \frac{\partial u}{\partial t} = c[f'(\alpha) - f'(\beta)] = c[f'(ct-x) - f'(ct+x)], \tag{117}$$

where

$$\alpha = ct-x \quad \text{and} \quad \beta = ct+x. \tag{118,119}$$

The strain ϵ is given by the expression

$$\epsilon = \frac{\partial u}{\partial x} = -[f'(ct-x) + f'(ct+x)]. \tag{120}$$

Initially the entire rope has a velocity V and no (dynamic) strain. Hence, Eqns. (117) and (120) yield, at $t = 0$,

$$c[f'(-x) - f'(x)] = V \qquad \text{for } 0<x<L, \tag{121}$$

and

$$f'(-x) + f'(x) = 0 \qquad \text{for } 0<x<L. \tag{122}$$

A combination of Eqns. (121) and (122) results in

$$f'(-x) = \frac{V}{2c} \qquad \text{for } 0<x<L, \tag{123}$$

and

$$f'(x) = -\frac{V}{2c} \qquad \text{for } 0<x<L. \tag{124}$$

Now let $f = f(\zeta)$ where ζ may be set equal to $ct-x$ or $ct+x$ as required. Hence

$$f'(-\zeta) = \frac{V}{2c} \qquad \text{for } 0<\zeta<L \tag{125}$$

and

$$f'(\zeta) = -\frac{V}{2c} \qquad \text{for } 0<\zeta<L. \tag{126}$$

Note that Eqn. (113) can be written as

$$mL\, f''(ct+L) + f'(ct+L) = mL\, f''(ct-L) - f'(ct-L), \tag{127}$$

and with the substitution $\zeta = ct+L$, this equation becomes

$$f''(\zeta) + \frac{1}{mL} f'(\zeta) = f''(\zeta-2L) - \frac{1}{mL} f'(\zeta-2L). \tag{128}$$

Equation (128) can now be regarded as determining $f'(\zeta)$ in the interval $L<\zeta<3L$ since the right-hand side of Eqn. (128) is known in the interval $L<\zeta<3L$.

The integral of Eqn. (128) can be written as:

$$f'(\zeta) = Ce^{-\frac{\zeta}{mL}} + e^{-\frac{\zeta}{mL}}\int e^{\frac{\zeta}{mL}}\left[f''(\zeta-2L) - \frac{1}{mL}f'(\zeta-2L)\right]d\zeta \tag{129}$$

where C is a constant of integration. Equation (129) becomes, for $L<\zeta<2L$,

$$f'(\zeta) = Ce^{-\frac{\zeta}{mL}} - \frac{V}{2c}. \tag{130}$$

Now at $x = L$, the velocity v is

$$v = c\,[f'(ct-L) - f'(ct+L)] \tag{131}$$

and hence for small positive values of t,

$$c\,[f'(0^+-L) - f'(0^++L)] = V. \tag{132}$$

Therefore

$$c\left[\frac{V}{2c} - \left[Ce^{-\frac{1}{m}} - \frac{V}{2c}\right]\right] = V, \tag{133}$$

and hence $C = 0$. It follows that

$$f'(\zeta) = -\frac{V}{2c} \qquad \text{for } L<\zeta<2L. \tag{134}$$

The process outlined here can be continued to determine $f'(\zeta)$ for subsequent intervals of ζ. Once $f(\zeta)$ is known in any interval, Eqns. (117) and (118) can be used to determine the velocity and the strain in that interval. For example, in the interval $2L<\zeta<4L$,

$$f'(\zeta) = -\frac{2V}{c}e^{-\frac{\zeta-2L}{mL}} + \frac{V}{2c}, \tag{135}$$

and in the interval $4L<\zeta<6L$,

$$f'(\zeta) = -\frac{2V}{c}\left[\frac{8}{m}e^{\frac{4}{m}} + e^{\frac{2}{m}}\right]e^{-\frac{\zeta}{mL}} + \frac{4V}{mLc}\zeta e^{-\frac{\zeta-4L}{mL}} - \frac{V}{2c}. \tag{136}$$

Some specific analytical results will now be presented for the case in which the weight of the suspended mass is equal to the mass of the rope, i.e. $m = 1$. Results will be given for the strain ϵ, from which the force in the rope can be calculated by means of the relation $T = K_1AE\epsilon$.

First, consider the state of strain in the rope at the time when the longitudinal wave just reaches the skip. It turns out that, at this moment, the entire rope is under a constant *dynamic* strain given by

$$\epsilon = \frac{V}{c} \qquad \text{for } 0<x<L \quad \text{at } t=L/c. \tag{137}$$

After this instant, a wave is reflected back toward the clamped end. When the reflected wave just reaches the top, the distribution of strain along the rope is given by

$$\epsilon = 2\frac{V}{c}e^{-\frac{x}{L}} \qquad \text{for } 0<x<L \quad \text{at } t=2L/c. \tag{138}$$

Note in particular that the dynamic strain at the top ($x = 0$) has doubled in value from the dynamic strain imposed by the initial clamping.

After the reflected wave reaches the top of the rope, it, too, is reflected back toward the skip. The fixed end condition at the clamp gives rise to an additional strain jump of magnitude V/c, so that, at this instant (i.e. $t=2L/c^+$), the total dynamic strain at the top of the rope is $3V/c$—*three* times the dynamic strain induced by the initial clamping. Actually, this result is obtained for any value of m (i.e. for any skip weight), as will be illustrated shortly in a representative example. It should be kept in

mind that, throughout this discussion, it is assumed that the rope is *instantaneously* arrested at its upper end.

When that twice-reflected wave reaches the skip, the distribution of strain along the rope is given by

$$\epsilon = 2\frac{V}{c}\left[e^{-\frac{L-x}{L}} + e^{-\frac{L+x}{L}}\right] - \frac{V}{c} \qquad \text{for } 0<x<L \quad \text{at } t=3L/c. \tag{139}$$

Waves will continue to propagate up and down the rope until dissipative mechanisms (not considered in this discussion) render the motion of the rope quasi-static.

A numerical example for a 1¼-in.-dia. Seale IWRC will now be presented. In this example,

L	= 3,000 ft.,
weight of skip	= 5,000 lb.,
E	= 29.0×10^6 lb./in.^{2},
A	= 0.727 in.^{2},
ρ	= (2.89 lb./ft.)/(32.2 ft./sec.^{2})
	= 0.0898 lb.-sec.^{2}/ft.^{2}
K_1	= 0.7
V	= 40 ft./sec.

The wavespeed c is computed to be

$$c = \left(\frac{AEK_1}{\rho}\right)^{1/2} = 12{,}800 \text{ ft./sec.},$$

and the mass ratio m has the value

$$m = \frac{M}{\rho L} = \frac{Mg}{\rho Lg} = 0.577,$$

that is, the skip weight is 0.577 times the weight of the rope.

The total *static* load at the top of the rope is

$$T_S = 2.89\times3000 + 5000 = 13{,}700 \text{ lb.}$$

The additional dynamic load T_D due to the sudden clamping at the top is plotted as a function of time in Fig. 18. Immediately upon clamping, a dynamic load of about 46,200 lb. is induced in the rope, for a combined (static and dynamic) load of about 60,000 lb., which is well below the rated strength of this type of rope—about 138,000 lb. However, when the wave is reflected back from the skip and again reflected at the clamped (upper) end, the total dynamic load reaches a peak value of about 138,800 lb., which when added to the static load of 13,700 lb., exceeds the rated strength of the rope considerably. The time at which the peak dynamic loading occurs is given by $t = 2L/c$, which (in this example) is about 0.47 seconds after the rope is clamped. As shown in Fig. 18, the dynamic load quickly decays from its peak value and even goes negative; presumably, if the rope did not break at time $t = 2L/c$, the rope would buckle soon thereafter when the negative dynamic load exceeded the positive static load.

Again it is pointed out that, in the derivation of these equations, it is assumed that the clamping occurs instantaneously. Even so, if the clamping occurs in a time that is much smaller than the time of transit of the longitudinal wave in the rope, serious dynamic overloading (of the order of $2AEK_1V/c$) could easily occur and cause rope failure.

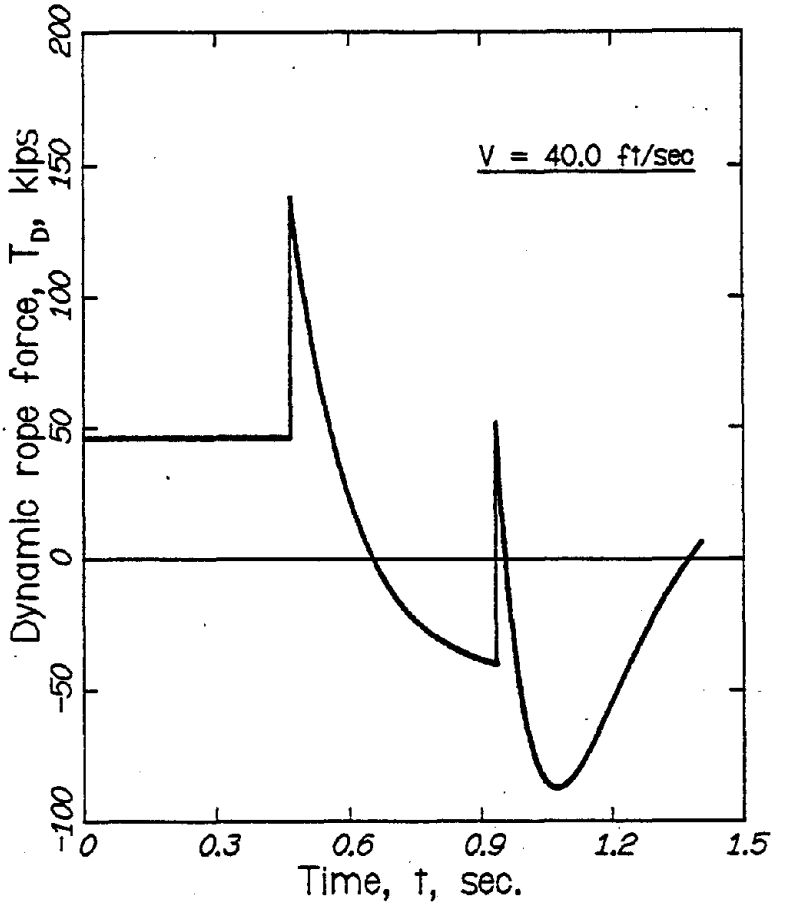

Fig. 18. Dynamic force, T_D, at the top of a rope that is suddenly clamped to arrest a descending skip, as a function of time, t.

Concluding remarks

Representative problems from the deep-shaft mining industry have been shown to be amenable to solution by the techniques that have been outlined. An important step toward the development of meaningful solutions was provided by Butson [31,32], who demonstrated that, with minimal error, one can neglect the effect of the rotational displacements on the predominantly longitudinal displacements of a rope.

III. Experiment

Some static tests on a representative wire rope and the wires and strands comprising the rope have been conducted in an effort to determine experimentally the relations between the elastic responses of wire, strand, and rope. Stress-strain curves have been obtained for each of the four different diameters of extra-improved-plow (EIP) steel wires that comprise the outer strands of a commercially available ½" 6x25F IWRC wire rope. Load-deflection curves have also been obtained for initially straight specimens of the 0.167"-dia. strands made from these wires; care was taken to minimize rotation of the ends of the specimen during these tests. Finally, load-deflection curves were also obtained for specimens of the rope itself; again, care was taken to minimize rotation of the ends of the specimen during the tests.

A. Stress-strain curves for wire

A clip gage with a nominal gage length of one inch was used to determine the strain in the wire samples, as illustrated in Fig. 19. It was found that the clip gage could be prevented from slipping on the specimen, if a drop of cyanoacrylate cement was applied at each of the contact points.

The load was determined by means of a calibrated load cell within the testing machine. A Riehle® 10-kip tension/compression machine was used for these tests. The specimen was loaded by file grips and fracture of the wire invariably occurred at a grip.

The actual diameter of each wire was measured with a micrometer caliper, and the data for wire diameters, reported in Table I, are felt to be accurate to within 0.0002 inch on the basis of a statistical analysis of several measured values of the wire diameter for a given wire.

Table I. Summary of results for elastic response of wires

Nominal wire diameter (in.)	*Actual wire diameter (in.)*	*Actual cross sectional area (sq. in.)*	*Spring rate* $\Delta T/\Delta\epsilon$ *(lb.)*	*Young's modulus* E *(psi)*
0.015	0.0149	0.1744×10^{-3}	5240	30.0×10^{6}
			5190	29.8×10^{6}
0.032	0.0322	0.8143×10^{-3}	22500	27.6×10^{6}
			24900	30.6×10^{6}
0.035	0.0349	0.9566×10^{-3}	28900	30.2×10^{6}
			29200	30.5×10^{6}
0.037	0.0379	1.128×10^{-3}	32500	28.8×10^{6}

Also reported in Table I are the corresponding spring rates for the various wires, and the resulting experimentally determined values of Young's modulus for the wires. The spring rate $\Delta T/\Delta\epsilon$ was determined by taking the slopes of one or more unloading/reloading portions of the load-deflection curve, such as portions 2 and 3 of the curve in Fig. 20. Only those unloading/reloading curves for which the offset yield strain was less than 0.3% were used.

On the basis of the results summarized in Table I, it can be concluded that the Young's modulus of the steel is

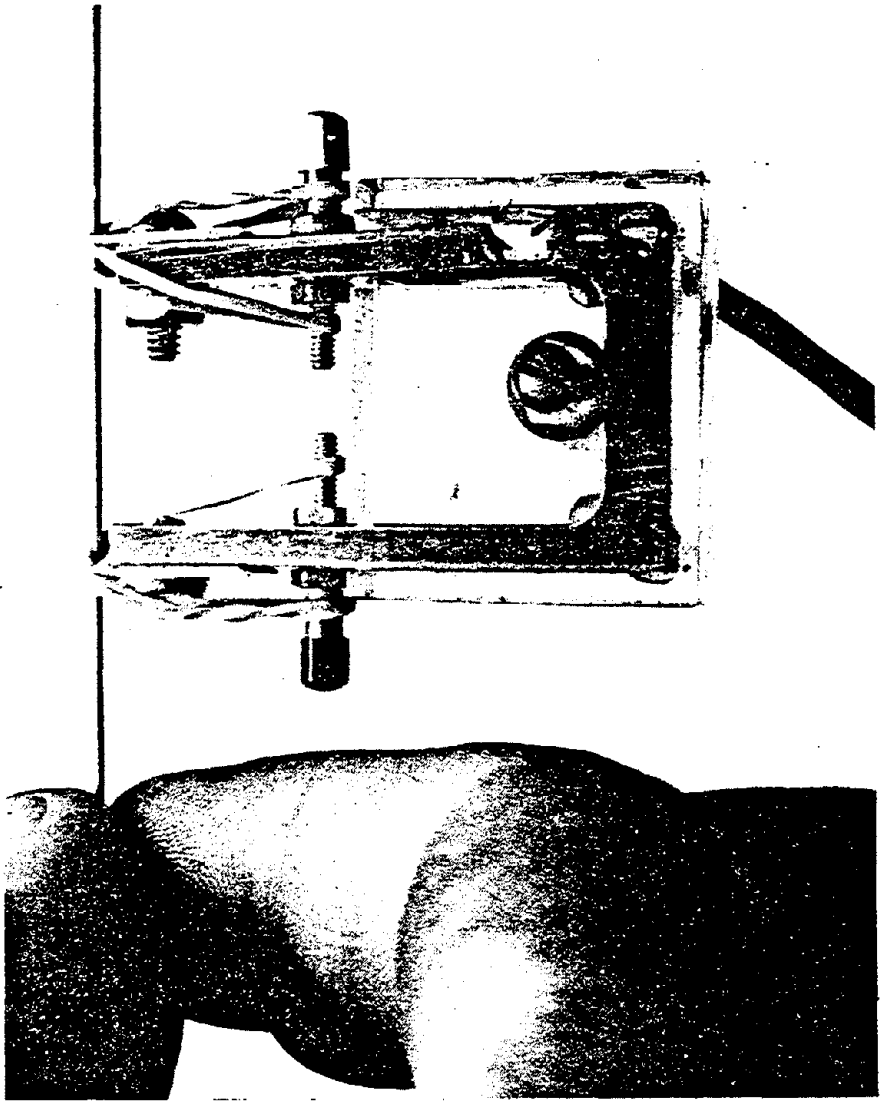

Fig. 19. Clip gage used for tension tests on wires.

$$E = (29.6 \pm 1.1) \times 10^6 \text{ lb./in.}^2.$$

The 0.2%-offset yield strength of the wire material was observed to be about $(280 \times 10^3 \pm 30 \times 10^3)$ lb./in.^{2}. The ultimate tensile strength was not accurately determined because failure never occurred away from the grips; however, it can be stated that the ultimate strength exceeds the 0.2%-offset yield strength by at least 5%.

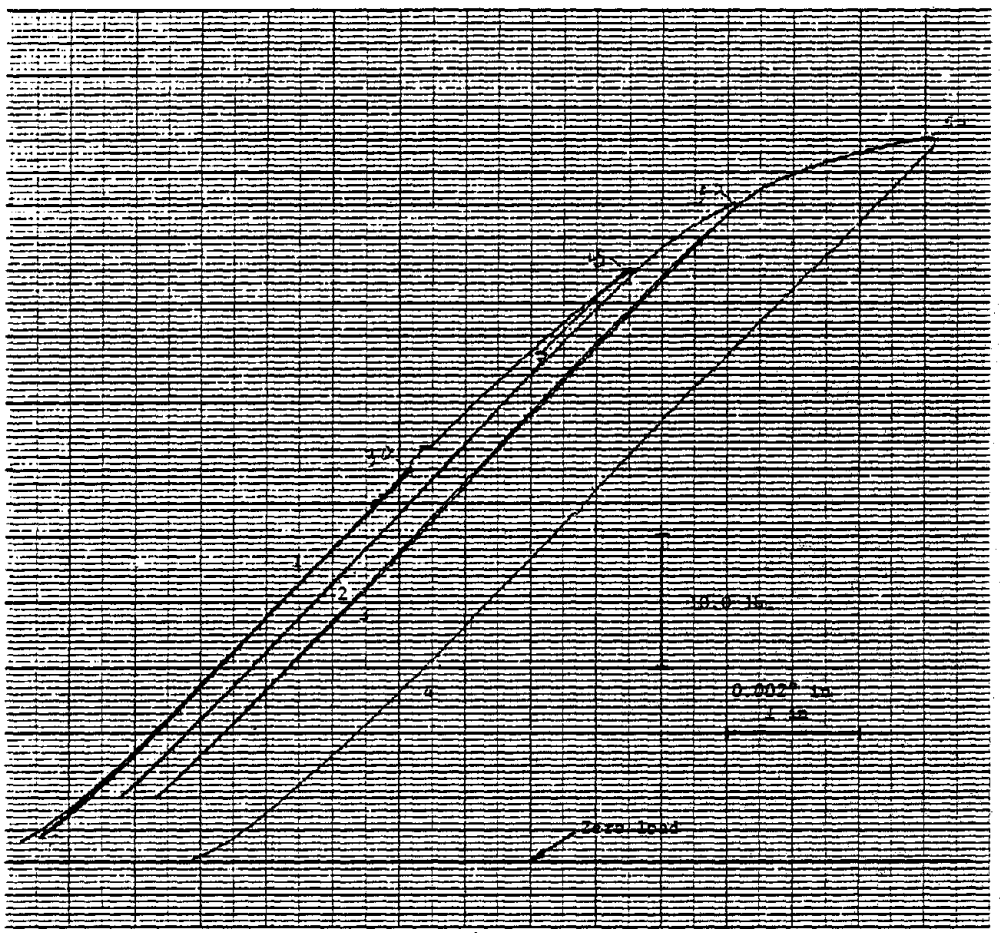

Fig. 20. Typical load-deflection curve for 0.015″ wire.

B. Load-deflection curves for strand and rope

Strand

Specimens of initially straight strand formed of a 0.037″ core wire wrapped left-handed, in turn, by six 0.035″ wires, six 0.015″ filler wires, and twelve 0.032″ wires, were tested in a Riehle® 200,000-lb. tension/compression machine as illustrated in Fig. 21. A 12-inch beam-type clip gage was used to determine the axial strain in the specimen. Four-inch-long steel collars with zinc-filled tapered internal bores were used to load the specimen; the individual wires within the strand had been splayed in the collar prior to the pouring of the molten zinc. In the testing machine, the collars were rigidly held by means of V-groove grips, as shown in Fig. 22. In view of the massiveness of the testing machine and the method of gripping that was employed, one can argue that the ends of the specimen were effectively prevented from rotating.

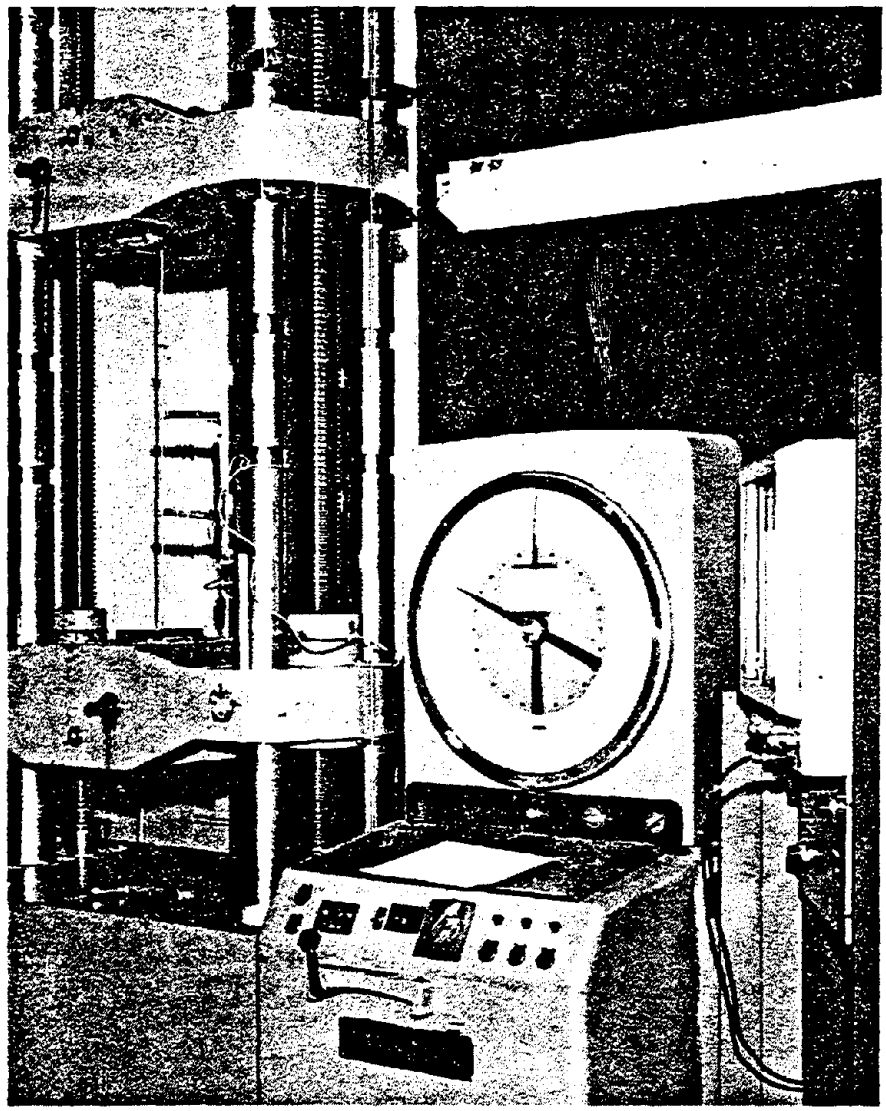

Fig. 21. Photograph of strand in 200,000-lb. machine.

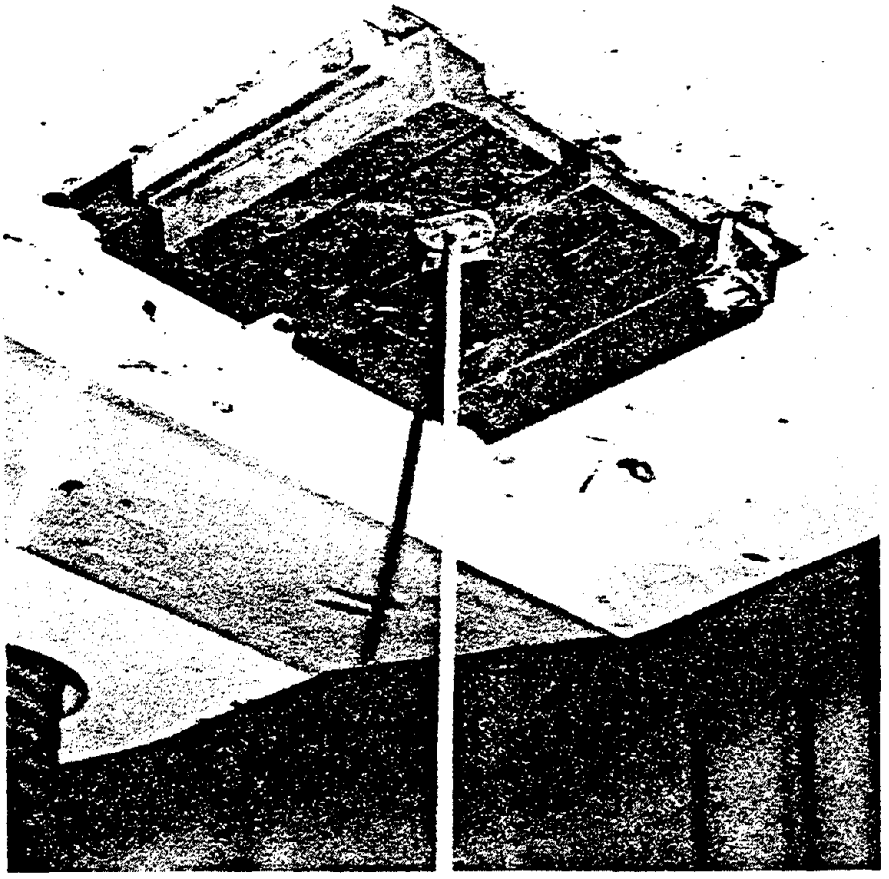

Fig. 22. View of upper strand socket in V-groove grip.

A typical load-deflection curve for the strand is shown in Fig. 23. In the test illustrated, the loading curve is essentially nonlinear right from the origin. The spring rate $\Delta T/\Delta\epsilon$ near the origin is approximately 0.42×10^6 lb.

In order to determine an effective Young's modulus E_e for the strand, one must know the metallic area A_s of the strand. Using the measured wire diameters from Table I, one finds that

$$\begin{aligned} A_s = {} & (1)\,\frac{\pi}{4}(0.0379)^2 + \\ & (6)\,\frac{\pi}{4}(0.0349)^2 + \\ & (6)\,\frac{\pi}{4}(0.0149)^2 + \\ & (12)\,\frac{\pi}{4}(0.0322)^2 \\ = {} & 0.01768\text{in.}^2 \end{aligned}$$

The effective Young's modulus is then given by

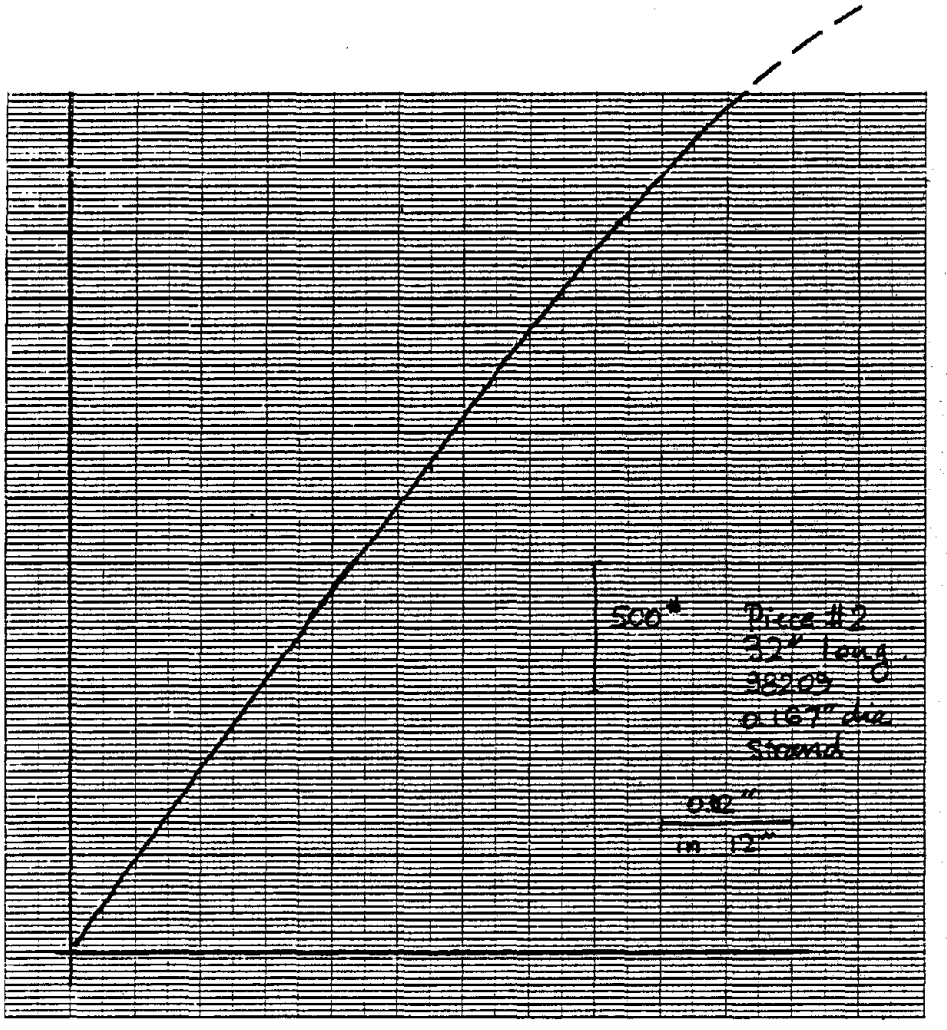

Fig. 23. Typical load-deflection curve for 0.167″ strand.

$$E_e = \frac{\Delta T/\Delta\epsilon}{A_s} = \frac{0.42\times10^6\,\text{lb.}}{0.01768\,\text{in.}^2}$$

$$= 24\times10^6\,\text{lb./in.}^2$$

It should be noted that the computed value of E_e is about 81% of the computed value of E for the wire material.

Wire rope

A regular-lay ½″ 6x25F IWRC wire rope is made from six of the left-lay strands just described, wrapped right-handed about a core which is itself a right-lay lang-lay 6x7 IWRC, the smaller IWRC being a 7-wire right-lay strand. The total metallic area A_{core} of the IWRC is computed to be

$$A_{core} = (7)\frac{\pi}{4}\left[\frac{0.086}{3}\right]^2 + (6)(7)\frac{\pi}{4}\left[\frac{0.076}{3}\right]^2 = 0.026 \text{ in.}^2,$$

based on the diameters of the strands comprising the core. The total metallic area A of the wire rope is therefore computed to be

$$A = A_{core} + 6A_s = 0.026 + 6(0.01768) = 0.132 \text{ in.}^2$$

An independent estimate of the metallic area is provided by measuring the weight w of a known length l of the wire rope and by deducing the *projected* area A_{proj} of the wire rope cross section according to the relation

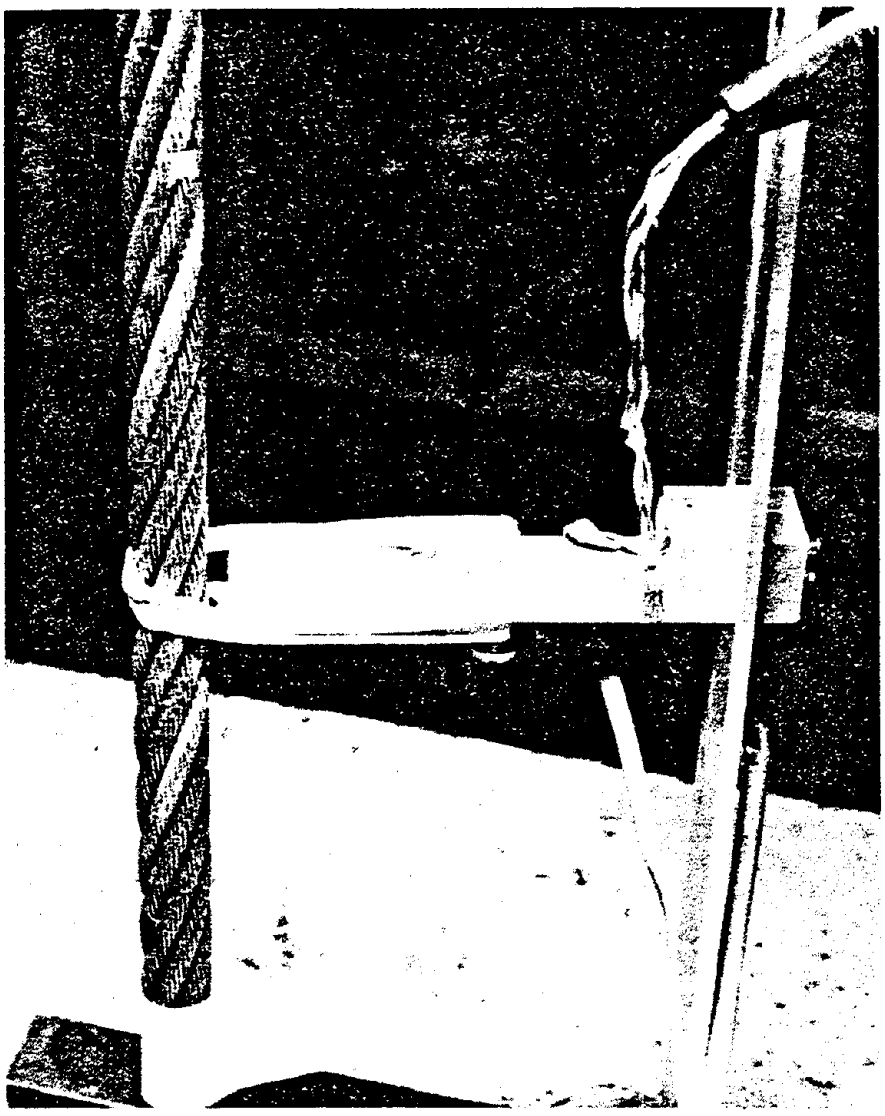

Fig. 24. Detail of 12" clip gage on ½" rope.

$$w = \gamma A_{proj} l$$

where γ denotes the specific weight of the wire material, taken here to be 490 lb./ft.^{3}. Two samples of the rope were measured and it was found experimentally that $w/l = 0.464$ lb./ft., which agrees with the manufacturer's stated value of 0.46 lb./ft. Consequently,

$$A_{proj} = \frac{1}{\gamma}\frac{w}{l} = \frac{0.464\,\text{lb./ft.}}{490\,\text{lb./ft.}^3} \times 144\,\frac{\text{in.}^2}{\text{ft.}^2} = 0.136\ \text{in.}^2$$

Now, the projected area A_{proj} is somewhat larger than the metallic area A because the projected area of each wire is $1/\cos\theta$ times the circular area of that wire, where θ denotes the the angle between the axis of the wire rope and the tangent to the centerline of the given wire as it penetrates the cross section. In principle, one would have to determine θ for every wire in the cross section in order to calculate A accurately by this method; but, just for purposes of checking, one can argue that most of the wires in the strands and in the IWRC make an "average" angle θ_{avg} of about 18° with respect to the wire rope axis, and consequently the metallic area A is approximately

$$A = A_{proj}\cos\theta_{avg} = 0.136\cos 18^\circ = 0.129\ \text{in.}^2,$$

which is seen to be within 3% of the value of A computed by measuring the diameters of the individual wires.

Consistent values of the metallic area A are difficult to obtain from the literature. For example, the *Wire Rope Users Manual* [40, p. 75] lists the "approximate metallic area" of 6x25F IWRC as 0.4830, which is based on an assumed 1.03 "target" diameter. Thus, for a ½" rope of the specified type, the area A should be equal to $0.4830 \times (½")^2$ or 0.121 in.^{2}. It will be seen that this value is considerably smaller than the values of the areas computed by either of the above methods for the given rope.

Tests on the ½" rope were run in the same Riehle® 200,000-lb. machine used for the strands, and the same 12"-gage-length clip gage was used to determine the axial deflection. Also, the ends of the rope specimens were held by zinc-filled cylindrical sockets that were gripped by V-groove grips to prevent rotation.

The detail of the contact between the clip gage and the rope is shown in Fig. 24. The clip gage spanned approximately twenty-two crests of the six-strand rope, which means that the ends of the clip gage were not in contact with the same strand within the rope. In some of the preliminary testing, where short zinc-filled end sockets were used, it was found that the strands would apparently pull out of the sockets one-by-one. This led to erratic strain measurements. Later, the sockets were redesigned and the wires were cleaned more thoroughly before the molten zinc was poured into the sockets. Seemingly satisfactory load-deflection curves were then obtained, as illustrated in Fig. 25. From this figure, one can calculate an effective stiffness of the rope by noting that the spring rate $\Delta T/\Delta\epsilon$ is approximately 2.2×10^6 lb. along the reloading curve (between about 9×10^3lb. and 15×10^3lb., where the curve is linear). A somewhat larger value is observed over a nearly linear region along the second unloading curve (between about 20×10^3lb. and 10×10^3lb.), where $\Delta T/\Delta\epsilon$ is approximately 2.3×10^6 lb. Of course, along the initial portion of the load-deflection curve of the virgin rope, the spring rate is rather small. At the origin, the spring rate is only about 0.8×10^6 lb. The effective Young's modulus E_e for the rope is calculated by the formula

$$E_e = \frac{1}{A}\Delta T/\Delta\epsilon,$$

where some judgment is required in picking the most meaningful values of both $\Delta T/\Delta\epsilon$ and A. It is felt that $\Delta T/\Delta\epsilon = 2.2\times10^6$ lb. is reasonable because it corresponds to the stiffness of the rope after it has been moderately preloaded. Also, the value 0.132 in.^{2} seems to be an appropriate one for A because it is based on the actual diameters of the component wires. If these two values are employed, then

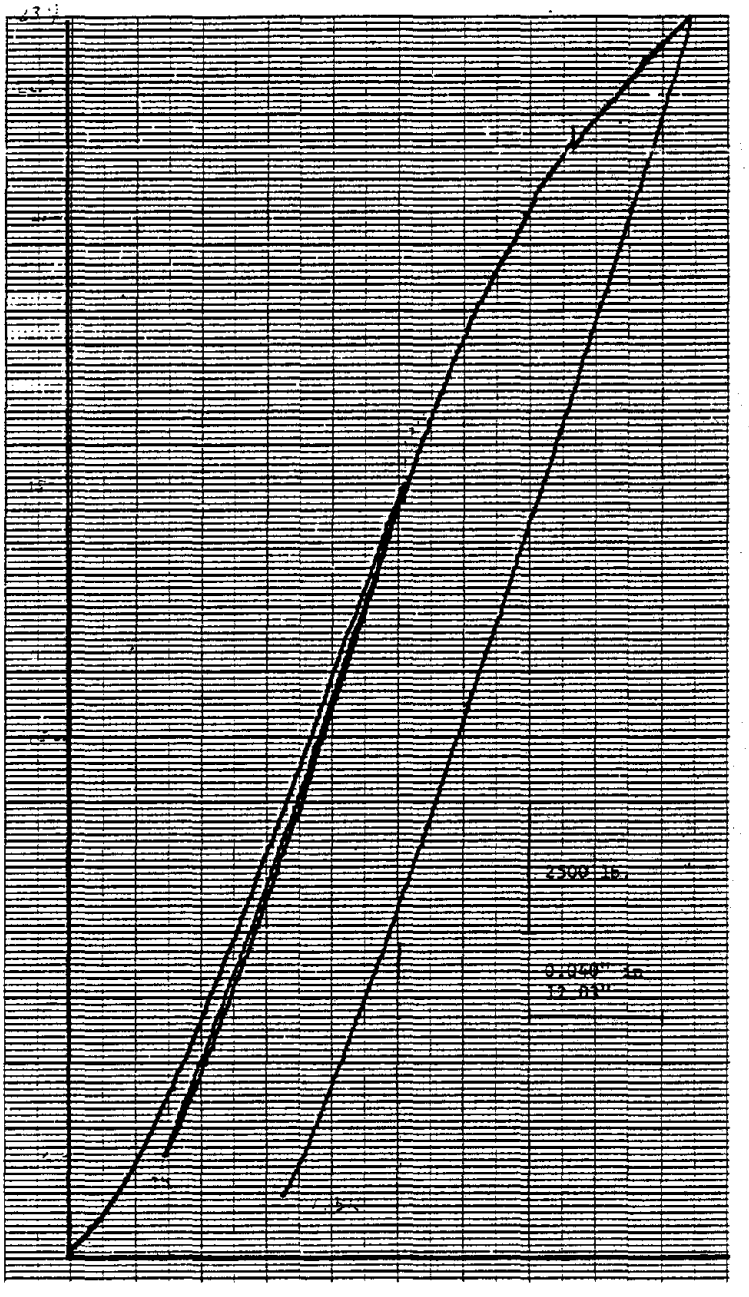

Fig. 25. Load-deflection curve for ½" wire rope.

$$E_e = \frac{2.2\times10^6\,\text{lb.}}{0.132\,\text{in.}^2} = 16.7\times10^6\ \text{lb./in.}^2$$

is the calculated value of E_e for the rope. It should be noted that the use of any of the other measures of A will only increase the computed value of E_e. As an extreme, if the value furnished by the *Wire Rope Users Manual* [40] is used, then E_e is calculated to be

$$E_e = \frac{2.2\times10^6 \text{ lb.}}{0.121 \text{ in.}^2} = 18.2\times10^6 \text{ lb./in.}^2.$$

These two values of E_e are, respectively, about 70% and 76% of the E_e for one of the outer strands, which in turn makes them, respectively, about 56% and 61% of E for the wire material.

Concluding remarks

A coherent set of tests were run on the wires and outer strands that comprise a particular wire rope of the type often used in mine hoists. Where rotation of the specimen ends could occur, special effort was made to minimize such rotation.

It was found that the effective Young's modulus for the outer strands was about 81% of the modulus for the wire material, and that, depending on the definition employed for the metallic area of the wire rope, the effective stiffness of the rope is approximately 75% of that of the strand, or about 60% of the modulus of the wire material.

IV. Factors affecting the useful life of a rope

A. Contact stresses

An important factor affecting the service life of a rope is the severe state of stress which occurs in regions of contact between wires. The stresses are a result of either a line contact or point contact between adjacent wires. This section is concerned with the determination of contact loads and the stresses resulting from such contact.

Consideration will be given at first to a simple straight strand, such as the one illustrated in the inset in Fig. 6. This strand consists of one straight wire surrounded by six helical wires. The strand will be loaded axially. Let the initial radius of the center wire be R_{11}, and let the initial radius and initial helix angle of the outer wire be R_{12} and α_{12}, respectively. The initial radius of the helix of the outer wire is

$$r_{12} = R_{11} + R_{12}.$$

For a given axial strand strain, ϵ_1, and a given strand twist, $\Delta\tau_1$, Eqns. (39) and (40) yield the axial wire strain, ϵ_{12}, the change in curvature, $\Delta\kappa'_{12}$, and the change in twist, $\Delta\tau_{12}$, of an outer wire. Equations (17) and (18) can then be used to determine the shear force, N'_{12}, and the normal force per unit length, X_{12}, acting on the outer wire. Once X_{12} is known, existing formulas [41] can be used to determine the elastic contact stresses.

It will be assumed, in calculating the contact stresses between the outer wire and the center wire, that the contact stresses are determined with sufficient accuracy by considering two cylindrical surfaces in contact along a straight line. The cross section of the circular cylinder will have a radius R_{12} and the cross section of the other cylindrical body (namely, the center wire) will have an elliptical cross section given by the equation

$$\frac{x^2}{(R_{11}/\sin\alpha_{12})^2} + \frac{y^2}{R_{11}^2} = 1,$$

where x and y are points on the boundary. The radius of curvature, ρ_1, at the point of contact is given by the expression

$$\rho_1 = \frac{R_{11}}{\sin^2\alpha_{12}}. \tag{140}$$

The maximum normal stress, σ_{zz}, at the surface of contact is given by the expression

$$\sigma_{zz} = -\frac{b}{\Delta}, \tag{141}$$

where

$$b = \left[\frac{-2X_{12}\Delta}{\pi}\right]^{1/2} \tag{142}$$

and

$$\Delta = \frac{4}{\dfrac{1}{R_{12}} + \dfrac{\sin^2\alpha_{12}}{R_{11}}} \frac{(1-\nu)}{E}. \tag{143}$$

Let, for example, $R_{11} = 0.0316$ in., $R_{12} = 0.0289$ in., $E = 30.0\times10^6$ psi, $\nu = 0.29$, and let the

pitch of an outer wire be 1.30 in. Hence $r_{12} = R_{11} + R_{12} = 0.0605$ in., and $\alpha_{12} = 73.7°$. Let the strand be loaded so that the ends of the strand are not allowed to rotate, i.e. $\Delta\tau_1 = 0$. Let the axial strain of the strand be $\epsilon_1 = 0.00222$. An application of Eqns. (39), (40), (19) and (8) yields:

$$T_{12} = 158 \text{ lb.},$$
$$H_{12} = -0.101 \text{ in.-lb.},$$

and

$$G'_{12} = -0.0990 \text{ in.-lb.}$$

Equations (17) and (18) then give

$$N'_{12} = 0.309 \text{ lb.}$$

and

$$X_{12} = -204 \text{ lb./in.}$$

Hence

$$\Delta = 1.91\times10^{-9} \text{ in.}^3\text{/lb.},$$
$$b = 498\times10^{-6} \text{ in.},$$

and

$$\sigma_{zz} = -260{,}000 \text{ psi.}$$

This large (compressive) stress occurs in both the center wire and in the helical outer wire, within the helical contact strip existing between the two wires. It is interesting to note that the axial stress in the center wire, in this example, has a value of only

$$E\epsilon_1 = 66{,}600 \text{ psi.}$$

The strand in this example is the same as that found in the center of the IWRC of a 6x19 Seale IWRC having a nominal rope diameter of 1¼ in. In such a rope, the strands surrounding the center strand tend to compress the center strand, thereby increasing the line contact force existing between the center wire and an outer wire of the core strand.

Furthermore, the IWRC strands surrounding the center strand of the IWRC contact the center strand along *points*, since the individual wires in the outer strands are in point contact with the wires of the center strand. As a consequence, the contact stresses that would be calculated on the basis of elastic contact-stress theory would be in the inelastic region; an elastic analysis of these contact stresses would be of questionable value.

B. Residual stresses

Another factor which may affect the useful life of a rope is the residual stresses. In general, residual tensile surface stresses are considered undesirable. In the case of wire ropes used in deep-shaft hoisting, however, the effect of residual stresses is minimized since the severe contact stresses (which give rise to a low-cycle fatigue problem) cause inelastic behavior of the material. This inelastic behavior tends to negate the effects of the residual stresses in fatigue. In the following paragraphs an estimate will be made of the residual stresses which occur as a result of preforming a wire into the helical shape it has in a strand.

The material properties of a given wire may be approximated by piecewise linear relationships in the elastic and inelastic regions, i.e.

$$\begin{aligned} \sigma &= E\epsilon, && \text{for } \epsilon \leqslant \epsilon_Y, \\ \sigma &= E_r\epsilon + (E-E_r)\epsilon_Y, && \text{for } \epsilon > \epsilon_Y, \end{aligned} \tag{144}$$

where σ is the stress, ϵ is the strain, E is Young's modulus, E_r is a reduced modulus, and ϵ_Y is the yield strain. The reduced modulus is the slope of the stress-strain diagram in the inelastic region.

When a wire is subjected to bending, the strain at a given distance y from the neutral axis of bending is given by the expression

$$\epsilon = \frac{y}{\rho}, \tag{145}$$

where ρ is the radius of curvature of the deformed wire. It is assumed, in writing Eqn. (145), that in the inelastic region plane sections remain plane and that the material properties of the wire in tension are the same as those in compression. Hence the stress distribution is given by the equations

$$\begin{aligned} \sigma &= E\, y/\rho, && \text{for } y \leqslant \epsilon_Y \rho, \\ \sigma &= E_r\, y/\rho + (E-E_r)\,\epsilon_Y, && \text{for } y > \epsilon_Y \rho. \end{aligned} \tag{146}$$

The momemt, M, resulting from this stress distribution is found by integrating the stress distribution according to the relation

$$M = \int_A \sigma\, y\, dA \tag{147}$$

over the cross-sectional area A; since the cross section is circular,

$$M = 4\int_0^R \sigma\, y\, (R^2-y^2)^{1/2}\, dy. \tag{148}$$

Thus the bending moment is given by

$$M = 4\int_0^{\epsilon_Y\rho} y^2\,(R^2-y^2)^{1/2}\,dy + 4\int_{\epsilon_Y\rho}^R \frac{E_r}{\rho}\, y^2\,(R^2-y^2)^{1/2}\,dy + 4\int_{\epsilon_Y\rho}^R \epsilon_Y\,(E-E_r)\,y\,(R^2-y^2)^{1/2}\,dy. \tag{149}$$

The integrals in Eqn. (149) can be readily evaluated by noting that

$$\int_a^b y^2\,(R^2-y^2)^{1/2}\,dy = -\frac{y\,(R^2-y^2)^{3/2}}{4} + \frac{R^2\,y\,(R^2-y^2)^{1/2}}{8} + \frac{R^4}{8}\sin^{-1}\left(\frac{y}{R}\right)\Bigg|_a^b$$

and

$$\int_a^b y\,(R^2-y^2)^{1/2}\,dy = -\frac{(R^2-y^2)^{3/2}}{3}\Bigg|_a^b.$$

Upon release of the moment M, the stress distribution is changed. The residual stress distribution can be obtained by superimposing on the stress distribution given by Eqns. (146) the elastic stress distribution given by the flexure formula for an equal but opposite bending moment, $-M$.

The change in curvature due only to the release of the moment M is given by the elastic-response relation, and hence the final curvature, $1/\rho_f$, is given by the formula

$$\frac{1}{\rho_f} = \frac{1}{\rho} - \frac{M}{EI}. \tag{150}$$

Consider a numerical example in which a wire with a radius R of 0.0289 in. is plastically deformed to a radius of curvature ρ of 0.768 in. The curvature, $1/\rho$, is then 1.30 in.$^{-1}$ and, if E and E_r are taken to be 28.0×10^6 psi and 7.0×10^6 psi, respectively, and the yield strain, ϵ_Y, is equal to 0.01 (corresponding to a yield stress of 280,000 psi), then Eqn. (149) yields a value of M of 11.6 lb.-in. Upon release of the bending moment, the maximum tensile residual stress has a value of 134,000 psi.

The maximum tensile residual stress occurs on the side closest to the center of curvature. The final curvature, from Eqn. (150), has the value

$$\frac{1}{\rho_f} = 0.551 \text{ in.}^{-1},$$

and the final radius of curvature, ρ_f, is therefore 1.81 in. It is interesting to note that if this wire is wrapped around a core wire having a radius of 0.0316 in., the curvature calculated here would correspond to a helix angle of 79.5°.

The numbers in this example are typical of the data pertaining to wires in the central strand of an IWRC. Although the wire radii and other geometrical factors will vary from wire to wire in a complex wire rope, it can be argued that the magnitudes of the residual stresses will be of the order of half the yield stress of the wire material, as found in this example.

Again it should be kept in mind that a wire has residual stresses before it is preformed into a strand or rope. Also, ropes may be pre-stretched in order to reduce the "constructional stretch" in the rope. This will also have an effect on the residual stresses.

C. Friction

Consider a strand consisting of one center wire surrounded by six helical wires. When the strand is unloaded, a line element in the normal direction of the outer helical wire passes through the centerline of the center wire. When the strand is loaded axially by a force and a twisting moment, this line element still passes through the centerline of the center wire in the deformed state. There is no shearing force in the normal direction on the cross section of an outer wire. There is also no relative motion between points of contact of the center wire and the other wire. The result is that no frictional force in the strand is generated even if the coefficient of friction has a nonzero value. This argument applies only if the strand is loaded axially.

If the strand is now bent over a sheave, relative motion does exist between the wires, and friction then becomes a factor. The frictional forces will cause shearing stresses on the surface of the wires and hence will be important in predicting the fatigue life of a rope. Determining the frictional forces analytically becomes an extremely difficult problem. It should be kept in mind that, while some parts of the wires slip relative to one another, other parts of the wires may not slip relative to one another and these portions will still develop frictional forces.

It is felt that, if a strand or rope is loaded axially, the frictional forces are minimal provided there are no broken wires. If a wire is broken, then there is relative motion between the wires and friction does become a factor. The analysis of broken wires is complicated by the same problem noted previously, namely, that some parts of the wires slip relative to one another, whereas other parts do not slip. In order to assess the importance of frictional effects on wire ropes used in hoisting operations, mechanical tests would be required.

It is interesting to note that, in the example considered in §IV.A above, some remarks can be made concerning the effects of a fracture of a center wire and the subsequent effects of friction. If the wires have a *very* large coefficient of friction and the center wire were to break, then no slipping would occur. If one were to invoke Saint-Venant's principle (namely, that a change in the distribution of the loads on an end, without change of the resultant, alters the stresses only near the end), then the stresses at a short distance away from the fractured center wire would remain essentially the same as those of the unfractured portion of the strand. The affected length would be of the order of the diameter of the strand.

If one assumes that the coefficient of friction is small, say $\mu \approx 0.1$, one can calculate a "slip length", L, over which the nominal stress, σ, in the center wire can be developed near a fractured end. The required slip length, L, can be deduced from the equilibrium condition

$$6 X_{12} \mu \frac{L}{\sin \alpha_{12}} = \sigma \pi R_{11}^2, \tag{151}$$

so that for the example given in §IV.A,

$$L = 1.64 \text{ in.}$$

The actual slip length will be somewhat less than L since X_{12} will increase in the vicinity of the fractured center wire; also, there will be a portion of the wire where the center wire does not slip relative to the outside wires even though frictional forces are involved. If the strand considered here is the center strand in an IWRC, the slip length, if any, would be very small since the normal loads are much greater than those produced by X_{12} alone.

Similar remarks can be made concerning the center wires in the outer strands of a rope. One can also make some estimates of the slip length of an outer wire. Each time an outer wire contacts the core of the rope, a normal force is generated. If the coefficient of friction is very large, a broken outer wire will pick up the nominal stress in a very short length after the contact point. If the coefficient of friction is small, it may take more than one contact point to develop the nominal stress in an outer wire.

V. Conclusions

It has been shown that the static response of a rope can be predicted by linearizing not only the equations governing the response of wires within a strand, but also those governing the response of strands within a rope. The procedure allows complex cross sections to be analyzed with relative ease, and the solution has been extended to treat the case of a rope passing over a sheave. A computer program has been written for plotting the maximum tensile stress in the individual wires of any rope whose cross section can be described by a fairly general set of rules. Specific results have been presented for some simple rope constructions, as well as for 6x19 Seale and 6x25 filler-wire ropes both with and without internal-wire-rope cores.

An interesting result is found for the Seale IWRC. When this rope is pulled axially, the maximum stress occurs in the center wire of the IWRC. As the rope is bent over a sheave, the maximum axial wire stress may shift to the center wire in the outer strands, since the center wire in the outer strand has a larger diameter than does the center wire in the IWRC. Whether or not this "crossover" occurs depends on the radius of the sheave since the size of the sheave and the diameters of the individual wires in the rope determine the primary bending stresses in the rope.

The numerical results of the static stress analysis of several types of rope are summarized in Table 2. The nondimensional "stress factors" z_{si}^T and z_{si}^B are used in the equation

$$\frac{\sigma_{max}}{\sigma_{nom}} = z_{si}^T + \frac{z_{si}^B}{\frac{D}{d}\cdot\frac{\sigma_{nom}}{E}},$$

where σ_{max} is the maximum tensile stress in a rope loaded axially and simultaneously bent over a sheave, σ_{nom} is the nominal stress given by the axial load divided by the metallic area of the rope, D/d denotes the ratio of the sheave diameter to the rope diameter, and E is Young's modulus of the wire material. The "crossover" referred to in the case of the Seale IWRC arises because the wire for which z_{si}^T is a maximum is not the wire for which z_{si}^B is a maximum.

A *conservative* estimate of the maximum stresses in a given rope can be made by selecting the maxima of both z_{si}^T and z_{si}^B, regardless of which wire(s) possess these maxima. Thus, for the Seale rope with no core,

$$\frac{\sigma_{max}}{\sigma_{nom}} = 1.29 + \frac{0.0847}{\frac{D}{d}\cdot\frac{\sigma_{nom}}{E}},$$

whereas for the Seale IWRC,

$$\frac{\sigma_{max}}{\sigma_{nom}} = 1.42 + \frac{0.0812}{\frac{D}{d}\cdot\frac{\sigma_{nom}}{E}}.$$

The corresponding formulas for the 6x25 filler-wire construction would be

$$\frac{\sigma_{max}}{\sigma_{nom}} = 1.21 + \frac{0.0686}{\frac{D}{d}\cdot\frac{\sigma_{nom}}{E}}$$

for the filler-wire with no core, and

$$\frac{\sigma_{max}}{\sigma_{nom}} = 1.31 + \frac{0.0656}{\frac{D}{d}\cdot\frac{\sigma_{nom}}{E}}$$

Table 2. Stress coefficients for various ropes

Type of rope	Strand (s)	Wire (i)	z_{si}^T	z_{si}^B
Solid rod	1	1	1.000	1.000
7-wire strand	1	1	1.128	0.3529
	1	2	1.103	0.3071
7x7 lang lay	1	1	1.253	0.1271
	1	2	1.225	0.1106
	2	1	1.127	0.1039
	2	2	1.117	0.0953
6x19 Seale	1	1	1.294	0.0847
	1	2	1.244	0.0402
	1	3	1.198	0.0675
6x19 Seale IWRC	1	1	1.424	0.0483
	1	2	1.392	0.0420
	2	1	1.281	0.0395
	2	2	1.270	0.0362
	3	1	1.262	0.0812
	3	2	1.214	0.0386
	3	3	1.168	0.0648
6x25 filler-wire	1	1	1.208	0.0686
	1	2	1.197	0.0620
	1	3	1.142	0.0262
	1	4	1.133	0.0543
6x25 filler-wire IWRC	1	1	1.312	0.0503
	1	2	1.308	0.0447
	2	1	1.293	0.0424
	2	2	1.289	0.0385
	3	1	1.154	0.0656
	3	2	1.144	0.0593
	3	3	1.091	0.0250
	3	4	1.081	0.0519

for the filler-wire with the IWRC. On the basis of these results, it can be concluded that the stresses in a filler-wire rope are less than the stresses in a Seale rope, and that, for either rope, the advantage of including an IRWC is that the maximum stresses due to bending are reduced somewhat—but only at the expense of introducing significant axial stresses in the straight or nearly straight wires of the IWRC.

An interesting result [34] for axially loaded ropes has been demonstrated. The axial stiffness, or effective modulus, given by

$$E_e = K_1 E,$$

where E is the Young's modulus of the wire material, is found to decrease as additional strands are added to a rope. Specifically, for the Seale IWRC, $E_e = 0.866E$ for the center (1x7) strand alone, $E_e = 0.798E$ for the (7x7) IWRC alone, and $E_e = 0.704E$ for the entire 6x19 Seale IWRC. Experiments described in this report and elsewhere [35] indicate that the actual effective modulus of rope is somewhat smaller than these theoretical results, even when care is taken to prevent rotation of the wire-rope grips during loading. It should be mentioned that the theory neglects contact deformation between the wires and consequently the theory should predict an upper bound on the effective modulus. Also, the inter-strand penetration which certainly occurs between the various layers of strands in a rope, is neglected; this penetration accounts, perhaps, for much of the decrease in modulus of the rope (as compared to the modulus of the wire material).

In related work [30] it has been shown that the contact stresses between wires in simple strands can be very large. Contact stresses are felt to be principally responsible for the initiation of internal failures, particularly those in axially fatigued rope. The computer program given in this report allows the normal forces on wires and strands to be calculated.

Estimates are made for the length from the fractured end of broken wire wherein the wire will again develop its nominal load-bearing capacity. One can predict this length on the basis of equilibrium, estimates of the coefficient of friction and of the normal contact force, and Saint-Venant's principle. For wires in the core of an IWRC rope, this length is very small (perhaps of the order of a strand diameter) since these wires are subjected to very large lateral compressive forces. The lengths in the outer wires of outside strands will of course be larger. The lengths can again be estimated since an outer wire comes in contact with the core each time a lay length of the outer wires in a strand is traversed. Knowing the normal force, one can then calculate the maximum frictional force and can hence estimate the length required to develop the nominal load-bearing capacity in the wire.

The dynamic equations of motion for an axially loaded rope are presented. The equations are based on the static response in which the axial force and the axial twisting moment are written as linear functions of the axial strain and the rotational strain. Expressions are presented for the strains and loads in a rope subjected to various dynamic loading conditions associated with deep-shaft hoisting. These expressions are based on an analysis in which the rotational strains are neglected; this assumption has been shown to be reasonable for the types of problem considered [31]. In predicting the useful life of a rope, the dynamic loads must be taken into account since it is the maximum stress which occurs during a cycle that affects the fatigue life.

Theoretically, the maximum stresses in a rope are generated when the skip is moving downward and the upper end of the rope is suddenly clamped. This condition, however, is difficult to produce since it is nearly impossible to arrest the motion of a particular point along a moving rope *instantaneously*. Of the dynamic loading situations considered in this study, the one which routinely gives rise to the largest stresses is the one in which a fully loaded skip is accelerated upward.

In the case where muck is being dumped into a suspended skip, it was found that the dumping times normally encounted in mining situations are long enough to allow the rope stresses to be computed statically with minimal error.

Residual stresses in the rope due to preforming were found theoretically to be of the order of one-half the yield strength of the wire material. However, the actual states of residual stress in individual wires could vary radically, depending upon the degree of stretching that accompanies the rope-forming process.

Estimates of the stresses in wires due to contact line loads are not consistent with the use of elastic contact-stress theory, if prior contact flattening is neglected.

In view of the difficulty of quantifying the state of residual stress and working values of the contact stresses, it is concluded that a prediction of the useful life of a rope can only be accomplished by bend-over-sheave tests. These tests should, however, be run on small-scale models of particular wire-rope constructions. The amount of testing can be considerably reduced by employing the theory of dimensional analysis. The small-scale tests can also be run at a higher cycling rate, since the temperature effects would not be as pronounced as they would be for large-scale ropes.

VI. Recommendations for further study

Expressions have been presented for a determination of the maximum tensile stresses on the wire cross sections and, in particular, curves have been drawn for these stresses in Seale rope, in 6x25 filler-wire rope, and in some simpler rope constructions. Similar results should be generated for other types of rope used in hoisting operations.

It is also known that the maximum stresses occur at the contact points between individual wires and this is also where the phenomenon of fretting fatigue takes place. The contact stress at these points are in the inelastic region and hence an analysis of the stresses at these points in bend-over-sheave tests would be extremely complex. Hence it is felt that fatigue tests must be resorted to in determining the useful life of a rope. Such tests would also eliminate the need of determining the residual stresses in individual wires.

In any testing program, the theory of dimensional analysis plays an important role. Use of such a theory reduces considerably the number of tests which must be performed. These tests would be performed on small-scale wire ropes, which are already available. The results of such tests would then be used to predict the life of large-diameter wire ropes. The use of small-scale tests also reduces the time to obtain fatigue data since the temperature effect is minimized.

References

[1] Suslov, B. M., "On the modulus of elasticity of wire ropes," *Wire and Wire Products*, **11**, 176-182 (1936).

[2] *Wire Rope Handbook* (St. Louis: Leschen Wire Rope Co., 1971).

[3] Scoble, W. A., "First Report of the Wire Rope Research Committee," *Proc. Institution of Mechanical Engineers*, **115**, 835-868 (1920). Second Report, *Proc.*, **119**, 1193-1290 (1924). Third Report, *Proc.*, **123**, 353-404 (1928). Fourth Report, *Proc.*, **125**, 553-602 (1930). Fifth Report, *Proc.*, **130**, 373-478 (1935).

[4] Woernle, R., "Drahlseilforschung," *Z. des Vereines Deutscher Ingenieure*, **73**, 417-426, 1623-1624 (1929). Also, *Z.*, **74**, 1417-1419 (1930). Also, *Z.*, **75**, 206-209, 1485-1489 (1931). Also, *Z.*, **76**, 557-560 (1932). Also, *Z.*, 77, 799-803 (1933). Also, *Z.*, **78**, 1492-1498 (1934). Also, *Z.*, **79**, 1281-1282 (1935). Also, *Z.*, **83**, 1056 (1939).

[5] de Forest, A. V. and Hopkins, L. W., "Testing of rope and wire rope," *Proc. American Society for Testing and Materials*, **32**, 398-412 (1932).

[6] Skillman, E., "Some tests of steel wire rope on sheaves," U. S. Bureau of Standards Technologic Paper No. 229, 227-243 (March 2, 1923).

[7] Drucker, D. C. and Tachau, H., "A new design criterion for wire rope," *Journal of Applied Mechanics, Trans. ASME*, **67**, A-33—A-38 (1945).

[8] Hall, H. M., "Stresses in small wire ropes," *Wire and Wire Products*, **26**, 257-259 (1951).

[9] Hruska, F. H., "Calculations of stresses in wire rope," *Wire and Wire Products*, **26**, 766-767, 799-801 (1951).

[10] Hruska, F. H., "Radial forces in wire rope," *Wire and Wire Products*, **27**, 459-463 (1952).

[11] Hruska, F. H., "Tangential forces in wire ropes," *Wire and Wire Products*, **28**, 455-460 (1953).

[12] Leissa, A. W., "Contact stresses in wire ropes," *Wire and Wire Products*, **34**, 307-314, 372-373 (1959).

[13] Starkey, W. L. and Cress, H. A., "An analysis of critical stresses and mode of failure of a wire rope," *Journal of Engineering for Industry, Trans. ASME*, **81**, 307-316 (1959).

[14] Bert, C. W. and Stein, R. A., "Stress analysis of wire rope in tension and torsion," *Wire and Wire Products*, **37**, 769-770 (1962).

[15] Machida, S. and Durelli, A. J., "Response of a strand to axial and torsional displacements," *Journal of Mechanical Engineering Science*, **15**, 241-251 (1973).

[16] Durelli, A. J. and Machida, S., "Response of epoxy oversized models of strands to axial and torsional loads," *Experimental Mechanics*, **13**, 313-321 (1973).

[17] Chi, M., "Analysis of multi-wire strands in tension and combined tension and torsion," *Developments in Mechanics* (Proc. 7th Southeastern Conf. on Theoretical and Applied Mechanics), **7**, 599-639 (1974).

[18] Phillips, J. W. and Costello, G. A., "Contact stresses in twisted wire cables," *Journal of the Engineering Mechanics Division, ASCE*, **99**, 331-341 (1973).

[19] Costello, G. A. and Phillips, J. W., "Contact stresses in thin twisted rods," *Journal of Applied Mechanics*, **40**, 629-630 (1973).

[20] Costello, G. A. and Phillips, J. W., "A more exact theory for twisted wire cables," *Journal of the Engineering Mechanics Division, ASCE*, **100**, 1096-1099 (1974).

[21] Love, A. E. H., *A Treatise on the Mathematical Theory of Elasticity* (New York: Dover Publications, 1944), chapters 18 and 19.

[22] Samras, R. K., Skop, R. A. and Milburn, D. A., "An analysis of coupled extension-torsional

oscillations in wire rope," *Journal of Engineering for Industry, Trans. ASME*, **96**, 1130-1135 (1974).

[23] Costello, G. A. and Phillips, J. W., "Effective modulus of twisted wire cables," *Journal of the Engineering Mechanics Division, ASCE*, **102**, 171-181 (1976).

[24] Phillips, J. W. and Costello, G. A., "Axial impact of twisted wire cables," *Journal of Applied Mechanics*, **44**, 127-131 (1977).

[25] Costello, G. A. and Sinha, S. K., "Static behavior of wire rope," *Journal of the Engineering Mechanics Division, ASCE*, **103**, 1011-1022 (1977).

[26] Costello, G. A., "Large deflections of helical springs due to bending," *Journal of the Engineering Mechanics Division, ASCE*, **103**, 481-487 (1977).

[27] Costello, G. A. and Miller, R. E., "Lay effect of wire rope," *Journal of the Engineering Mechanics Division, ASCE*, **105**, 597-608 (1979).

[28] Costello, G. A. and Sinha, S. K., "Torsional stiffness of twisted wire cables," *Journal of the Engineering Mechanics Division, ASCE*, **103**, 766-770 (1977).

[29] Costello, G. A. and Miller, R. E., "Static response of reduced rotation rope," *Journal of the Engineering Mechanics Division, ASCE*, **106**, 623-631 (1980).

[30] Phillips, J. W., Miller, R. E., and Costello, G. A., "Contact stresses in a straight cross-lay wire rope," Proc. 1st Annual Wire Rope Symposium (March 1980, Denver) (published by Washington State University, Pullman, 1980), 177-199 (1980).

[31] Butson, G. J., "Static and dynamic analysis of axially loaded wire rope," Ph.D. thesis, Department of Theoretical and Applied Mechanics, University of Illinois at Urbana-Champaign, 99 pp. (1981).

[32] Butson, G. J., Phillips, J. W., and Costello, G. A., "Stresses in wire rope due to dynamic loads associated with deep shaft hoisting systems," Proc. 1st Annual Wire Rope Symposium (March 1980, Denver) (published by Washington State University, Pullman, 1980), 243-273 (1980).

[33] Costello, G. A. and Butson, G. J., "A simplified bending theory for wire rope," *Journal of the Engineering Mechanics Division, ASCE*, **108**, 219-227 (1982).

[34] Velinsky, S. A., "Analysis of wire ropes with complex cross sections," Ph.D. thesis, Department of Theoretical and Applied Mechanics, University of Illinois at Urbana-Champaign, 87 pp. (1981).

[35] Velinsky, S. A., Anderson, G. L., and Costello, G. A., "Wire rope with complex cross sections," University of Illinois at Urbana-Champaign Technical Report UILU-ENG 81-6002 (Theoretical and Applied Mechanics Report No. 448), 22 pp. (1981).

[36] Hoeppner, D. W. and Gates, F. L., "Fretting fatigue conditions in engineering design," *Wear*, **70**, 155-164 (1981).

[37] McConnell, K. G. and Zemke, W. P., "The measurement of flexural stiffness of multistranded electrical conductors while under tension," *Experimental Mechanics*, **20**(6), 198-204 (1980).

[38] *Code of Federal Regulations*, **30** (Mineral Resources), §57.19-39 (1980).

[39] Timoshenko, S., Young, D. H., and Weaver, W., Jr., *Vibration Problems in Engineering*, 4th ed. (New York: John Wiley, 1974), 380-399.

[40] *Wire Rope Users Manual* (Washington, DC: American Iron and Steel Institute, 1979).

[41] Boresi, A. P., Sidebottom, O. M., Seely, F. B., and Smith, J. O., *Advanced Mechanics of Materials*, 3rd ed. (New York: John Wiley, 1978), Chapter 14.

APPENDIX

Computer program for stresses in wire rope loaded axially and bent over a sheave

Note 1: This program is written in ANSI 77 Fortran and has been compiled successfully on a CDC Cyber 175. An attempt has been made to avoid CDC extensions to the ANSI 77 Fortran, so that the code should work on any computer for which an ANSI 77 Fortran compiler is available.

Note 2: The 'PROGRAM' statement may have to be removed when running the code on a non-CDC computer.

Note 3: A sample of printed output is given at the end of this computer listing. In addition to the output print file (TAPE6 in this listing), an output plot file (TAPE9 in this listing--see the CALL PLOTS statement) is also created when the program is run. The plot file contains the plotter instructions for drawing two figures, side by side, on 11-in.-wide plotter paper. The first of these two figures is a plot of the ratio of the maximum wire stress to the nominal stress, as a function of the parameter (D/d)*signom/E. The second of these two figures is a detailed drawing of the wire cross section, like the one in Fig. 3 of this report. For plotters equipped with two or more pens, it is suggested that pen #1 be fine tipped and pen #2 be broad tipped.

Note 4: Routines not supplied in this listing are the standard plotting routines PLOTS, PLOT, NEWPEN, AXIS, LINE, SYMBOL, and NUMBER. These routines will be found in the plotting software supplied by the manufacturer of the user's plotter.

Note 5: The user may have to modify the character strings appearing in the CALL AXIS statement in the main program, as well as those in the DATA statement in subroutine GEOM, in order to make the strings recognizable by the user's vendor-supplied SYMBOL routine. The character strings given in this listing are compatible with a locally available SYMBOL routine that allows the plotting of upper- and lower-case English and Greek letters and special mathematical symbols.

Note 6: The notation used in this computer listing follows, as closely as possible, the notation used in the section of this Report entitled, "Theoretical Analysis of Wire Rope: Static Analysis."

Note 7: Questions concerning the implementation of this computer program on the user's computing system may be directed to Prof. J. W. Phillips at 217/333-4388.

```
      PROGRAM        SHEAVE (INPUT,OUTPUT,TAPE5=INPUT,TAPE6)
C
C     MAIN PROGRAM FOR PULLING A ROPE OVER A SHEAVE
```

Computer Program: Stresses in Loaded Wire Rope Bent over a Sheave

```
C
C     INPUT DATA REQUIRED OF USER --
C
C     -        TYPE OF ROPE        SEE SUBROUTINE 'GEOM'
C
C-----------------------------------------------------------------
      PARAMETER      (PI=3.14159265,
     &                K=4)
C
C     K = MAX (MAX# WIRE LAYERS IN A STRAND, # STRAND LAYERS IN A ROPE)
C
      REAL           ALPHA(K,0:K), BIGR(0:K,0:K), ETA(0:K,0:K,K),
     &               EPS(0:K,0:K), DTAU(0:K,0:K), DKAP(0:K,0:K),
     &               DRDEPS(K),    DRDTAU(K),
     &               NU, SOL(3)
      INTEGER        S, T, M(K,0:K), LAYERS(0:K)
      COMMON /VAR/   ALPHA, BIGR, ETA, EPS, DTAU, DKAP,
     &               DRDEPS, DRDTAU, NU, M, LAYERS
      REAL           BIGT(0:K,0:K), GPRIME(0:K,0:K),
     &               BIGH(0:K,0:K), NPRIME(0:K,0:K),
     &               KAP(0:K,0:K),  TAU(0:K,0:K),
     &               R(0:K,0:K),    E,
     &               OFFANG(K,0:K)
      COMMON /VAR/   BIGT, GPRIME, BIGH, NPRIME,
     &               KAP, TAU, R, E, OFFANG
      CHARACTER*60   DESC
      COMMON /CVAR/ DESC
C-----------------------------------------------------------------
C
      REAL           X(102), Y(102), ZT(K,K), ZB(K,K)
      LOGICAL        YES, NO, LABEL
      DATA           YES/.TRUE./, NO/.FALSE./,
     &               DX/0.05/, DY/1./,
     &               UP/1.5/, OVER/1.3/
      FACTOR(X) = SIN(PI*X/180.)/(1.+NU/2.*COS(PI*X/180.)**2)
C
C     DEFINE THE ROPE
C
      CALL   GEOM
C
C     SEE WHAT AN AXIAL STRAIN WILL DO, WITH NO TWIST
C
      EPS00  = 0.001000
      DTAU00 = 0.
      CALL   ROPE   (EPS00, DTAU00, YES)
C
C      AT THIS STAGE, THE GENERALIZED FORCES ACTING ON ALL WIRES
C      IN THE STRAIGHT ROPE ARE KNOWN FOR THE PRESCRIBED AXIAL
C      STRAIN OF THE ROPE.  NOW CONSIDER THE EFFECT OF BENDING THE
C      ROPE OVER A SHEAVE OF A GIVEN D/D RATIO.
C
C     COMPUTE THE METALLIC AREA OF THE ROPE
```

```
C
      A = 0.
      DO 20 S = 1, LAYERS(0)
         AS = 0.
         DO 10 I = 1, LAYERS(S)
   10       AS = AS + M(S,I)*PI*BIGR(S,I)**2
   20    A = A + M(S,0)*AS
C
C     NOTE THE RADIUS OF THE ROPE
C
      BIGR(0,0) = R(LAYERS(0),0) + BIGR(LAYERS(0),0)
C
C     COMPUTE THE NOMINAL STRESS
C
      SIGNOM = BIGT(0,0)/A
C
      WRITE  (6,25) DESC, EPS(0,0), DTAU(0,0), BIGT(0,0), A, SIGNOM
   25 FORMAT (///' FOR A STRAIGHT ', A
     &          /'          -------- '
     &          /' SUBJECTED TO EPS(0,0) =', F9.6,
     &           ' AND DTAU(0,0) =', F9.6, ', THE NOMINAL'
     &          /' STRESS GIVEN BY BIGT(0,0)/A IS COMPUTED AS FOLLOWS:'
     &         //20X, 'BIGT(0,0) =', F10.1, ' LB., AND'
     &          /20X, 'A       =', F10.4, ' IN.**2; HENCE'
     &          /20X, 'SIGNOM    =', F10.0, ' LB./IN.**2.')
C
C     SET UP PLOTTER:  OPEN TAPE9; MOVE ORIGIN
C
      CALL   PLOTS  (0, 0, 9)
      CALL   PLOT   (OVER, UP, -3)
C
C     DETERMINE A GOOD LOWER BOUND FOR THE INDEX N1 THAT GOVERNS
C     THE MINIMUM VALUE OF (D/D)*SIGNOM/E THAT WILL BE PLOTTED
C
      YMAX   = 8.*DY
      N1     = 1
      DO 29 S = 1, LAYERS(0)
         DO 28 I = 1, LAYERS(S)
            ZTSI1  = BIGT(S,I)/(PI*BIGR(S,I)**2) / SIGNOM
            ZTSI2  = 4./(PI*BIGR(S,I)**3) * ABS(GPRIME(S,I)) / SIGNOM
            ZTSI3  = E * FACTOR(ALPHA(S,I))*BIGR(S,I)*ABS(DKAP(S,0))
     &               / SIGNOM
            ZT(S,I)= ZTSI1 + ZTSI2 + ZTSI3
            ZB(S,I)= BIGR(S,I)/BIGR(0,0)
     &               * FACTOR(ALPHA(S,I)) * FACTOR(ALPHA(S,0))
            N1SI   = 1 + ZB(S,I)/((0.1*DX)*(YMAX-ZT(S,I)))
   28       N1     = MAX(N1,N1SI)
   29    CONTINUE
C
C     PRINT OUT THE ZT(S,I) AND ZB(S,I)
C
      WRITE (6,30) DESC, ((S,I,ZT(S,I),ZB(S,I),I=1,LAYERS(S)),
```

Computer Program: Stresses in Loaded Wire Rope Bent over a Sheave

```
     &                                                S=1,LAYERS(0))
    30 FORMAT (//' FOR A ', A
     &          /' BENT AROUND A SHEAVE AND LOADED AXIALLY, THE FACTORS'
     &          /' ZT(S,I) AND ZB(S,I) IN THE FORMULA'
     &         //'           SIGMAX                    ZB(S,I)    '
     &          /'           ------  =  ZT(S,I) + --------------'
     &          /'           SIGNOM                 (D/D)SIGNOM/E'
     &         //' ARE:'
     &         //'    S     I    ZT(S,I)    ZB(S,I)'
     &          /'    -     -    -------    -------'
     &          /(   I5,   I5,     F9.3,     F11.5  ))
      WRITE (6,31)
    31 FORMAT (//' NUMERICAL RESULTS BASED ON THESE VALUES OF ZT(S,I)'
     &          /' AND ZB(S,I) ARE GIVEN BELOW.')
C
      DO 50 S = 1, LAYERS(0)
         DO 40 I = 1, LAYERS(S)
            NPTS = 0
C
C           N1 IS DETERMINED ABOVE
C
            N2   = 60
            DO 32 N = N1, N2
               NPTS = NPTS + 1
               DBYDSE = 0.1*DX * N
               X(NPTS)= DBYDSE
    32         Y(NPTS)= ZT(S,I) + ZB(S,I)/DBYDSE
            WRITE  (6,33) I, S, (X(N),Y(N), N=1,NPTS)
    33 FORMAT (//' SIGMAX/SIGNOM--WIRE', I2, ', STRAND', I2,
     &          ' [X = (D/D)SIGNOM/E; Y = SIGMAX/SIGNOM]:'
     &         //5('     X     Y     ')
     &         //(5(F6.3,F5.2,3X)))
            X(NPTS+1) = 0.
            X(NPTS+2) = DX
            Y(NPTS+1) = 0.
            Y(NPTS+2) = DY
C
C           DRAW LINE THROUGH POINTS
C
            L       = K*(S-1) + (I-1)
            CALL    NEWPEN (1)
            CALL    NEWPEN (2)
            CALL    LINE   (X, Y, NPTS, 1, 10, L)
    40      CONTINUE
    50   CONTINUE
C
C     LABEL PLOT WITH TYPE OF ROPE
C
      CALL   NEWPEN (1)
      CALL   NEWPEN (2)
      CALL   SYMBOL (0.5, 0.3, 0.25, DESC, 0., 60)
C
```

```
C     FURNISH KEY TO SYMBOLS ON PLOT
C
      CALL    NEWPEN (2)
      CALL    NEWPEN (1)
      CALL    XSECTN (3.8, 5.8, 2.0, NO, YES, 1, 1)
C
C     DRAW AXES
C
      CALL    NEWPEN (2)
      CALL    NEWPEN (1)
      CALL    AXIS   (0., 0.,
     &                '                (D/!2D)!0(!4S!7!2NOM!8/!1E  ',
     &                -36, 6., 0., X(NPTS+1), X(NPTS+2))
      CALL    AXIS   (0., 0.,
     &                '                ' //
     &                'N!2ORMALIZED MAX. TENSILE WIRE STRESS, ' //
     &                '!4S!7!2MAX!8/!4S!7!2NOM!8                ',
     &                +80, 8., 90., Y(NPTS+1), Y(NPTS+2))
      CALL    AXIS   (0., 8., ' ', +1, 6.,  0., X(NPTS+1), 0.)
      CALL    AXIS   (6., 0., ' ', -1, 8., 90., Y(NPTS+1), 0.)
C
C     SKIP OVER AND PLOT THE CROSS SECTION OF THE ROPE
C
      CALL    PLOT   (-OVER, -UP, -3)
      CALL    PLOT   (8.5, 0., -3)
      CALL    NEWPEN (1)
      CALL    NEWPEN (2)
      CALL    XSECTN (4.25, 5., 3.5, YES, NO, 2, 1)
C
C     SHUT DOWN PLOTTER
C
      CALL    PLOT   (8.5, 0., 999)
      STOP    'SUCCESSFUL RUN FOR THIS ROPE.'
      END
C
C=====================================================================
C
      SUBROUTINE    ROPE (EPS00, DTAU00, WANTED)
      LOGICAL       WANTED
C
C     SUBROUTINE FOR ANALYZING STRAINS IN A STRAIGHT ROPE
C
C     NOMENCLATURE
C     ------------
C        EPS00      IMPOSED AXIAL STRAIN ON STRAIGHT ROPE
C        DTAU00     IMPOSED AXIAL TWIST ON STRAIGHT ROPE (1/IN.)
C        WANTED     = .TRUE. IF PRINTOUT WANTED; OTHERWISE, .FALSE.
C
C---------------------------------------------------------------------
      PARAMETER     (PI=3.14159265,
     &               K=4)
C
```

Computer Program: Stresses in Loaded Wire Rope Bent over a Sheave

```
C      K = MAX (MAX# WIRE LAYERS IN A STRAND, # STRAND LAYERS IN A ROPE)
C
       REAL           ALPHA(K,0:K), BIGR(0:K,0:K), ETA(0:K,0:K,K),
      &               EPS(0:K,0:K), DTAU(0:K,0:K), DKAP(0:K,0:K),
      &               DRDEPS(K),    DRDTAU(K),
      &               NU, SOL(3)
       INTEGER        S, T, M(K,0:K), LAYERS(0:K)
       COMMON /VAR/   ALPHA, BIGR, ETA, EPS, DTAU, DKAP,
      &               DRDEPS, DRDTAU, NU, M, LAYERS
       REAL           BIGT(0:K,0:K), GPRIME(0:K,0:K),
      &               BIGH(0:K,0:K), NPRIME(0:K,0:K),
      &               KAP(0:K,0:K),  TAU(0:K,0:K),
      &               R(0:K,0:K),    E,
      &               OFFANG(K,0:K)
       COMMON /VAR/   BIGT, GPRIME, BIGH, NPRIME,
      &               KAP, TAU, R, E, OFFANG
       CHARACTER*60   DESC
       COMMON /CVAR/  DESC
C-----------------------------------------------------------------
C
C      NOMENCLATURE (ROPE VARIABLES)
C      -----------------------------
C
C      DKAP   (0,0)   CHANGE IN CURVATURE OF ROPE
C      BIGH   (0,0)   TWISTING MOMENT     ON ROPE
C      BIGT   (0,0)   AXIAL FORCE         ON ROPE
C      DTAU   (0,0)   CHANGE IN TWIST     OF ROPE
C      EPS    (0,0)   AXIAL STRAIN        OF ROPE
C      GPRIME(0,0)    BENDING MOMENT      ON ROPE
C      KAP    (0,0)   INITIAL CURVATURE   OF ROPE (=0.)
C      LAYERS(0)      NUMBER OF LAYERS OF STRANDS WITHIN ROPE
C      NPRIME(0,0)    SHEAR FORCE         ON ROPE (=0.)
C      TAU    (0,0)   INITIAL TWIST       OF ROPE (=0.)
C
C      NOMENCLATURE (STRAND VARIABLES)
C      -------------------------------
C
C      ALPHA  (S,0)   HELIX ANGLE         OF STRAND S WITHIN ROPE
C      BIGH   (S,0)   TWISTING MOMENT     ON STRAND S WITHIN ROPE
C      BIGT   (S,0)   AXIAL FORCE         ON STRAND S WITHIN ROPE
C      BIGR   (S,0)   STRAND RADIUS       OF STRAND S WITHIN ROPE
C      DKAP   (S,0)   CHANGE IN CURVATURE OF STRAND S WITHIN ROPE
C      DRDEPS(S)      RATE OF CHANGE OF STRAND RADIUS OF STRAND S
C                     WITH RESPECT TO AXIAL STRAIN OF STRAND S
C      DRDTAU(S)      RATE OF CHANGE OF STRAND RADIUS OF STRAND S
C                     WITH RESPECT TO CHANGE IN TWIST OF STRAND S
C      DTAU   (S,0)   CHANGE IN TWIST     OF STRAND S WITHIN ROPE
C      EPS    (S,0)   AXIAL STRAIN        OF STRAND S WITHIN ROPE
C      ETA    (0,S,T) R(S,0)    = SUM ON T OF ETA(0,S,T)*BIGR(T,0)
C                     (T=1,...,S)
C      ETA    (S,0,J) BIGR(S,0)= SUM ON J OF ETA(S,0,J)*BIGR(S,J)
C                     (J=1,...,LAYERS(S))
```

```
C     GPRIME(S,0)   BENDING MOMENT       ON STRAND S WITHIN ROPE
C     KAP   (S,0)   INITIAL CURVATURE    OF STRAND S WITHIN ROPE
C     LAYERS(S)     NUMBER OF LAYERS OF WIRES IN STRAND S
C     M     (S,0)   NUMBER OF STRANDS IN STRAND LAYER S OF ROPE
C     NPRIME(S,0)   SHEAR FORCE          ON STRAND S WITHIN ROPE
C     TAU   (S,0)   INITIAL TWIST        OF STRAND S WITHIN ROPE
C
C     NOMENCLATURE (WIRE VARIABLES)
C     -----------------------------
C
C     ALPHA (S,I)   HELIX ANGLE          OF WIRE I IN STRAND S
C     BIGH  (S,I)   TWISTING MOMENT      ON WIRE I IN STRAND S
C     BIGT  (S,I)   AXIAL FORCE          ON WIRE I IN STRAND S
C     BIGR  (S,I)   WIRE RADIUS          OF WIRE I IN STRAND S
C     DKAP  (S,I)   CHANGE IN CURVATURE OF WIRE I IN STRAND S
C     DTAU  (S,I)   CHANGE IN TWIST      OF WIRE I IN STRAND S
C     EPS   (S,I)   AXIAL STRAIN         OF WIRE I IN STRAND S
C     ETA   (S,I,J) R(S,I) = SUM ON J OF ETA(S,I,J)*BIGR(S,J)
C                   (J=1,...,I)
C     GPRIME(S,I)   BENDING MOMENT       ON WIRE I IN STRAND S
C     KAP   (S,I)   INITIAL CURVATURE    OF WIRE I IN STRAND S
C     M     (S,I)   NUMBER OF WIRES IN LAYER I OF STRAND S
C     NPRIME(S,I)   SHEAR FORCE          ON WIRE I IN STRAND S
C     R     (S,I)   HELIX RADIUS         OF WIRE I IN STRAND S
C     TAU   (S,I)   INITIAL TWIST        OF WIRE I IN STRAND S
C
C
C     LET EPS(0,0) AND DTAU(0,0) BE PRESCRIBED
C
      EPS(0,0)  = EPS00
      DTAU(0,0) = DTAU00
C
      DO 6 S = 1, LAYERS(0)
C
C        COMPUTE THE STRAND RADIUS BIGR(S,0) OF THIS STRAND,
C        BY NOTING THAT THE STRAND RADIUS IS ALWAYS EQUAL TO
C        THE HELIX RADIUS OF THE OUTERMOST WIRE PLUS THE WIRE
C        RADIUS OF THE OUTERMOST WIRE.
C
         BIGR(S,0) = 0.
         DO 1 J = 1, LAYERS(S)
            IF (J.NE.LAYERS(S)) THEN
               ETA(S,0,J) = ETA(S,LAYERS(S),J)
            ELSE
               ETA(S,0,J) = ETA(S,LAYERS(S),J) + 1.
            END IF
    1       BIGR(S,0) = BIGR(S,0) + ETA(S,0,J)*BIGR(S,J)
C
C        COMPUTE THE HELIX RADIUS R(S,0) (WHICH DEPENDS ON THE RADII
C        OF THE UNDERLYING STRANDS AS WELL AS ON THIS ONE)
C
         R(S,0) = 0.
```

```
      DO 2 T = 1, S
    2    R(S,0) = R(S,0) + ETA(0,S,T)*BIGR(T,0)
C
C     NEXT, COMPUTE THE IMPOSED CHANGE IN HELIX RADIUS DUE TO
C     THE UNDERLYING STRANDS
C
      DRPS   = 0.
      DO 3 T = 1, S-1
    3    DRPS   = DRPS + ETA(0,S,T)*
     &                    (DRDEPS(T)*EPS(T,0) + DRDTAU(T)*DTAU(T,0))
C
C     NOW COMPUTE THE RATE OF CHANGE OF STRAND RADIUS WITH RESPECT
C     TO THE STRAND STRAIN AND THE STRAND TWIST
C
      EPS(S,0)  = 1.
      DTAU(S,0) = 0.
      CALL   STRAND (S)
      DRDEPS(S) = 0.
      DO 4 J = 1, LAYERS(S)
    4    DRDEPS(S) = DRDEPS(S) - NU*ETA(S,0,J)*BIGR(S,J)*EPS(S,J)
C
      EPS (S,0) = 0.
      DTAU(S,0) = 1.
      CALL   STRAND (S)
      DRDTAU(S) = 0.
      DO 5 J = 1, LAYERS(S)
    5    DRDTAU(S) = DRDTAU(S) - NU*ETA(S,0,J)*BIGR(S,J)*EPS(S,J)
C
C     NOW SOLVE FOR THE STRAND STRAIN
C
      CDTAU  = ETA(0,S,S)*DRDTAU(S)
      CEPS   = ETA(0,S,S)*DRDEPS(S)
      CALL   DEFORM (PI*ALPHA(S,0)/180., CDTAU, CEPS, R(S,0),
     &                EPS(0,0), DTAU(0,0), DRPS, SOL)
      DTAU(S,0) = SOL(1)
      DKAP(S,0) = SOL(2)
      EPS (S,0) = SOL(3)
C
C     LEAVE THE CORRECT STRAINS IN COMMON /VAR/
      CALL STRAND (S)
    6 CONTINUE
C
C     ------------------- GENERALIZED FORCES ------------------
C
C     AT THIS STAGE, THE GEOMETRY OF DEFORMATION IS KNOWN.  NOW
C     THE INTERNAL FORCES CAN BE COMPUTE.
C
      IF (WANTED) WRITE (6,11) DESC, EPS(0,0), DTAU(0,0)
   11 FORMAT (///' FOR A STRAIGHT ', A
     &          /' ', 8('-'), ' '
     &          /' SUBJECTED TO EPS(0,0) =', F9.6
     &          ,' AND DTAU(0,0) =', F9.6, ' ',/
```

```
     &          /' THE GENERALIZED STRAINS AND FORCES ARE:')
      DO 40 S = 1, LAYERS(0)
         IF (WANTED) WRITE (6,12) S, LAYERS(S)
   12 FORMAT(//' ---- STRAND #', I1,
     &          ' (CONTAINING', I2, ' LAYERS OF WIRES):'
     &        /' S I  EPS(SI) DTAU(SI) DKAP(SI)'
     &        ,'  T(SI)  G''(SI)   H(SI)  N''(SI)'
     &        ,'   X(SI)'
     &        /' # #            (1/IN)    (1/IN) '
     &        ,'  (LB)   (LB-IN) (LB-IN)    (LB) '
     &        ,' (LB/IN)'
     &       //29X, 'WIRE VARIABLES:')
         DO 20 I = 1, LAYERS(S)
C
C           GENERALIZED FORCES ON INDIVIDUAL WIRES
C
            BIGT  (S,I) = PI   *E              *BIGR(S,I)**2 *  EPS(S,I)
            GPRIME(S,I) = PI/4.*E              *BIGR(S,I)**4 * DKAP(S,I)
            BIGH  (S,I) = PI/2.*E/(2.*(1.+NU))*BIGR(S,I)**4 * DTAU(S,I)
C
            R(S,I) = 0.
            DO 13 J = 1, I
   13          R(S,I) = R(S,I) + ETA(S,I,J)*BIGR(S,J)
            IF (R(S,I).EQ.0) THEN
               KAP(S,I) = 0.
               TAU(S,I) = 0.
            ELSE
               ANG      = PI*ALPHA(S,I)/180.
               KAP(S,I) = COS(ANG)**2/R(S,I)
               TAU(S,I) = COS(ANG)*SIN(ANG)/R(S,I)
            END IF
C
C           FROM EQUILIBRIUM,
C
            NPRIME(S,I) = BIGH(S,I)*KAP(S,I) - GPRIME(S,I)*TAU(S,I)
            BIGX        = NPRIME(S,I)*TAU(S,I) - BIGT(S,I)*KAP(S,I)
            IF (WANTED) WRITE (6,14) S, I, EPS(S,I), DTAU(S,I),
     &          DKAP(S,I), BIGT(S,I), GPRIME(S,I), BIGH(S,I),
     &          NPRIME(S,I), BIGX
   14 FORMAT (I2, I2, 3F9.6, F7.1, 3F8.3, F8.1)
   20       CONTINUE
C
C        GENERALIZED FORCES ON STRANDS
C
         BIGT  (S,0) = 0.
         BIGH  (S,0) = 0.
         GPRIME(S,0) = 0.
         DO 21 I = 1, LAYERS(S)
            ANG         = PI*ALPHA(S,I)/180.
            COSANG      = COS(ANG)
            SINANG      = SIN(ANG)
            BIGT  (S,0) = BIGT  (S,0)
```

```
     &                    + M(S,I)*(BIGT(S,I)*SINANG + NPRIME(S,I)*COSANG)
           BIGH   (S,0) = BIGH   (S,0)
     &                    + M(S,I)*(BIGH(S,I)*SINANG + GPRIME(S,I)*COSANG
     &                              +R(S,I)*(BIGT(S,I)*COSANG
     &                                      -NPRIME(S,I)*SINANG))
C
C          THE BENDING MOMENT APPLIED TO THE STRAND IS COMPUTED BY
C          TREATING THE STRAND AS A COLLECTION OF SMOOTH HELICAL WIRES.
C          SEE: COSTELLO, G. A., ''LARGE DEFLECTIONS OF HELICAL SPRING
C          DUE TO BENDING,'' JOURNAL OF THE ENGINEERING MECHANICS DIV.,
C          ASCE, VOL. 103, NO. EM3, PP. 479-487 (JUNE 1977).
C
           GPRIME(S,0) = GPRIME(S,0)
     &                    + M(S,I)*SINANG/(1.+NU/2.*COSANG**2)
     &                            *PI/4.*BIGR(S,I)**4*E*DKAP(S,0)
   21      CONTINUE
C
        IF (R(S,0).EQ.0.) THEN
           KAP(S,0) = 0.
           TAU(S,0) = 0.
        ELSE
           ANG      = PI*ALPHA(S,0)/180.
           KAP(S,0) = COS(ANG)**2/R(S,0)
           TAU(S,0) = COS(ANG)*SIN(ANG)/R(S,0)
        END IF
C
C       FROM EQUILIBRIUM,
C
        NPRIME(S,0) = BIGH(S,0)*KAP(S,0) - GPRIME(S,0)*TAU(S,0)
        BIGX        = NPRIME(S,0)*TAU(S,0) - BIGT(S,0)*KAP(S,0)
        IF (WANTED) THEN
           WRITE (6,22)
   22 FORMAT (/28X,'STRAND VARIABLES:')
           WRITE (6,14) S, 0, EPS(S,0), DTAU(S,0),
     &                  DKAP(S,0), BIGT(S,0), GPRIME(S,0),
     &                  BIGH(S,0), NPRIME(S,0), BIGX
        END IF
   40   CONTINUE
C
C     GENERALIZED FORCES ON ROPE
C
      BIGT   (0,0) = 0.
      BIGH   (0,0) = 0.
C     GPRIME(0,0) = 0. FOR A STRAIGHT ROPE
C
      DO 50 S = 1, LAYERS(0)
         ANG      = PI*ALPHA(S,0)/180.
         COSANG   = COS(ANG)
         SINANG   = SIN(ANG)
         BIGT(0,0) = BIGT(0,0)
     &             + M(S,0)*(BIGT(S,0)*SINANG + NPRIME(S,0)*COSANG)
         BIGH(0,0) = BIGH(0,0)
```

```
     &              + M(S,0)*(BIGH(S,0)*SINANG + GPRIME(S,0)*COSANG
     &                       +R(S,0)*(BIGT(S,0)*COSANG
     &                                -NPRIME(S,0)*SINANG))
C
C        FOR A STRAIGHT ROPE, KAP(0,0) (IF IT WERE INTRODUCED) WOULD
C        BE EQUAL TO ZERO; AND ALSO:
C
C        GPRIME(0,0) WOULD = 0.
C        NPRIME(0,0) WOULD = 0.
C        BIGX        WOULD = 0.
C
   50    CONTINUE
      IF (WANTED) WRITE (6,51) 0, 0, EPS(0,0), DTAU(0,0),
     &                         BIGT(0,0), BIGH(0,0)
   51 FORMAT (//21X, 'ROPE VARIABLES (STRAIGHT ROPE):'
     &         /21X, '                 --------      '
     &         /I2, I2, 2F9.6,
     &          '     ---  ', F7.1, '   ---  ', F8.3, 2('   ---  '))
      RETURN
      END
C
C=======================================================================
C
      SUBROUTINE    STRAND (S)
C
C     SOLVE FOR ALL WIRE VARIABLES IN STRAND S, GIVEN
C     EPS(S,0) AND DTAU(S,0) (WHICH ARE IN COMMON BLOCK /VAR/)
C
C-----------------------------------------------------------------
      PARAMETER     (PI=3.14159265,
     &               K=4)
C
C     K = MAX (MAX# WIRE LAYERS IN A STRAND, # STRAND LAYERS IN A ROPE)
C
      REAL          ALPHA(K,0:K), BIGR(0:K,0:K), ETA(0:K,0:K,K),
     &              EPS(0:K,0:K), DTAU(0:K,0:K), DKAP(0:K,0:K),
     &              DRDEPS(K),    DRDTAU(K),
     &              NU, SOL(3)
      INTEGER       S, T, M(K,0:K), LAYERS(0:K)
      COMMON /VAR/  ALPHA, BIGR, ETA, EPS, DTAU, DKAP,
     &              DRDEPS, DRDTAU, NU, M, LAYERS
      REAL          BIGT(0:K,0:K), GPRIME(0:K,0:K),
     &              BIGH(0:K,0:K), NPRIME(0:K,0:K),
     &              KAP(0:K,0:K),  TAU(0:K,0:K),
     &              R(0:K,0:K),    E,
     &              OFFANG(K,0:K)
      COMMON /VAR/  BIGT, GPRIME, BIGH, NPRIME,
     &              KAP, TAU, R, E, OFFANG
      CHARACTER*60  DESC
      COMMON /CVAR/ DESC
C-----------------------------------------------------------------
C
```

```
      LOGICAL         WANTED
      DATA            WANTED /.FALSE./
      DO 3 I=1, LAYERS(S)
C
C        COMPUTE HELIX RADIUS
C
         RSI     = 0.
         DO 1 J = 1, I
    1       RSI     = RSI + ETA(S,I,J)*BIGR(S,J)
C
C        COMPUTE IMPOSED RADIUS CHANGE DUE TO WIRES BENEATH
C        THE CURRENT LAYER OF WIRES
C
         DRPSI   = 0.
         DO 2 J = 1, I-1
    2       DRPSI   = DRPSI - NU*ETA(S,I,J)*BIGR(S,J)*EPS(S,J)
         CDTAU   = 0.
         CEPS    = -NU*ETA(S,I,I)*BIGR(S,I)
         CALL    DEFORM (PI*ALPHA(S,I)/180., CDTAU, CEPS, RSI,
     &                   EPS(S,0), DTAU(S,0), DRPSI, SOL)
         DTAU(S,I) = SOL(1)
         DKAP(S,I) = SOL(2)
         EPS (S,I) = SOL(3)
    3    CONTINUE
      IF (WANTED) WRITE (6,10) S, S, EPS(S,0), S, DTAU(S,0),
     &             (I,I=1,3), (EPS(S,I),I=1,3),
     &             (DTAU(S,I),I=1,3), (DKAP(S,I),I=1,3)
   10 FORMAT (
     &//'WHEN STRAND', I2, ' IS STRAINED WITH EPS(', I1, ',0) ='
     & /F9.6, ' AND DTAU(', I1, ',0) =', F9.6, ', WE HAVE:'
     &//10X, 3(' WIRE', I2, '    ')
     & /' STRAIN    ', 3F10.6
     & /' D TWIST   ', 3F10.6
     & /' D KAPPA   ', 3F10.6)
      RETURN
      END
C
C=======================================================================
C
      SUBROUTINE    DEFORM (ALPHA, CDTAU, CEPS, R, EPS, DTAU, DRP,
     *                      SOL)
      REAL          SOL(3)
C
C     SOLUTION FOR CHANGE IN TWIST, CHANGE IN CURVATURE, AND
C     STRAIN OF A WIRE OR STRAND:
C
C        SOL(1)  =  DELTA TAU
C        SOL(2)  =  DELTA KAPPA
C        SOL(3)  =  EPSILON
C
      REAL          A(3,3), B(3)
      COTALP = COT(ALPHA)
```

```
C
C     THIS ROUTINE WORKS WITH STRANDS IN A ROPE [OR]
C     WIRES IN A STRAND, AS FOLLOWS:
C
C     --- GIVEN:
C
C     ALPHA      HELIX ANGLE OF STRAND [WIRE]                    RADIANS
C     CDTAU      RATE OF CHANGE OF STRAND [WIRE] RADIUS          L**2
C                   WITH RESPECT TO
C                   CHANGE IN STRAND [WIRE] TWIST
C     CEPS       RATE OF CHANGE OF STRAND [WIRE] RADIUS          L
C                   WITH RESPECT TO
C                   AXIAL STRAIN OF STRAND [WIRE]
C     R          HELIX RADIUS OF STRAND [WIRE]                   L
C     EPS        PRESCRIBED AXIAL STRAIN OF ROPE [STRAND]        L
C     DTAU       PRESCRIBED CHANGE IN TWIST OF ROPE [STRAND]     1/L
C     DRP        THAT PORTION OF THE CHANGE IN STRAND [WIRE]     L
C                   HELIX RADIUS IMPOSED BY UNDERLYING
C                   STRANDS [WIRES] (IF ANY)
C
C     --- DETERMINE:
C
C     SOL(1)     CHANGE IN TWIST OF STRAND [WIRE]                1/L
C     SOL(2)     CHANGE IN CURVATURE OF STRAND [WIRE]            1/L
C     SOL(3)     AXIAL STRAIN IN STRAND [WIRE]                   1
C
      IF (COTALP.NE.0.) THEN
         A(1,1) = COTALP
         A(1,2) = -1.
         A(1,3) = +1.
C
         A(2,1) = +1.
         A(2,2) = COTALP
         A(2,3) = COTALP
C
         A(3,1) = - 2.*COTALP - (COTALP**2/R**2) * CDTAU
         A(3,2) = 1. - COTALP**2
         A(3,3) = - (COTALP**2/R) * CEPS
C
         B(1)   = EPS
         B(2)   = R*DTAU
         B(3)   = (COTALP**2/R) * DRP
C
         CALL   SOL3B3 (A, B, SOL)
         SOL(1) = SOL(1)/R
         SOL(2) = SOL(2)/R
C        SOL(3) IS O.K.
      ELSE
         SOL(1) = DTAU
         SOL(2) = 0.
         SOL(3) = EPS
      END IF
```

```
      RETURN
      END
C
C=====================================================================
C
      SUBROUTINE    SOL3B3 (A, B, X)
      REAL          A(3,3), B(3), X(3)
C
C     FIND SOLUTION TO  A X = B  BY CRAMER'S RULE
C
      D       = A(1,1)*(A(2,2)*A(3,3) - A(3,2)*A(2,3))
     &        + A(2,1)*(A(3,2)*A(1,3) - A(1,2)*A(3,3))
     &        + A(3,1)*(A(1,2)*A(2,3) - A(2,2)*A(1,3))
      IF (D.EQ.0.) THEN
         WRITE  (6, '(''  TOO BAD: COEFFICIENT DETERMINANT VANISHED.'')')
         STOP    ' MATRIX ''A'' PASSED TO ''SOL3B3'' WAS SINGULAR.'
      END IF
      X(1)    = B(1)*(A(2,2)*A(3,3) - A(3,2)*A(2,3))
     &        + B(2)*(A(3,2)*A(1,3) - A(1,2)*A(3,3))
     &        + B(3)*(A(1,2)*A(2,3) - A(2,2)*A(1,3))
      X(2)    = B(1)*(A(2,3)*A(3,1) - A(3,3)*A(2,1))
     &        + B(2)*(A(3,3)*A(1,1) - A(1,3)*A(3,1))
     &        + B(3)*(A(1,3)*A(2,1) - A(2,3)*A(1,1))
      X(3)    = B(1)*(A(2,1)*A(3,2) - A(3,1)*A(2,2))
     &        + B(2)*(A(3,1)*A(1,2) - A(1,1)*A(3,2))
     &        + B(3)*(A(1,1)*A(2,2) - A(2,1)*A(1,2))
      DO 1 I = 1, 3
    1    X(I) = X(I)/D
      RETURN
      END
C
C=====================================================================
C
      REAL FUNCTION COT(ALPHA)
      DATA PI /3.14159265/
      IF (ABS(ABS(ALPHA)-PI/2.) .LT. 0.000001) THEN
         COT = 0.
      ELSE
         COT = 1./TAN(ALPHA)
      END IF
      RETURN
      END
C
C=====================================================================
C
      SUBROUTINE    XSECTN (XCTR, YCTR, RADIUS,
     &                      NUMBRS, SYMBLS, NPEN1, NPEN2)
      LOGICAL       SYMBLS, NUMBRS
C
C     DRAW CROSS SECTION OF THE ROPE, CENTERED AT (XCTR,YCTR), WITH
C     RADIUS (IN INCHES OF DRAWING) OF 'RADIUS'.  IF 'SYMBLS' =
C     .TRUE., THEN LABEL ALL THE WIRES IN THE FIRST OCCURRENCE OF
```

```
C     A STRAND WITH PLOTTING SYMBOLS; IF 'NUMBRS' = .TRUE., THEN
C     LABEL ALL THE WIRES IN THE FIRST OCCURRENCE OF A STRAND
C     WITH NUMBER PAIRS S,I.
C
C-----------------------------------------------------------------
      PARAMETER      (PI=3.14159265,
     &                K=4)
C
C     K = MAX (MAX# WIRE LAYERS IN A STRAND, # STRAND LAYERS IN A ROPE)
C
      REAL           ALPHA(K,0:K), BIGR(0:K,0:K), ETA(0:K,0:K,K),
     &               EPS(0:K,0:K), DTAU(0:K,0:K), DKAP(0:K,0:K),
     &               DRDEPS(K),    DRDTAU(K),
     &               NU, SOL(3)
      INTEGER        S, T, M(K,0:K), LAYERS(0:K)
      COMMON /VAR/   ALPHA, BIGR, ETA, EPS, DTAU, DKAP,
     &               DRDEPS, DRDTAU, NU, M, LAYERS
      REAL           BIGT(0:K,0:K), GPRIME(0:K,0:K),
     &               BIGH(0:K,0:K), NPRIME(0:K,0:K),
     &               KAP(0:K,0:K),  TAU(0:K,0:K),
     &               R(0:K,0:K),    E,
     &               OFFANG(K,0:K)
      COMMON /VAR/   BIGT, GPRIME, BIGH, NPRIME,
     &               KAP, TAU, R, E, OFFANG
      CHARACTER*60   DESC
      COMMON /CVAR/  DESC
C-----------------------------------------------------------------
C
      REAL           IS(3),  JS(3),  KS(3),
     &               ISI(3), JSI(3), KSI(3)
      LOGICAL        LABEL
      CHARACTER      NUMB(0:9)*1, STRING*3
C
      DATA           HMAX  /0.1/,
     &               NUMB  /'0','1','2','3','4','5','6','7','8','9'/
C
      XPLOT() = XCTR + SCALE*X
      YPLOT() = YCTR + SCALE*Y
C
C
      BIGR(0,0) = R(LAYERS(0),0) + BIGR(LAYERS(0),0)
      SCALE     = RADIUS/BIGR(0,0)
      DO  6 S = 1, LAYERS(0)
         LABEL = .TRUE.
         COSAS  = COS(PI/180.*ALPHA(S,0))
         SINAS  = SIN(PI/180.*ALPHA(S,0))
         DO  5 M1 = 1, M(S,0)
            PHIS   = PI/180.*OFFANG(S,0) + 2.*PI*(M1-1)/M(S,0)
            COSPS  = COS(PHIS)
            SINPS  = SIN(PHIS)
C
C           STRAND TRIAD
```

```
C           ------ -----
C
            IS(1)  =  COSPS
            IS(2)  =  SINPS
            IS(3)  =  0.
C
            JS(1)  = -SINAS*SINPS
            JS(2)  =  SINAS*COSPS
            JS(3)  = -COSAS
C
            KS(1)  = -COSAS*SINPS
            KS(2)  =  COSAS*COSPS
            KS(3)  =  SINAS
C
            DO  4 I = 1, LAYERS(S)
               COSASI = COS(PI/180.*ALPHA(S,I))
               SINASI = SIN(PI/180.*ALPHA(S,I))
               DO  3 M2 = 1, M(S,I)
                  PHISI  = PI/180.*OFFANG(S,I) + 2.*PI*(M2-1)/M(S,I)
                  COSPSI = COS(PHISI)
                  SINPSI = SIN(PHISI)
C
C                 WIRE TRIAD
C                 ---- -----
C
                  DO  1 J = 1, 3
                     ISI(J) =  COSPSI*IS(J) + SINPSI*JS(J)
                     JSI(J) = -SINASI*SINPSI*IS(J)
     &                        +SINASI*COSPSI*JS(J)
     &                        -COSASI*KS(J)
     1               KSI(J) = -COSASI*SINPSI*IS(J)
     &                        +COSASI*COSPSI*JS(J)
     &                        +SINASI*KS(J)
C
C                 INTERSECTION OF WIRE CENTERLINE WITH ROPE
C                 CROSS SECTION--NEEDED ONLY IF WIRE IS LABELLED
C
                  IF (LABEL .AND. (NUMBRS.OR.SYMBLS)) THEN
                     DIST = R(S,I)*SINPSI*COSAS
     &                     /(SINASI*SINAS-COSASI*COSPSI*COSAS)
                     X    = R(S,0)*IS(1) + R(S,I)*ISI(1) + DIST*KSI(1)
                     Y    = R(S,0)*IS(2) + R(S,I)*ISI(2) + DIST*KSI(2)
                     CALL NEWPEN (NPEN2)
                     IF (NUMBRS) THEN
                        STRING = NUMB(S)//',''//NUMB(I)
                        H      = MIN(HMAX,0.6*SCALE*BIGR(S,I))
                        CALL   SYMBOL (XPLOT()-1.0*H,
     &                                 YPLOT()-0.5*H, H, STRING, 0., 3)
                     ELSE
                        L      = K*(S-1) + (I-1)
                        H      = MIN(HMAX,2.*SCALE*BIGR(S,I))
                        CALL   SYMBOL (XPLOT(), YPLOT(), H, L, 0., -1)
```

```
                  END IF
               END IF
C
C              INTERSECTION OF WIRE PERIPHERY WITH ROPE CROSS SECTION
C              ------------ -- ---- --------- ---- ---- ----- -------
C
               IC     = 3
               CALL   NEWPEN (NPEN1)
               IANGLS = 2.*PI*SCALE*BIGR(S,I)/0.10
               IANGLS = MAX(IANGLS,20)
               DO  2 IANG = 0, IANGLS
                  ANG    = 2.*PI*IANG/IANGLS
                  COSANG = COS(ANG)
                  SINANG = SIN(ANG)
                  DIST   = (R(S,I)*SINPSI*COSAS
     &                     +BIGR(S,I)*(COSANG*SINPSI*COSAS
     &                                +SINANG*(SINASI*COSPSI*COSAS
     &                                        +COSASI*SINAS)))
     &                     /(SINASI*SINAS - COSASI*COSPSI*COSAS)
                  X      = R(S,0)*IS(1) + R(S,I)*ISI(1)
     &                     +BIGR(S,I)*(COSANG*ISI(1)+SINANG*JSI(1))
     &                     +DIST*KSI(1)
                  Y      = R(S,0)*IS(2) + R(S,I)*ISI(2)
     &                     +BIGR(S,I)*(COSANG*ISI(2)+SINANG*JSI(2))
     &                     +DIST*KSI(2)
                  CALL   PLOT (XPLOT(), YPLOT(), IC)
     2            IC     = 2
     3         CONTINUE
     4      CONTINUE
     5      LABEL = .FALSE.
     6   CONTINUE
       RETURN
       END
C
C=======================================================================
C
       SUBROUTINE    GEOM
C
C      ROUTINE FOR DEFINING THE ROPE UNDER CONSIDERATION.
C      THIS PARTICULAR ROPE IS A SEALE 6X19 IWRC, WHERE THE
C      IWRC IS A 6X7 ROPE WITH A 7-WIRE STRAND CORE.
C
C-----------------------------------------------------------------
       PARAMETER     (PI=3.14159265,
      &               K=4)
C
C      K = MAX (MAX# WIRE LAYERS IN A STRAND, # STRAND LAYERS IN A ROPE)
C
       REAL          ALPHA(K,0:K), BIGR(0:K,0:K), ETA(0:K,0:K,K),
      &              EPS(0:K,0:K), DTAU(0:K,0:K), DKAP(0:K,0:K),
      &              DRDEPS(K),    DRDTAU(K),
      &              NU, SOL(3)
```

Computer Program: Stresses in Loaded Wire Rope Bent over a Sheave

```
      INTEGER        S, T, M(K,0:K), LAYERS(0:K)
      COMMON /VAR/   ALPHA, BIGR, ETA, EPS, DTAU, DKAP,
     &               DRDEPS, DRDTAU, NU, M, LAYERS
      REAL           BIGT(0:K,0:K), GPRIME(0:K,0:K),
     &               BIGH(0:K,0:K), NPRIME(0:K,0:K),
     &               KAP(0:K,0:K),  TAU(0:K,0:K),
     &               R(0:K,0:K),    E,
     &               OFFANG(K,0:K)
      COMMON /VAR/   BIGT, GPRIME, BIGH, NPRIME,
     &               KAP, TAU, R, E, OFFANG
      CHARACTER*60   DESC
      COMMON /CVAR/  DESC
C-----------------------------------------------------------------
      DATA           E/30.E+6/, NU/0.29/
      DATA           DESC
     &/'6!2X19 !1S!2EALE !1IWRC (!26X7 CORE)                      '/
C    &/'6!2X7 LANG-LAY ROPE                                       '/
C    &/'7-!2WIRE STRAND                                           '/
C    &/'S!2OLID CIRCULAR BAR                                      '/
C
C     STRAND VARIABLES: NUMBER OF STRANDS IN EACH LAYER,
C     AND HELIX ANGLES OF THE STRANDS WITHIN THE ROPE
C
      DATA
     &     LAYERS(0)           /3/,
     &     (    M(S,0),S=1,3) /    1,     6,     6/,
     &     (ALPHA(S,0),S=1,3) /90.00, 70.83, 70.24/,
C
C     WIRE VARIABLES: NUMBER OF WIRES IN EACH LAYER, HELIX
C     ANGLES OF WIRES WITHIN THE STRANDS, AND WIRE RADII
C
C    &     LAYERS(1)           /1/,
     &     LAYERS(1)           /2/,
     &     (    M(1,I),I=1,2) /      1,       6/,
     &     (ALPHA(1,I),I=1,2) /  90.00,   73.71/,
     &     ( BIGR(1,I),I=1,2) /0.03155, 0.02893/,
C
     &     LAYERS(2)           /2/,
     &     (    M(2,I),I=1,2) /      1,       6/,
     &     (ALPHA(2,I),I=1,2) /  90.00,   81.07/,
     &     ( BIGR(2,I),I=1,2) /0.02773, 0.02582/,
C
     &     LAYERS(3)           /3/,
     &     (    M(3,I),I=1,3) /      1,       9,       9/,
     &     (ALPHA(3,I),I=1,3) /  90.00,  102.27,  111.23/,
     &     ( BIGR(3,I),I=1,3) /0.05731, 0.02805, 0.04993/
C
C     ----- GEOMETRICAL FACTORS ETA(*,*,*) -----
C
C     FACTORS FOR HELIX RADIUS OF THE STH STRAND, ETA(0,S,T)
C     IN TERMS OF THE RADII OF THE STRANDS
C
```

```
      DATA
     &      ETA(0,1,1)          /0.          /,
     &     (ETA(0,2,T),T=1,2) /1., 1.     /,
     &     (ETA(0,3,T),T=1,3) /1., 2., 1./
C
C     FACTORS FOR THE HELIX RADII OF WIRES WITHIN STRANDS--THE
C     FIRST TWO STRANDS ARE SIMPLE STRANDS
C
      DATA
     &     ((ETA(1,I,J),J=1,I),I=1,2) /0.,    1., 1./,
     &     ((ETA(2,I,J),J=1,I),I=1,2) /0.,    1., 1./
C
C     THE SEALE STRAND HAS A SIMPLE STRAND FOR ITS FIRST TWO LAYERS
C
      DATA
     &     ((ETA(3,I,J),J=1,I),I=1,2) /0.,    1., 1./
C
C     BUT THE HELIX RADIUS OF THE OUTER [3,3] LAYER DEPENDS ON
C     BIGR(3,1), BIGR(3,2), AND BIGR(3,3) IN A SOMEWHAT MORE
C     INVOLVED MANNER:
C
      ETA(3,3,1) = COS(PI/M(3,2))
      GAMMA      = ASIN((BIGR(3,1)+BIGR(3,2))
     &                 /(BIGR(3,2)+BIGR(3,3))
     &                 *SIN(PI/M(3,2)))
      ETA(3,3,2) = COS(PI/M(3,2)) + COS(GAMMA)
      ETA(3,3,3) = COS(GAMMA)
C
C     THE FOLLOWING DATA ARE FOR COSMETIC PURPOSES.  IT IS
C     HELPFUL TO KNOW, WHEN DRAWING THE CROSS SECTION OF THE
C     ROPE, WHERE THE FIRST WIRE IN A GIVEN LAYER OF WIRES
C     IS LOCATED IF IT IS NOT "LINED UP" WITH THE OTHERS.
C
      DATA           (OFFANG(S,0),S=1,3) /0., 0., 0./
C
      DATA           (OFFANG(1,I),I=1,2) /0., 0./,
     &               (OFFANG(2,I),I=1,2) /0., 0./,
     &               (OFFANG(3,I),I=1,3) /0., 0., 20./
      RETURN
      END
C
C=======================================================================
C
```

Computer Program: Stresses in Loaded Wire Rope Bent over a Sheave

Sample Output
for 6x19 Seale IWRC (7x7 core)

FOR A STRAIGHT 6!2X19 !1S!2EALE !1IWRC (!27X7 CORE)

SUBJECTED TO EPS(0,0) = .001000 AND DTAU(0,0) = 0.000000,
THE GENERALIZED STRAINS AND FORCES ARE:

---- STRAND #1 (CONTAINING 2 LAYERS OF WIRES):

S #	I #	EPS(SI)	DTAU(SI) (1/IN)	DKAP(SI) (1/IN)	T(SI) (LB)	G'(SI) (LB-IN)	H(SI) (LB-IN)	N'(SI) (LB)	X(SI) (LB/IN)
				WIRE VARIABLES:					
1	1	.001000	0.000000	0.000000	93.8	0.000	0.000	0.000	0.0
1	2	.000900	-.003558	-.002700	71.0	-.045	-.046	.139	-91.7
				STRAND VARIABLES:					
1	0	.001000	0.000000	0.000000	502.7	0.000	6.837	0.000	0.0

---- STRAND #2 (CONTAINING 2 LAYERS OF WIRES):

S #	I #	EPS(SI)	DTAU(SI) (1/IN)	DKAP(SI) (1/IN)	T(SI) (LB)	G'(SI) (LB-IN)	H(SI) (LB-IN)	N'(SI) (LB)	X(SI) (LB/IN)
				WIRE VARIABLES:					
2	1	.000864	-.001339	0.000000	62.6	0.000	-.014	0.000	0.0
2	2	.000827	-.003566	-.001265	51.9	-.013	-.029	.025	-23.3
				STRAND VARIABLES:					
2	0	.000864	-.001339	-.001269	370.5	-.096	2.384	1.700	-233.6

---- STRAND #3 (CONTAINING 3 LAYERS OF WIRES):

S #	I #	EPS(SI)	DTAU(SI) (1/IN)	DKAP(SI) (1/IN)	T(SI) (LB)	G'(SI) (LB-IN)	H(SI) (LB-IN)	N'(SI) (LB)	X(SI) (LB/IN)
				WIRE VARIABLES:					
3	1	.000858	-.000506	0.000000	265.6	0.000	-.100	0.000	0.0
3	2	.000817	.001406	-.000784	60.6	-.011	.016	-.019	-32.0
3	3	.000741	.000941	-.001134	174.0	-.166	.107	-.276	-149.0
				STRAND VARIABLES:					
3	0	.000858	-.000506	-.000497	2259.5	-.789	-94.538	-23.424	-589.7

ROPE VARIABLES (STRAIGHT ROPE):

0	0	.001000	0.000000	---	15317.0	---	1731.165	---	---

Computer Program: Stresses in Loaded Wire Rope Bent over a Sheave

FOR A STRAIGHT 6!2X19 !1S!2EALE !1IWRC (!27X7 CORE)

SUBJECTED TO EPS(0,0) = .001000 AND DTAU(0,0) = 0.000000, THE NOMINAL STRESS GIVEN BY BIGT(0,0)/A IS COMPUTED AS FOLLOWS:

BIGT(0,0) = 15317.0 LB., AND
A = .7271 IN.**2; HENCE
SIGNOM = 21065. LB./IN.**2.

FOR A 6!2X19 !1S!2EALE !1IWRC (!27X7 CORE)
BENT AROUND A SHEAVE AND LOADED AXIALLY, THE FACTORS ZT(S,I) AND ZB(S,I) IN THE FORMULA

$$\frac{SIGMAX}{SIGNOM} = ZT(S,I) + \frac{ZB(S,I)}{(D/D)SIGNOM/E}$$

ARE:

S	I	ZT(S,I)	ZB(S,I)
1	1	1.424	.04831
1	2	1.392	.04204
2	1	1.281	.03949
2	2	1.270	.03620
3	1	1.262	.08124
3	2	1.214	.03860
3	3	1.168	.06475

NUMERICAL RESULTS BASED ON THESE VALUES OF ZT(S,I) AND ZB(S,I) ARE GIVEN BELOW.

SIGMAX/SIGNOM--WIRE 1, STRAND 1 [X = (D/D)SIGNOM/E; Y = SIGMAX/SIGNOM]:

X	Y	X	Y	X	Y	X	Y	X	Y
.015	4.64	.020	3.84	.025	3.36	.030	3.03	.035	2.80
.040	2.63	.045	2.50	.050	2.39	.055	2.30	.060	2.23
.065	2.17	.070	2.11	.075	2.07	.080	2.03	.085	1.99
.090	1.96	.095	1.93	.100	1.91	.105	1.88	.110	1.86
.115	1.84	.120	1.83	.125	1.81	.130	1.80	.135	1.78
.140	1.77	.145	1.76	.150	1.75	.155	1.74	.160	1.73
.165	1.72	.170	1.71	.175	1.70	.180	1.69	.185	1.69
.190	1.68	.195	1.67	.200	1.67	.205	1.66	.210	1.65
.215	1.65	.220	1.64	.225	1.64	.230	1.63	.235	1.63
.240	1.63	.245	1.62	.250	1.62	.255	1.61	.260	1.61
.265	1.61	.270	1.60	.275	1.60	.280	1.60	.285	1.59

.290 1.59 .295 1.59 .300 1.59

SIGMAX/SIGNOM--WIRE 2, STRAND 1 [X = (D/D)SIGNOM/E; Y = SIGMAX/SIGNOM]:

X	Y	X	Y	X	Y	X	Y	X	Y
.015	4.20	.020	3.49	.025	3.07	.030	2.79	.035	2.59
.040	2.44	.045	2.33	.050	2.23	.055	2.16	.060	2.09
.065	2.04	.070	1.99	.075	1.95	.080	1.92	.085	1.89
.090	1.86	.095	1.83	.100	1.81	.105	1.79	.110	1.77
.115	1.76	.120	1.74	.125	1.73	.130	1.72	.135	1.70
.140	1.69	.145	1.68	.150	1.67	.155	1.66	.160	1.66
.165	1.65	.170	1.64	.175	1.63	.180	1.63	.185	1.62
.190	1.61	.195	1.61	.200	1.60	.205	1.60	.210	1.59
.215	1.59	.220	1.58	.225	1.58	.230	1.58	.235	1.57
.240	1.57	.245	1.56	.250	1.56	.255	1.56	.260	1.55
.265	1.55	.270	1.55	.275	1.55	.280	1.54	.285	1.54
.290	1.54	.295	1.53	.300	1.53				

SIGMAX/SIGNOM--WIRE 1, STRAND 2 [X = (D/D)SIGNOM/E; Y = SIGMAX/SIGNOM]:

X	Y	X	Y	X	Y	X	Y	X	Y
.015	3.91	.020	3.26	.025	2.86	.030	2.60	.035	2.41
.040	2.27	.045	2.16	.050	2.07	.055	2.00	.060	1.94
.065	1.89	.070	1.85	.075	1.81	.080	1.77	.085	1.75
.090	1.72	.095	1.70	.100	1.68	.105	1.66	.110	1.64
.115	1.62	.120	1.61	.125	1.60	.130	1.58	.135	1.57
.140	1.56	.145	1.55	.150	1.54	.155	1.54	.160	1.53
.165	1.52	.170	1.51	.175	1.51	.180	1.50	.185	1.49
.190	1.49	.195	1.48	.200	1.48	.205	1.47	.210	1.47
.215	1.46	.220	1.46	.225	1.46	.230	1.45	.235	1.45
.240	1.45	.245	1.44	.250	1.44	.255	1.44	.260	1.43
.265	1.43	.270	1.43	.275	1.42	.280	1.42	.285	1.42
.290	1.42	.295	1.41	.300	1.41				

SIGMAX/SIGNOM--WIRE 2, STRAND 2 [X = (D/D)SIGNOM/E; Y = SIGMAX/SIGNOM]:

X	Y	X	Y	X	Y	X	Y	X	Y
.015	3.68	.020	3.08	.025	2.72	.030	2.48	.035	2.30
.040	2.17	.045	2.07	.050	1.99	.055	1.93	.060	1.87
.065	1.83	.070	1.79	.075	1.75	.080	1.72	.085	1.70
.090	1.67	.095	1.65	.100	1.63	.105	1.61	.110	1.60
.115	1.58	.120	1.57	.125	1.56	.130	1.55	.135	1.54
.140	1.53	.145	1.52	.150	1.51	.155	1.50	.160	1.50
.165	1.49	.170	1.48	.175	1.48	.180	1.47	.185	1.47
.190	1.46	.195	1.46	.200	1.45	.205	1.45	.210	1.44
.215	1.44	.220	1.43	.225	1.43	.230	1.43	.235	1.42

.240 1.42	.245 1.42	.250 1.41	.255 1.41	.260 1.41
.265 1.41	.270 1.40	.275 1.40	.280 1.40	.285 1.40
.290 1.39	.295 1.39	.300 1.39		

SIGMAX/SIGNOM--WIRE 1, STRAND 3 [X = (D/D)SIGNOM/E; Y = SIGMAX/SIGNOM]:

X Y	X Y	X Y	X Y	X Y
.015 6.68	.020 5.32	.025 4.51	.030 3.97	.035 3.58
.040 3.29	.045 3.07	.050 2.89	.055 2.74	.060 2.62
.065 2.51	.070 2.42	.075 2.35	.080 2.28	.085 2.22
.090 2.17	.095 2.12	.100 2.07	.105 2.04	.110 2.00
.115 1.97	.120 1.94	.125 1.91	.130 1.89	.135 1.86
.140 1.84	.145 1.82	.150 1.80	.155 1.79	.160 1.77
.165 1.75	.170 1.74	.175 1.73	.180 1.71	.185 1.70
.190 1.69	.195 1.68	.200 1.67	.205 1.66	.210 1.65
.215 1.64	.220 1.63	.225 1.62	.230 1.62	.235 1.61
.240 1.60	.245 1.59	.250 1.59	.255 1.58	.260 1.57
.265 1.57	.270 1.56	.275 1.56	.280 1.55	.285 1.55
.290 1.54	.295 1.54	.300 1.53		

SIGMAX/SIGNOM--WIRE 2, STRAND 3 [X = (D/D)SIGNOM/E; Y = SIGMAX/SIGNOM]:

X Y	X Y	X Y	X Y	X Y
.015 3.79	.020 3.14	.025 2.76	.030 2.50	.035 2.32
.040 2.18	.045 2.07	.050 1.99	.055 1.92	.060 1.86
.065 1.81	.070 1.77	.075 1.73	.080 1.70	.085 1.67
.090 1.64	.095 1.62	.100 1.60	.105 1.58	.110 1.57
.115 1.55	.120 1.54	.125 1.52	.130 1.51	.135 1.50
.140 1.49	.145 1.48	.150 1.47	.155 1.46	.160 1.46
.165 1.45	.170 1.44	.175 1.43	.180 1.43	.185 1.42
.190 1.42	.195 1.41	.200 1.41	.205 1.40	.210 1.40
.215 1.39	.220 1.39	.225 1.39	.230 1.38	.235 1.38
.240 1.38	.245 1.37	.250 1.37	.255 1.37	.260 1.36
.265 1.36	.270 1.36	.275 1.35	.280 1.35	.285 1.35
.290 1.35	.295 1.35	.300 1.34		

SIGMAX/SIGNOM--WIRE 3, STRAND 3 [X = (D/D)SIGNOM/E; Y = SIGMAX/SIGNOM]:

X Y	X Y	X Y	X Y	X Y
.015 5.48	.020 4.41	.025 3.76	.030 3.33	.035 3.02
.040 2.79	.045 2.61	.050 2.46	.055 2.35	.060 2.25
.065 2.16	.070 2.09	.075 2.03	.080 1.98	.085 1.93
.090 1.89	.095 1.85	.100 1.82	.105 1.78	.110 1.76
.115 1.73	.120 1.71	.125 1.69	.130 1.67	.135 1.65
.140 1.63	.145 1.61	.150 1.60	.155 1.59	.160 1.57
.165 1.56	.170 1.55	.175 1.54	.180 1.53	.185 1.52

Computer Program: Stresses in Loaded Wire Rope Bent over a Sheave

.190 1.51	.195 1.50	.200 1.49	.205 1.48	.210 1.48
.215 1.47	.220 1.46	.225 1.46	.230 1.45	.235 1.44
.240 1.44	.245 1.43	.250 1.43	.255 1.42	.260 1.42
.265 1.41	.270 1.41	.275 1.40	.280 1.40	.285 1.40
.290 1.39	.295 1.39	.300 1.38		